TÉCNICO LISBOA

A 0-D Off-Design Performance Prediction Model of the CFM56-5B Turbofan Engine

Francisco Miguel da Costa Baptista

Thesis to obtain the Master of Science Degree in

Aerospace Engineering

Supervisors: Prof. André Calado Marta
Eng. António Miguel Abreu Ribeiro Henriques

Examination Committee

Chairperson: Prof. Filipe Szolnoky Ramos Pinto Cunha
Supervisor: Prof. André Calado Marta
Member of the Committee: Prof. Virginia Isabel Monteiro Nabais Infante

October 2017

To the women of my life. Those who take care of me and those who watch over me.

Acknowledgments

I would like to thank Chief Engineer António Ferreira for granting me the opportunity to develop the present work at TAP Portugal Engine Department.

To both my supervisors, Engineer António Miguel Henriques and Professor André Calado Marta, for all the support and encouragements. Their dedication and valuable guidance were of crucial importance in the development of this thesis.

To all the Engineering team of the Engine Department, particularly João Pedro Fernandes and Ricardo Santos.

To my friends, Arnaldo Tungumuna, Luis Janeiro, Rita Neves, Odelma Teixeira, Ricardo Oliveira, Jorge Aurélio and Paulo Valadas.

To Andreia Guerreiro, for all her love and for always keeping my head up all these years.

And finally to my parents, for giving me the possibility to conclude my studies and for the all support they gave me. All that I am, I owe to them.

Resumo

A perda de desempenho de turbinas a gás pode ser identificado a nível modular do motor, em termos de redução de caudal e eficiência dos seus componentes. A identificação de componentes com mau desempenho irá permitir focar os recursos humanos e financeiros num plano de trabalhos de manutenção eficaz.

Nesta tese, um modelo de desempenho para o motor CFM56-5B foi desenvolvido utilizando o software *GasTurb*®, de maneira a estudar o impacto que o desempenho do compressor de alta pressão tem no desempenho global do motor. A modelação inicia-se por seleccionar um ponto de referência de operação, seguindo se a modelação em condições não nominais, onde o modelo é equiparado com o desempenho de um motor existente.

As ferramentas do *GasTurb*® permitem avaliar a condição de um motor, ao introduzir parâmetros do motor testado no software. Uma base de dados foi criada, utilizando VBA macros do Excel, para facilitar o processamento de dados e armazenar dados de desempenho de diferentes motores. Desta maneira, é possível identificar quais os componentes menos eficientes.

A tese foca-se no desempenho do compressor de alta pressão, e na diferença de desempenho quando são utilizados pás reparadas ou novas. Foi demonstrado que os compressores de alta pressão são mais eficientes, quanto maior for a percentagem de pás novas instaladas. O estudo desenvolvido realça a importância dos primeiros andares no desempenho do compressor.

Com o trabalho desenvolvido, a TAP M&E tem em seu poder, uma ferramenta que permite avaliar a condição de motores CFM56-5B, e ajudar os engenheiros de manutenção a optimizar os seus recursos de maneira a alcançar o desempenho desejado dos seus clientes.

Palavras-chave: Pás de compressor, Perda de desempenho, Motor Turbofan, Modelo de Desempenho, Manutenção, Ferramenta de decisão

Abstract

Gas turbines performance loss can be identified at the engine module level, in terms of reduction in the component mass flow and efficiency. The identification of the faults will facilitate and allow to focus the financial and human resources in an effective engine maintenance work scope.

In this thesis, a performance model for the CFM56-5B engines was developed using the gas turbine computer simulator *GasTurb*®, in order to study the impact that the high pressure compressor performance has on the overall performance of the engine. The modelling phase begins by selecting an appropriate cycle reference point, followed by the off-design, where the model is matched to the performance of an existing engine.

GasTurb® tools allow the assessment of the condition of an engine and its components, by inputting parameters of the tested engine in the software. A database using Excel VBA macros was created to ease the data processing and store the performance of different engines. This allows to identify which components of the engine that are at fault.

The thesis focus primarily in the performance of the HPC, and the difference in performance when using repaired or new blades. It was demonstrated that the HPC is more efficient when the percentage of new blades installed is greater. The developed study emphasizes the importance the first stages of the HPC have on its performance

With the work developed in this thesis, TAP M&E has been offered a decision making tool that can be used to evaluate the condition of the CFM56-5B engine components, and help the maintenance engineers to optimize the resources in time and cost to meet the desired engine performance of their customers.

Keywords: Compressor blades, Performance loss, Turbofan Engine, Performance Model, Maintenance repair, Decision making tool

Contents

List of Tables

List of Figures

Nomenclature

Greek symbols

α	Angle of attack (fig. 3.13); Flow angle in cascade terminology
β	Flow angle in rotor terminology
Δ	Variation
δ	Standard day pressure correction factor; Deviation angle
η	Efficiency
γ	Stagger angle; Heat capacity ratio
κ	Blade angle with meridional direction
μ	Dynamic viscosity
ρ	Density
θ	Standard day temperature correction factor
ϖ	Total pressure loss

Roman symbols

A	Facility Modifiers coefficients
c	Blade chord
C_D	Total drag coefficient
C_L	Total lift coefficient
C_{DA}	Annulus drag coefficient
C_{DP}	Profile drag coefficient
C_{DS}	Secondary drag coefficient
D	Drag
F	Force

F_N Net thrust

H Enthalpy

h Blade height

i Incidence angle

L Characteristic length; Lift

M Mach number

N Spool rotational speed

o Throat opening

P Pressure

PR Pressure ratio

R R-squared value; Reaction degree

Re Reynolds number

s Blade pitch

T Temperature

t Thickness

V Velocity

W Relative velocity; Mass flow

x x Cartesian coordinate

Subscripts

0 Total property

1 Parameter at blade inlet

2 Parameter at blade outlet

a Axial

ADJ Adjustment

amb Ambient temperature and pressure conditions

$ambStd$ Standard day ambient conditions

b Blade row

c Compressor

$corr$	Corrected value
f	Fuel
ind	Indicated value
is	Isentropic
LE	Leading edge
m	Mean
max	Maximum value
$read$	Measured value
s	Static conditions
stg	Stage
t	Turbine
TE	Trailing edge
th	Theoretical
$true$	Real value

Glossary

BPR Bypass ratio, is the ratio between the secondary and the primary airflow in a turbofan engine.

CBM Condition Based Maintenance is a maintenance strategy that monitors the actual condition of the asset to decide what maintenance needs to be done. CBM dictates that maintenance should only be performed when certain indicators show signs of decreasing performance or upcoming failure.

CDP Compressor Discharge Pressure is a seal after the HPC 9th stage, in which the airflow that goes through it, is directed to cool the LPT nozzle.

CMM Coordinate measuring machine is a device for measuring the physical geometrical characteristics of an object. This machine may be manually controlled by an operator or it may be computer controlled.

EASA European Aviation Safety Agency is an agency of the European Union with regulatory and executive tasks in the field of civilian aviation safety. Its responsibilities includes authorizing foreign operators, giving advice for the drafting of EU legislation, implementing and monitoring safety rules, giving type-certification of aircraft and components as well as the approval of organizations involved in the design, manufacture and maintenance of aeronautical products.

EGT Exhaust Gas Temperature is the temperature measured on the 2nd stage of the LPT. It is a key parameter in order to determine an engine health.

FAA Federal Aviation Administration is the national authority within the United States of America that regulates all aspects of civil aviation. These include the construction and operation of airports, the management of air traffic, the certification of personnel and aircraft.

FM Facility Modifiers and factors that correlate the performance of an engine in different test cells.

FRT Flat Rate Temperature is the temperature at which the EGT margin is kept constant due to reducing the maximum available thrust.

HD Hot Day is the Standard Day atmosphere with a temperature of a 30^{o}C.

HPC High Pressure Compressor, is a component of the engine.

IGV Inlet Guide Vanes are airfoils located at the HPC inlet that guide the incoming airflow. These airfoils are adjustable between different speed regimes.

LLP Life limited parts are parts in an engine that have a limited number of operating cycles or a specified time.

LPC Low Pressure Compressor, is a component of the engine, which in this thesis is described as Fan.

MBTA Model Based Test Analysis is the method that GasTurb uses to analyze the performance of engines.

MRO Maintenance Repair and Overhaul are facilities that perform maintenance actions in order to restore components performance.

NDT Non-destructive testing is a group of analysis techniques used in science and technology industries to evaluate the properties of a material, component or system without causing damage.

NGV Nozzle Guide Vanes are airfoils with a convergent shape.

OAT Outside Air Temperature, or static air temperature refers to the temperature of the air around an aircraft, but unaffected by the passage of the aircraft through it.

OEM Original Equipment Manufacturer, is a company that makes a part or subsystem that is used in another company's end product.

OGV Outlet Guide Vanes are airfoils in the secondary flow that straighten out the flow incoming from the fan.

OVH Overhauled is the definition for a part that has been removed, disassembled, cleaned, inspected, repaired as necessary and tested using factory service manual approved procedures.

TSFC Thrust Specific Fuel Consumption is the mass of fuel needed to provide the net thrust for a given period. It is used to describe the fuel efficiency of an engine design with respect to thrust output.

VBV Variable Bleed Valves are valves located between the booster and HPC, that control the primary airflow in low speed regimes, preventing surge to occur in the compressor.

VSV Variable Stator Vanes, are vane blades that can be adjusted to prevent stall to occur in the compressor.

Chapter 1

Introduction

A turbomachine is a machine that exchanges energy between the continuous flow of a fluid and a continuously rotating blade system. Energy can be transferred from the flow to the rotating machine components or vice versa. It includes among others, steam turbines and gas turbines. In aviation, the most used engine types are gas turbines. These can be turboprop, turbojet and turbofan. All of the mentioned are composed of at least one compressor, combustion chamber, and one turbine, the difference being the way they operate and how thrust is produced. Turboprops (illustrated in figure 1.1a) are gas turbines that have a mechanical gearbox connected to a propeller. Turbojets (illustrated in figure 1.1c) are the simplest form of gas turbines that produce thrust through the exhaust nozzle that accelerates the gases out of the back of the engine. Turbofans (illustrated in figure 1.1b) are similar to turbojets but the air is separated into two streams, the secondary and primary airflow. The fan in the front of the engine provides a great amount of the total engine thrust through its secondary nozzle. These are much more fuel efficient when compared to turbojets.

The aerospace industry has been the leader of gas turbine engines as illustrated in figure 1.2, where it is possible to verify the evolution of the maximum pressure ratio and maximum temperatures within gas turbines. Throughout the years, new designs and materials allowed to withstand greater firing temperatures and pressure ratios within the engine and maintaining reliability levels. With that increase, it was possible to obtain higher values of thermal efficiency in the thermodynamic cycle characterized as the Brayton Cycle. It is possible to see in figure 1.2c that the increase in pressure ratio increases the thermal efficiency when accompanied with the increase in turbine firing temperature. This is true to a certain limit, where it is possible to see that beyond certain values of pressure ratio, the gain in thermal efficiency is very small or none [2].

Turbofans are gas turbine engines that have a bypass airflow (secondary airflow). The air goes through the fan and is separated into two streams, the secondary and primary airflow. The secondary airflow goes through the fan, passes the outlet guide vanes (OGV) and leaves the engine. The primary airflow passes through the Booster and the High Pressure Compressor (HPC) where it is compressed, entering the combustion chamber where it is mixed with fuel and ignited. It then goes through the High Pressure Turbine (HPT) and Low Pressure Turbine (LPT) where the combustion gases are expanded

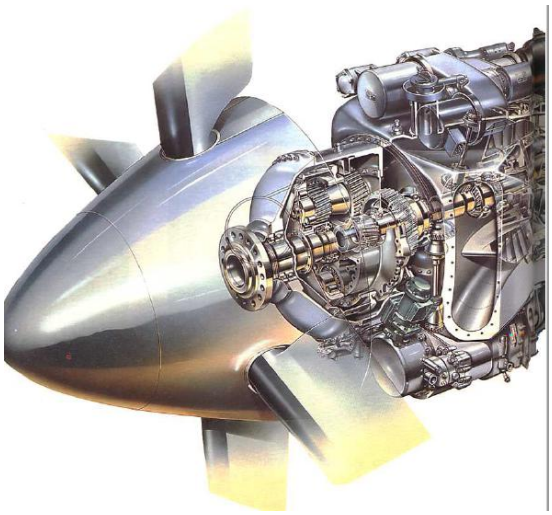

(a) Turboprop engine configuration

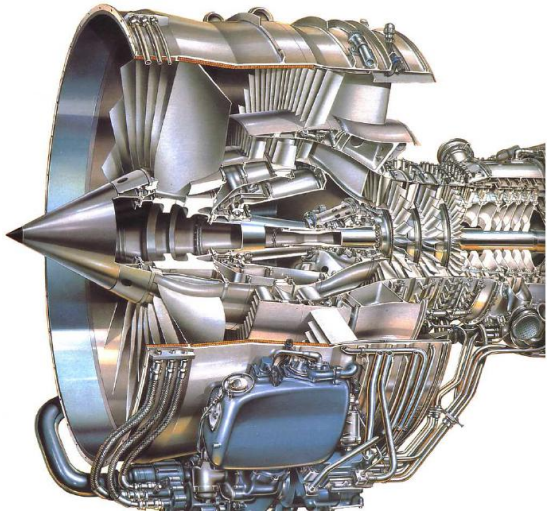

(b) Turbofan engine configuration

(c) Turbojet engine configuration

Figure 1.1: Aircraft engines configuration examples [1]

and finally exits the engine through a convergent nozzle. The majority of the produced thrust originates from the bypass flow. A schematic of a turbofan engine configuration is presented in figure 1.3.

The performance of Gas Turbines, specifically Turbofan engines depends on the efficiency of each engine component, that are the Fan, Compressor (Booster and HPC), Combustion Chamber and Turbine (LPT and HPT). A knowledge of the true state of each component is essential in order to evaluate its deterioration and, by doing so, to perform a CBM (Condition Based Maintenance) individually. This practice is an effective strategy to improve engine availability and reduce maintenance costs and failure hazards. With the continuous operation of the engine, deterioration affects the engine components and these become less and less efficient. To overcome the lower efficiency of the engine, fuel flow is increased in order to produce the same amount of thrust. The increase of fuel flow leads to a rise in the exhaust gas temperature (EGT) and thrust specific fuel consumption (TSFC). When a specified EGT limit is reached, the engine has to perform a shop visit in order to do a performance restoration where its parts are repaired and cleaned or replaced. The Maintenance, Repair & Overhaul (MRO) company and the customer agree to reach to a new EGT margin taking into account the best use of the financial resources. Usually it is installed a mix of repaired (which are also called overhauled blades) and new parts parts to restore the engine performance.

Although EGT is a very important parameter in the engine performance, it should be known in an engine, its individual components performance and the effect these components have on crucial parameters as EGT and TSFC. To have that knowledge, it is necessary to know how each of these components

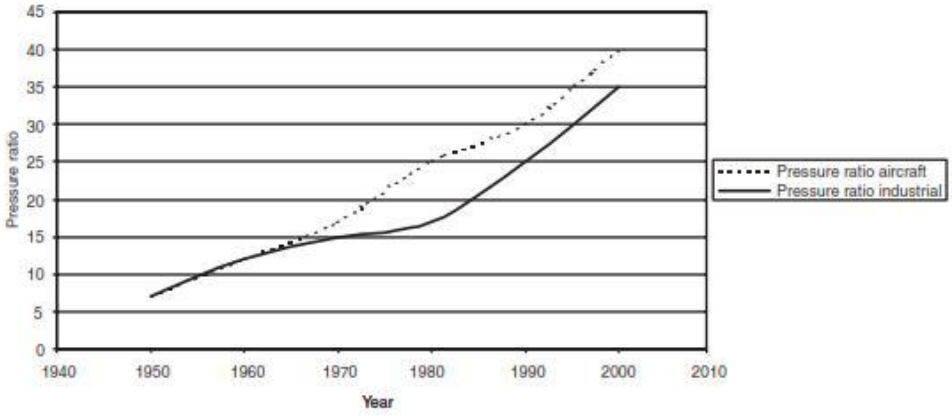

(a) Evolution of gas turbine engine pressure ratio

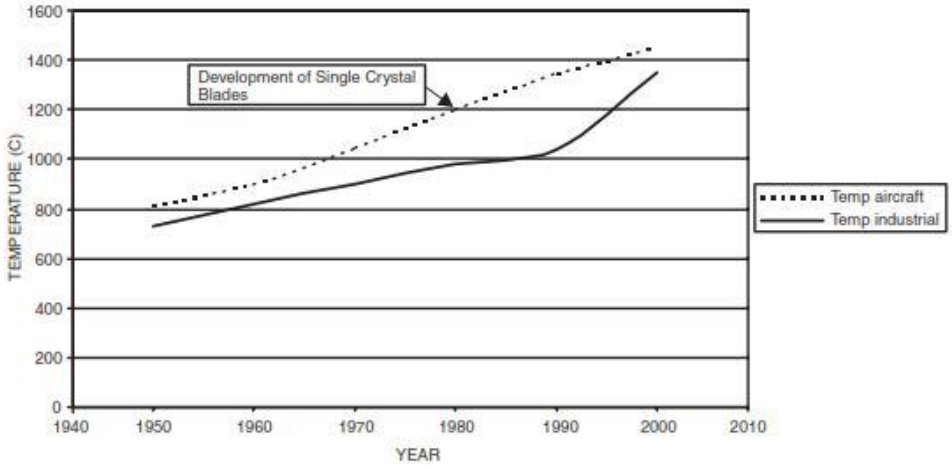

(b) Evolution of gas turbine engine firing temperature

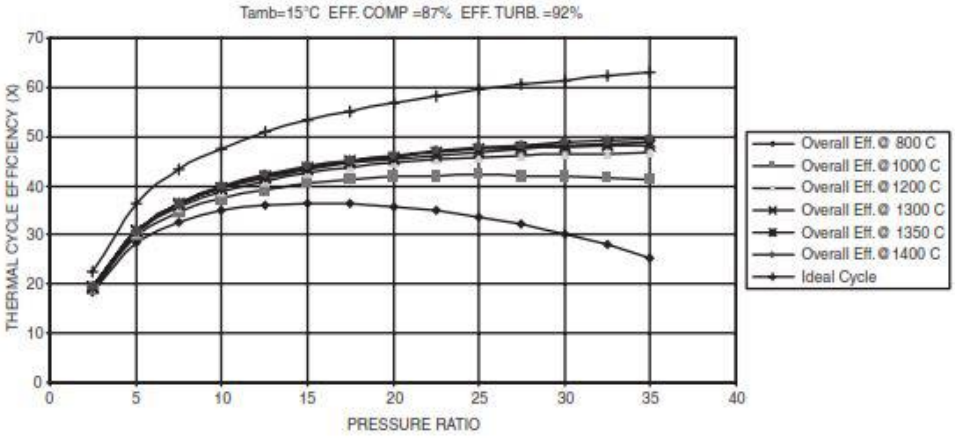

(c) Gas turbine engine overall efficiency

Figure 1.2: Gas turbine pressure ratio and firing temperatures impact on efficiency in the thermodynamic cycle [2]

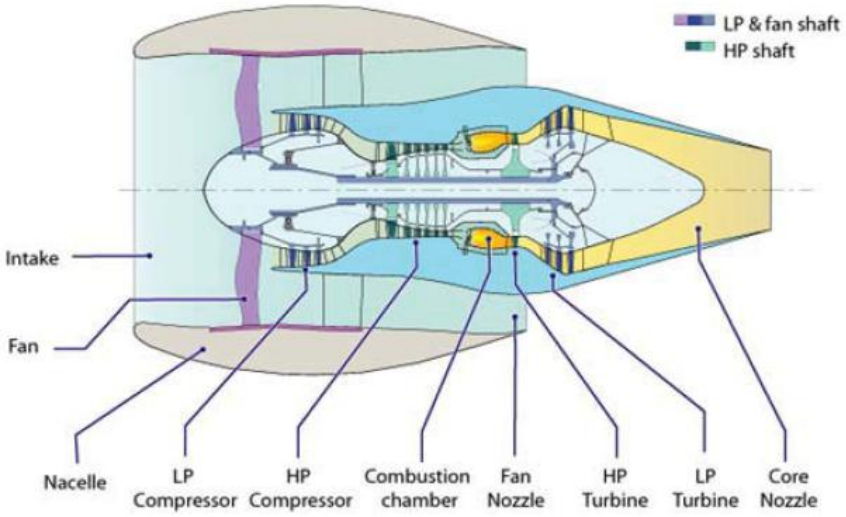

Figure 1.3: Turbofan engine schematic [3]

is expected to perform and only then it is possible to evaluate its performance.

Gas turbines have always been studied with the use of thermodynamic models. If the behaviour of an engine and its respective components is known, the maintenance and engineering teams of MRO companies can act accordingly to solve potential performance problems. *GasTurb*® is a commercial gas turbine computer simulator [4] that allows the user to model an engine for research and industry purposes. This software is currently on its 13^{th} version, however, the work developed in this thesis will be made using *GasTurb*® 11. The capabilities between versions are very much the same, the only major difference is the user interface.

1.1 Motivation

The increasing pressure on costs forces Maintenance, Repair and Overhaul (MRO) Companies, such as TAP M&E, to improve their repair processes and to carefully develop a strategy for its financial and human resources in the critical matters.

Throughout the years, maintenance practices have been facing an evolution process in order to remain competitive in the market, which can be easily noticed as the change from a time-based maintenance to a condition based maintenance. In this safety and economically sensitive business, where maintenance works can cost up to millions of dollars, MRO companies are forced to reduce costs as much as possible.

Gas turbines are very complex machines. Without a full knowledge of their performance, the impact that specific maintenance tasks have on the engine performance will not be understood.

1.2 Objectives

The main objective within this thesis evaluate the impact that the HPC has on the overall performance of the CFM56-5B engine. To aid that purpose, the existing model that TAP M&E possesses for the turbofan engine will be of crucial importance, however, this model proved unfit for performance studies, and so, a new model will be created. Within the objectives of this thesis, the following steps will be taken:

- The first step is to define the engine design-point and off-design operation points. This will be done using the software *GasTurb®*.
- Secondly, to develop a database using Excel Visual Basic (VBA) macros that will store the CFM56-5B engine components performance and provide a basis of comparison to other engines in the future. This will be accomplished using the Model Based Test Analysis (MBTA) tool that *GasTurb®* offers, that will allow to compare the engines performance with the developed model. The database will be of crucial importance because it will permit to compare components performance between different engines. This will help TAP M&E to identify potential problems in the future if an engine is rejected in a performance test, and so save valuable time in troubleshooting and also avoiding unnecessary costs.
- Regarding the HPC, it will be studied the effects that an improvement in its efficiency has on the overall performance of the engine. This will be done using the MBTA and Modifiers tool in *GasTurb®*. HPC blades have a set of geometric parameters that will define the aerothermodynamics performance of the compressor. With the use of empirical formulas, an attempt to relate the HPC efficiency with the use of OVH and new blades is made.
- An analysis to the HPC stages will be accomplished to understand which stages affect the HPC performance the most and why.
- Lastly, a cost analysis will be done to HPC rotor blades in order to understand its financial impact.

1.3 Thesis Outline

An introduction of aircraft engine maintenance concepts, TAP M&E facilities and a description of the CFM56-5B engine is given in chapter 2. A brief description of the compressor, types of deterioration and control and repair of compressor blades in TAP M&E is mentioned in the same chapter.

In chapter 3 it is described the loss sources and mechanisms in axial flow compressors, with emphasis in the entropy production in boundary layers and mixing processes. It is also depicted the effect that non-recoverable deterioration has on the compressor performance.

The modelling of the CFM56-5B engine is made in chapter 4, beginning with a description of the exhaust gas temperature, the correlation test report and a brief introduction to *GasTurb®*. The modelling initiates with the cycle reference point, followed by the off-design and lastly, the verification and validation of the model.

In chapter 5 the *GasTurb*® tools are applied to the the model, in order to study the effect that component deterioration has on the overall engine performance. Various engine tests were analysed using *GasTurb*® and the results were stored in an Excel file that will allow to compare the performance between engines. It was also studied the effect that an increase of the compressor efficiency has on the performance of the tested engines.

In chapter 6 it was studied the effect that compressor blades have on the performance of the compressor itself, and an analytical study was conducted to understand why the first stages are more important in the compressor performance.

In chapter 7, a maintenance, performance and cost analysis was accomplished. Two test cases were used as an example of the benefit that the *GasTurb*® tools can have in the evaluation of component performance. A maintenance and cost analysis was also accomplished to the various engines analysed with *GasTurb*®.

In the last chapter the conclusions of the work developed in this thesis are presented.

Chapter 2

Maintenance Concepts, MRO Facilities and the CFM56-5B Engine

Commercial aircraft maintenance costs can be divided into three main areas: airframe, engines and components. These three areas represent the majority of an aircraft's maintenance exposure over its service life, although engine maintenance costs will often represent the most significant, and consequently will have an important impact in the market of commercial flights. As it can bee seen in figures 2.1a and 2.1b, engine maintenance costs represent 35% to 40% of the total maintenance costs. These costs grow as time on-wing increases, since the level of deterioration that affects the engine is greater. Nonetheless, engines have to spend as much time as possible on-wing in order for the airlines operations to be profitable.

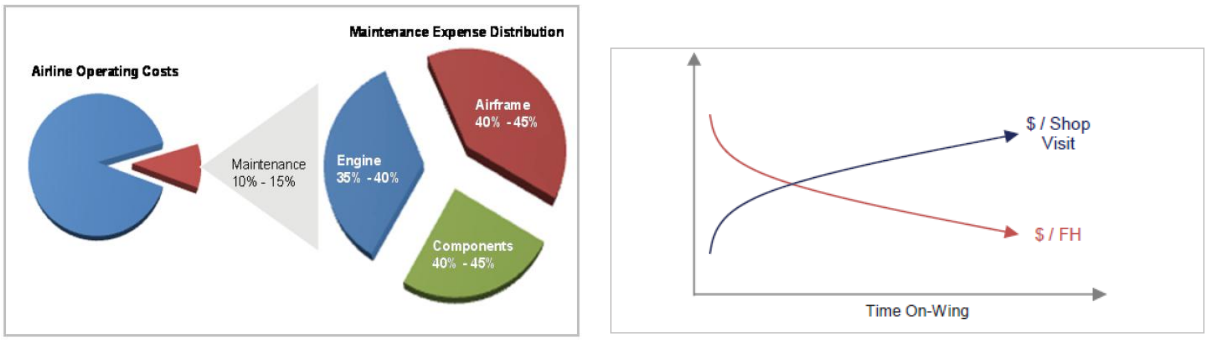

(a) Maintenance costs distribution

(b) Engine time on-wing vs costs

Figure 2.1: Engine maintenance costs [3]

When an engine comes to a shop visit, its maintenance works can be of two types:

- Performance Restoration: The components parts deteriorate due to heat, erosion and fatigue. This type of deterioration affects the engine core the most. During the continuous operation of the engine, its EGT increases constantly, causing an accelerated wear of the parts, thus decreasing further the engine performance. A critical EGT is established by the engine manufacturer and, before the engine reaches that limit, performance restoration works must be accomplished;

- Life Limited Parts Replacement (LLP): The rotating compressor and turbine shafts and disks have a defined operating life. When it is reached, these parts must be replaced and never used again.

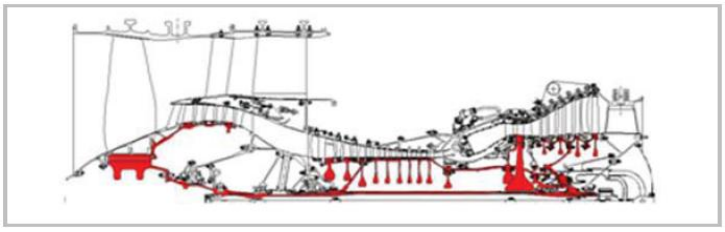

Figure 2.2: Life limited parts of a turbofan engine [3]

This thesis will only focus on performance restoration.

2.1 TAP Maintenance and Engineering

TAP Maintenance & Engineering is a global MRO solution provider for Airbus, Boeing and Embraer. The MRO services ranges from airframe, engines and components:

- $Care^2 Airframe$: It includes from light to heavy maintenance, TAP M&E covers pre-flight, transit and daily checks, troubleshooting and engine trend monitoring;
- $Care^2 Components$: It incorporates overhaul, repair, test, and modification for more than 15,000 components equipping Airbus, Boeing and Embraer fleets and their engines. This includes line-replaceable units and landing gears;
- $Care^2 Engines$: It includes MRO services to commercial and military aircraft engines. The Turbofan engine centre is located in Lisbon, Portugal, while the Turboprop engine centre is located in Porto Alegre, Brazil. ;
- $Care^2 Engineering$: Provides customised maintenance solutions and technical services that includes:
    1. CAMO (Part M): Full Continuing Airworthiness Management services;
    2. Design Organization Approvals, DOA (Part 21): Airframe and engine repair modifications;
    3. Technical labs: NDT, Physical & Chemical and Calibrations.

Based in Portugal and with two main centres in Brazil, it comprises a total workforce of about 4,000 employees. The facilities in Portugal are located in Lisbon and offer a vast span of services ranging from line maintenance to heavy maintenance checks, engine overhaul, components maintenance, engineering and planning services, material support and integrated maintenance packages for Airbus A300-600, A310, A330, A340, A320 family and for engine models CFM56-3, -5A, -5B, -5C, -7B and CF6-80C2.

At TAP M&E engine shop, the work scope can be of the type of preventive maintenance or corrective maintenance. Although for this thesis, it is only of concern the performance parameters, it is possible that

the engines perform maintenance of both types, but in general, preventive maintenance is the common case since this type of maintenance allows to develop time plans in coordination with the operation of the engine.

TAP Test Bed Description:

On completion of the maintenance works and assembly of the engine, every engine must be tested before being installed on wing to ensure that it meets the contractualized performance. Test Bed facilities can be of two types: high altitude test cells or sea-level test cells. In sea-level test facilities, these can also be of two different types:

- Outdoor test facility;
- Indoor test facility.

(a) Outdoor test facility [5]

(b) Indoor test facility of TAP M&E [6]

Figure 2.3: Engine test facilities

At TAP M&E the test cell facility is of the sea-level indoor type (illustrated in figure 2.3b), where the engine runs at ambient temperatures and pressure conditions. The resulted performance is corrected to the International Standard Atmosphere (ISA) sea-level conditions as described in section 4.2. In figures 2.3a and 2.3b the two types sea-level of test cells are illustrated.

The engines are tested to a flight evaluation test schedule that covers characteristics as anti-icing, combustion and reheat efficiencies, performance, mechanical reliability, oil and fuel consumptions at the variety of speed conditions to which the engine is subjected during its operational life [1]. Within this variety of test characteristics, it will only be of concern for this thesis the performance of the engine since the performance variables are the ones that are possible to control and evaluate in *GasTurb*®.

The TAP M&E test cell is a large state of-the-art test facility having a cross section of approximately 9.75$\times$8.65m. Its configuration is of the “L” type as illustrated in figure 2.4. The facility uses a down-draft inlet with turning vanes as it can be seen on the left side of figure 2.4. The incoming flow passes through noise reduction splitters and a bird screen before entering the cell working section. Exhaust gases pass in a cylindrical augmenter with a diffuser section and then upwards through a folded vertical exhaust stack [7].

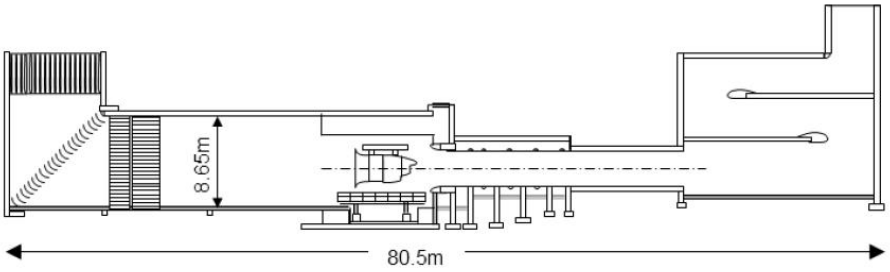

Figure 2.4: Schematic of the test cell of the ”L” type [6]

2.2 The CFM56-5B Turbofan Engine

The CFM56 engine is manufactured by CFM International and is a high-bypass turbofan engine. CFM is the association of two major aircraft engine manufacturers, Safran Aircraft Engines (formerly known as Snecma) from France and GE Aviation from USA. The name CFM56 is derived from both companies commercial engines designations: GE's CF6 and Snecma's M56. It made its first run in 1974 and 7 years later and approximately 1 billion dollars of investment, the FAA and the European civil aviation authority (currently EASA) issued the type certificate for the engine [8]. Almost 40 years later and the CFM56 is one of the most widely used turbofan engines in aircrafts. It has been developed into 4 variants as summarized in table 2.1

Model	Thrust (lbf)	BPR	Applications
CFM56-2	22,000 - 24,000	6	Douglas DC-8-70
CFM56-3	20,000 - 23,500	5.9 - 6.0	Boeing 737
CFM56-5	22,000 - 34,000	5.4 - 6.6	Airbus A319, A320, A321
CFM56-7	18,500 - 27,300	5.1 - 5.6	Boeing 737

Table 2.1: CFM56 models [9]

Within the CFM56-5 model, different engine rates are available. The engine that will be modelled in chapter 4 is a CFM56-5B3, that has a bypass ratio (BPR) of 5.3 and produces approximately 32,000lbf of thrust.

The CFM56-5B exists in 9 different versions and it can power every model in the A320 family (A318, A319, A320, A321). Throughout the different versions, thrust varies from 22,000lbf up to 34,000lbf with different BPR (ranging from 5.4 up to 6.6) and overall pressure ratios (ranging from 32.6 up to 35.5). These are all reference values and will differ from engine to engine.

All aircraft engines are composed by many parts, all which play an important role in this complex thermodynamic machine. For simplicity, it will only be mentioned in its constitution the modules and subsequent parts that are relevant to the aerothermodynamic operation of the engine. A more detailed description of the engine is available in reference [10]. It is constituted by 4 major modules:

- Fan Major Module
- Core Engine Major Module

- Low Pressure Turbine Major Module
- Accessory Drive Module

For a better understanding of the engine composition, figure 2.5 illustrates the CFM56-5B in a cut view.

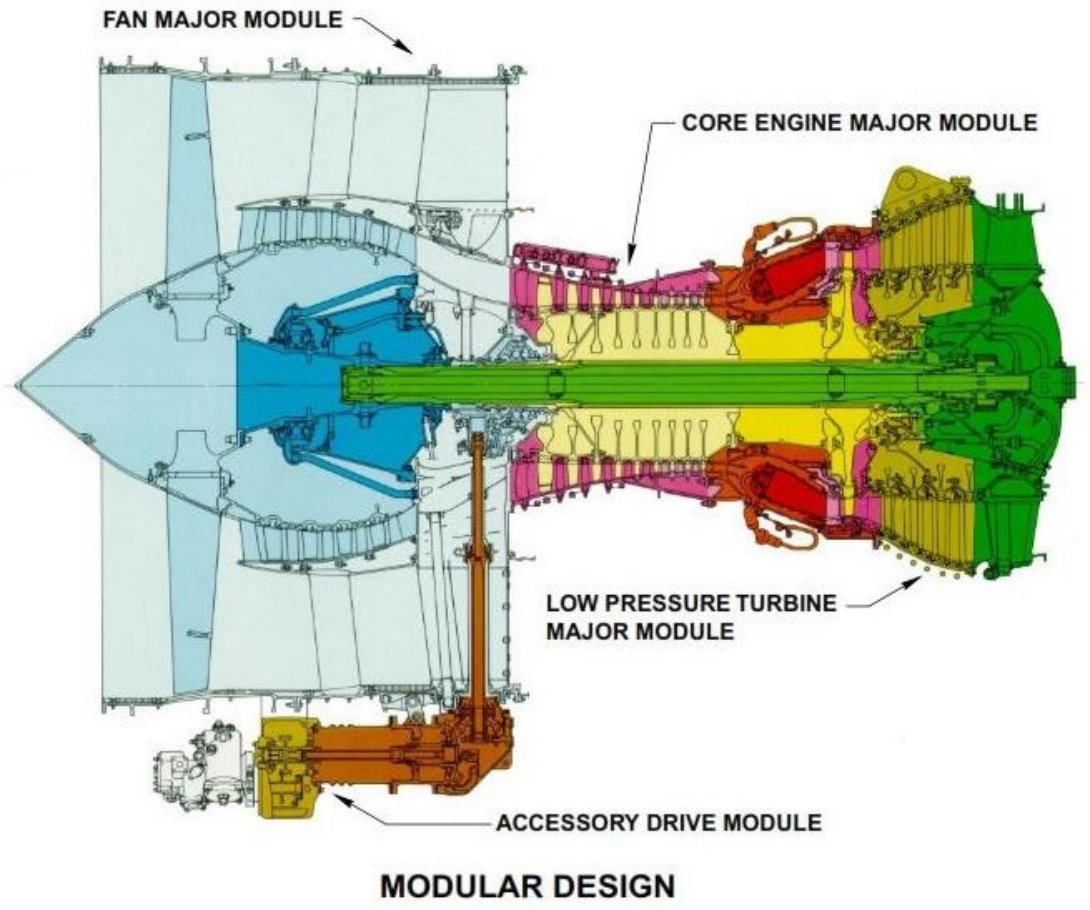

Figure 2.5: CFM56-5B cut view [10]

The Fan Major Module is part of the Low Pressure section of the engine and it consists of:

- Single stage fan rotor, constituted by 36 titanium alloy blades;
- Four stage axial booster (4 rotors and stators). The booster rotor is coupled to the fan and to the LPT rotor;
- Fan frame is the structure that supports the Fan, booster and HPC shafts bearings, which in turn support the rotors;
- Outlet Guiding Vanes (OGV), that guide the secondary flow;
- Variable Bleed Valves (VBV), located circumferentially in the Fan frame between the booster and the HPC. These valves control the primary airflow in low speed regimes and by doing so, prevent surge to occur in the compressor.

The Core Engine Module is the High Pressure section, and it is composed by:

- High Pressure Compressor (HPC), which has 9 stages (9 rotors and stators) and the HPC rotor is coupled with the HPT rotor;
- Single stage inlet guide vane (IGV), that guides the primary airflow into the HPC;
- Combustion chambers, where the compressed primary airflow is mixed with fuel and ignited;
- High Pressure Turbine and the first stage of the Low Pressure Turbine (LPT). The HPT is a single stage turbine.

The Low Pressure Turbine Module completes the Low Pressure section of the engine and is composed by:

- Low Pressure Turbine (LPT), which has 4 stages;
- Turbine rear frame, that supports the LPT and HPT shafts bearings.

The engine has a weight of 2,391kg and a length of 2.94m. The CFM56-5B was an improvement to the CFM56-5A series. In 2008, CFM developed a tech insertion program to upgrade the core performance of the engine, where the arfoils of the HPC and HPT were redesigned. According to the manufacturer, the CFM56 Tech Insertion Program is designed to provide operators a longer time on wing through an equivalent 15ºC-20ºC additional EGT margin, up to 5% lower maintenance costs through enhanced durability and up to 1% better specific fuel consumption [10].

2.2.1 Thermodynamic Stations

The nomenclature used in the locations of the engine at TAP Test Bed differs from the one that is used in *GasTurb*®. Whenever a thermodynamic station is mentioned, it will always be in reference to the *GasTurb*® nomenclature, except in the cases where that specific station does not exist in *GasTurb*®, e.g., the case of station 49.5, that is the station where the EGT is measured. In figure 2.6 it is presented the *GasTurb*® nomenclature. In table 5.2 is presented the description of the numbers preceded by a letter ”T”, which signifies temperature, or ”P”, which signifies pressure.

Some stations are instrumented with temperature and pressure sensors in order to have information about the performance of the different components. To completely isolate a component it would be required to have temperature and pressure sensors immediately before and after the component. On the other hand, a sensor is also a potential hazard to the engine in the sense that it can break loose and do irreparable damages. TAP M&E opts to only have the necessary sensors to evaluate the overall performance of the engine in order to reduce the risk of damaging the engine. This risk management policy also has some drawbacks, as it can be difficult to do troubleshooting without having measurements that can permit to assess the condition of the individual components.

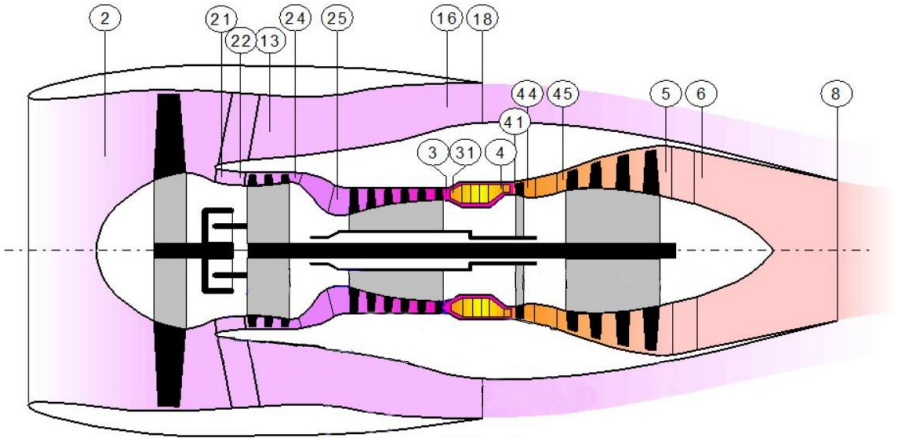

Figure 2.6: Thermodynamic stations in *GasTurb*®

2.2.2 High Pressure Compressor Description

The High Pressure Compressor (HPC) is a very complex component that is constituted by many parts. In this section it will be provided only its basic composition. The HPC is constituted by two main parts: the rotor and the stator.

The HPC rotor is a 9 stage axial flow compressor which comprises a total of 590 blades. Stages 1 to 3 are made of a titanium alloy and stages 4 to 9 are made of a nickel alloy. Close to the tip, on the concave side, the blades are coated with tungsten carbide to limit erosion. Between the rotor blades and the annulus wall, a tip clearance exists, which is usually of the order of 1% of the blade height.

The HPC stator is composed by an inlet guide vane (IGV), variable stator vanes (VSV) in stages 1 to 3 and fixed Stator Vanes from stages 4 to 9. Between the stator and the compressor hub is located a labyrinth seal to limit the leakage jet from the mainstream. A similar seal exists downstream of stage 9, that is called compressor discharge pressure (CDP). Through the CDP seal flows the air mass flow that cools the HPT nozzle guide vanes (NGV), HPT rotor blades and the LPT nozzle. The leakage jets from the rotor tip clearance and the stator labyrinth seal are one of loss sources of the compressor that will be discussed in the next chapter.

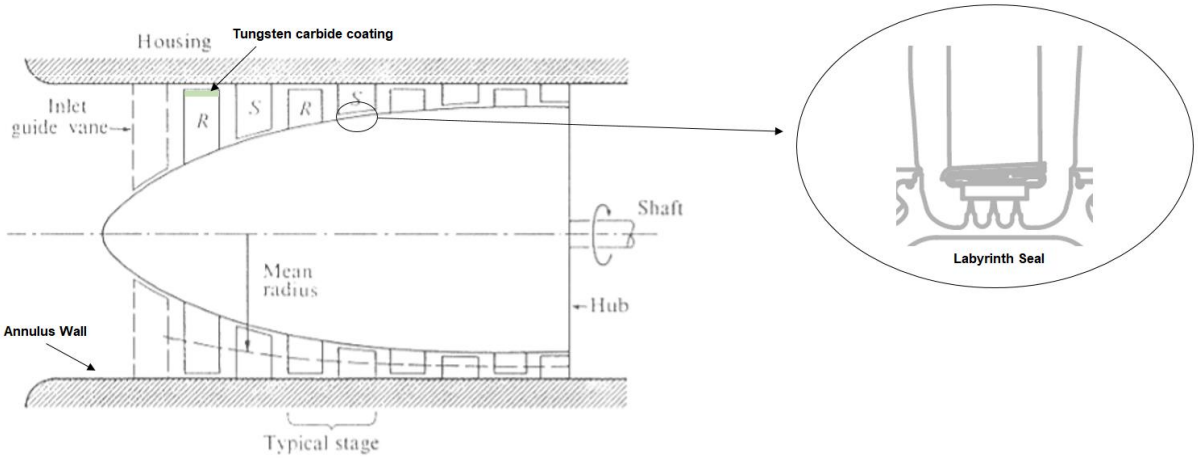

Figure 2.7: HPC schematic [11]

Chapter 3

Aerothermodynamics and Loss Sources of Axial Compressors

In this chapter it will be discussed the mechanisms responsible for losses in axial compressors. Some of the concepts are very complex and have been studied thoroughly, however, it is only meant to be described in this chapter the general concepts to understand these loss sources. Many correlations have been developed to help designing turbomachines, however, caution must be taken when using such correlations. A good physical understanding of the origins of loss may be more valuable than a quantitative prediction [12].

Loss is defined in terms of entropy increase. The sources of entropy are, in general: viscous effects in boundary layers, viscous effects in mixing processes, shock waves and heat transfer. It is assumed subsonic and adiabatic conditions, as such, only the first two sources of loss are of interest. Viscous shearing occurs wherever velocity gradients exist. In axial flow compressors velocity gradients will exist in boundary layers on the blades, annulus walls and in mixing processes. Figure 3.1 illustrates the different loss mechanisms present in axial-flow compressors.

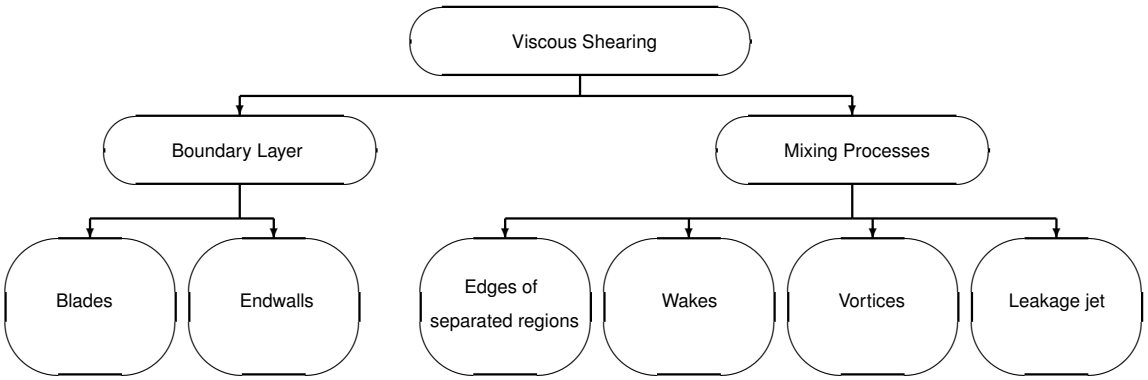

Figure 3.1: Diagram of loss mechanisms in axial flow compressors [13]

Howell [14] categorized the losses in compressors in three different groups:

- Annulus losses;
- Secondary losses;
- Profile losses.

Annulus losses appear due to the boundary layers that develop in the compressor wall annulus. Secondary losses are associated with the vorticity of secondary flows. This is a similar phenomenon to what happens in a finite wing. Lastly, profile losses are related to the boundary layers that develop in the compressor blades [11]. In figure 3.2 it is presented a graphic that illustrates the stage efficiency as a function of the flow coefficient and the losses considered. Annulus losses represent approximately 2.2%, secondary losses 4.4% and profile losses 4.2%. These losses tend to increase with engine operation, as erosion reshapes the annulus walls and compressor blades. As mentioned in section 3.2, some of the performance is restorable. In the case of the compressor blades, these can be repaired or replaced by new ones.

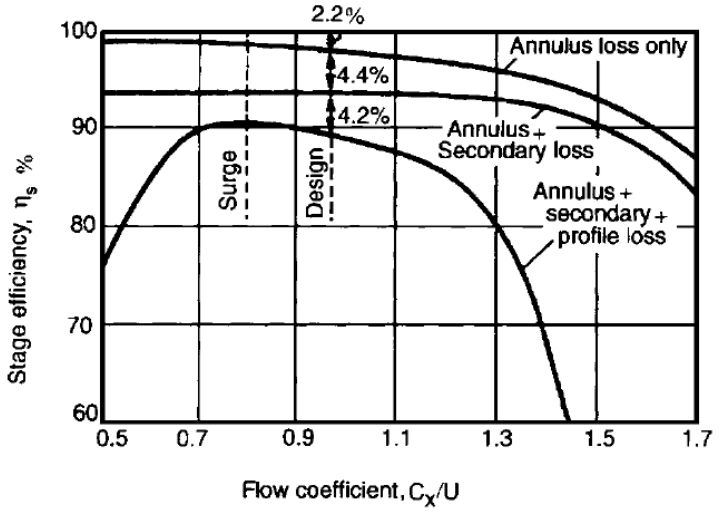

Figure 3.2: Losses in a compressor stage [15]

3.1 Entropy Production in Boundary Layers and Mixing Processes

Due to the viscosity in fluids, shear stresses occur that oppose the motion of the fluid, which in turn increase the internal energy and entropy of the fluid. The boundary layer mass-flow flows from the blade wall and enters the wake region. The wake formed on the trailing edge of the blade is a consequence of the mixing process between the flow of the airfoil pressure and suction side. Figure 3.3a illustrates this concept.

In the case of low incidence and low turbulence intensity, the two-dimensional boundary layer is formed near the leading edge, and at point 2 transits from laminar to the turbulent regime, as seen in Figure 3.4(c). At point 3 it becomes fully turbulent and in that region a very thin laminar sublayer

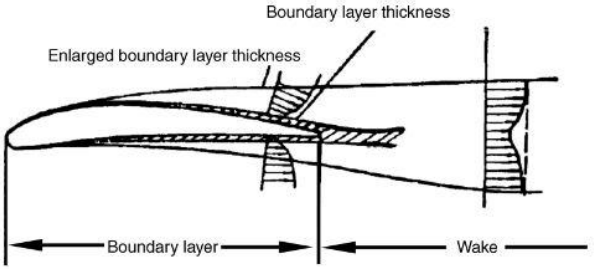

(a) Boundary layer flow on blade profile surfaces [16]

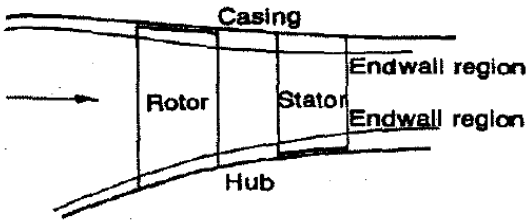

(b) Annulus boundary layer representation [13]

Figure 3.3: Boundary layer representations in an airfoil and annulus wall

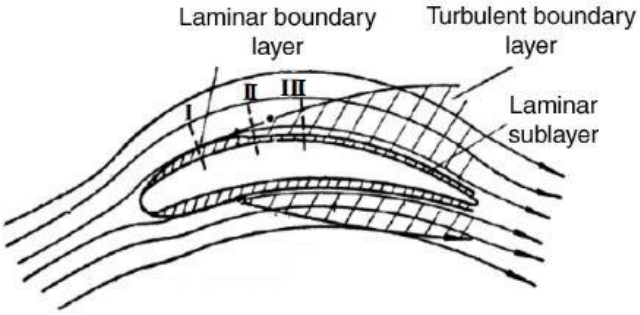

(a) Nature of the two-dimensional boundary layer regimes

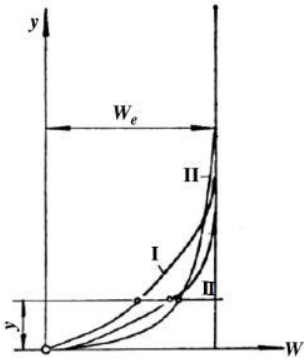

(b) Boundary layer velocity distribution

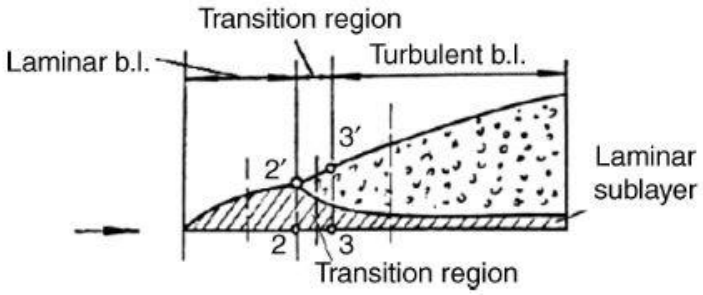

(c) Boundary layer transition region

Figure 3.4: Boundary layer formed on a compressor blade airfoil [16]

coexists. The velocity distribution in the normal direction to the flow of the three different regimes is also illustrated in figure 3.4(b) [16]. With the increase of the flow angle relative to the blade, i.e., greater incidence angles, the transition point moves closest to the leading edge until it reaches a point where the flow will separate and stall occurs. During this condition the entropy increases rapidly due to the high shear stresses. A similar phenomenon occurs on the endwall regions of the compressor, however it is much more difficult to analyse due to the complexity of the interactions with the mixing processes and the boundary layer.

Relatively high rates of shearing occur in wakes at the edges of separated regions, in vortices and in leakage jets. Since these are usually associated with turbulent flow, the local entropy creation rates are considerable. Due to the tip clearance between blades and the compressor annulus, the mass flow that passes through that gap possesses different velocity when compared with the mainstream, both in magnitude and direction, and a vortex is formed at their interface as illustrated in figure 3.5a. A similar

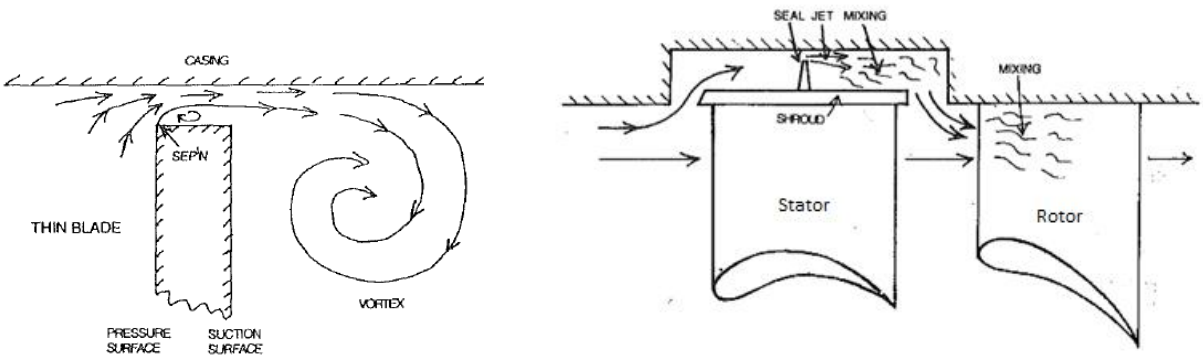

(a) Tip clearance leakage flow

(b) Flow over a shrouded tip seal

Figure 3.5: Losses in a compressor due to mixing processes [12]

phenomenon occurs with the mass flow that passes through the labyrinth seals between the stator and the compressor hub. When the fluid is re-injected into the main stream, the difference in velocity will generate further mixing loss as illustrated in figure 3.5b.

3.2 Types of Deterioration

During operation, the performance of each component in a gas turbine engine gradually deteriorates. This deterioration can be categorized into three different groups [17]:

- Recoverable Deterioration
- Non-Recoverable Deterioration
- Permanent Deterioration

The first one is caused essentially due to fouling and can be partially or totally recovered with washing. This deterioration leads to a continuous increase of the EGT as illustrated in figure 3.6.

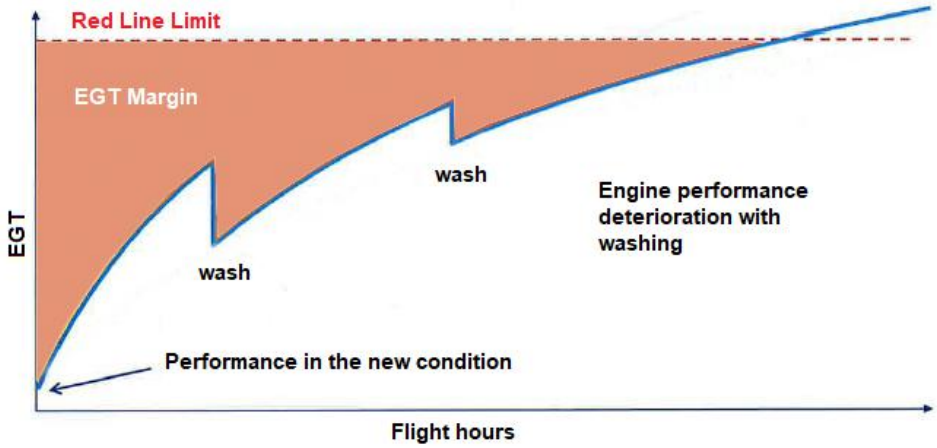

Figure 3.6: EGT margin restoration with washing

At the same time, the non-recoverable deterioration occurs due to surface erosion, airfoil roughness, corrosion and tip clearance increases. This type of deterioration cannot be recovered with washing and

it is the reason why washing has less effect in restoring the EGT with increasing operational times. The non-recoverable deterioration will depend upon the operational environment of the engine. In figure 3.7 it is possible to verify how the operational parameters and environment can affect the EGT.

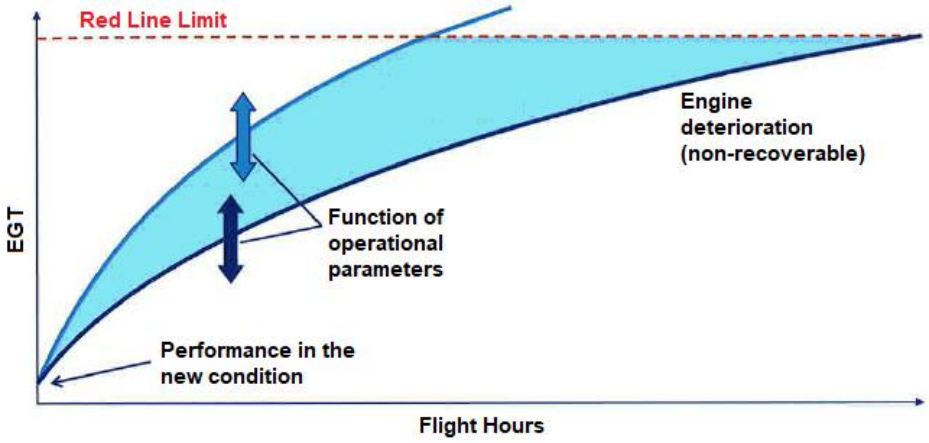

Figure 3.7: EGT margin as a function of the operational environment

A physical illustration of this type of deterioration can be seen in figures 3.8 and 3.9. Solid particles in the air, either ingested along the air flow or by-product of combustion (the latter will only affect turbine blades) experience different flow paths due the differences in their inertia. Depending on their size and weight, the solid particles tend not to follow the flow in the blade passage and impact on the blade surface along the stage channel height. This erosion manifests mainly with a reduction of the blade chord, height, bluntness of leading edge and a general increase in the blade surface roughness [18], however, it does as well alter a variety of other geometric properties that will be discussed in section 3.4.

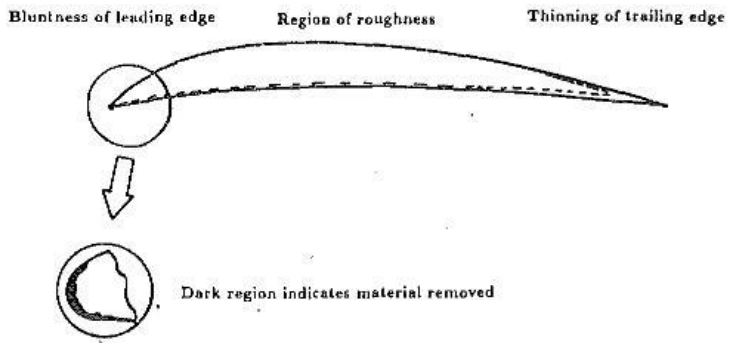

Figure 3.8: Airfoil from a compressor blade [19]

Finally, the permanent deterioration is characterized by casing and airfoil distortion [17]. In this thesis, the main focus will be in the non-recoverable deterioration caused by surface erosion which is responsible for altering the airfoil shape. This type of deterioration cannot be recovered unless the defective parts are repaired or replaced.

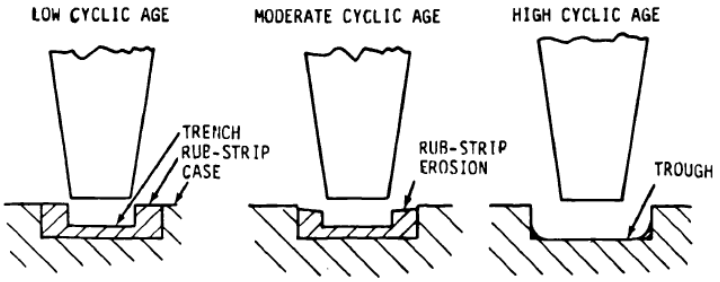

Figure 3.9: Tip clearance increase due to erosion [18]

3.3 Control and Repair of HPC Blades Geometric Parameters

Because TAP M&E engine department core business is maintenance, it is counter-productive to measure the various geometric properties of all the blades of a compressor, considering that this would have to be done manually and would consequently delay maintenance works. For investigation purposes, these measurements would be desirable, however, because it is not possible, the only geometric property that is currently possible to control is the airfoil chord, in which the blade is placed in a Go/NoGo tool to verify if its chord is within the minimum limits (illustrated in figure 3.10). Be that as it may, this tool does not give any indication of the actual chord and no documentation is generated. Difficulties arise when attempting to correlate any geometric property with the HPC performance. The solution is to venture in another direction, more concretely, to investigate if there could be a possible relation between the HPC performance and the use of OVH and new blades.

Regarding the HPC of the CFM56-5B engine, it is known that the repair processes are limited within the different stages. The first three stages are made of a titanium alloy, that is not repairable in chord extension due to the difficulties of the weld process. From stage 4 to 9, this restrain does not exist and so these stages can fully repaired.

(a) Go/NoGo tool of the HPC blades for all stages

(b) Side view of the Go/NoGo tool

(c) HPC blade Measurement in the Go/NoGo tool

Figure 3.10: Go/NoGo tool of the HPC blades

3.4 Non-Recoverable Deterioration in HPC Blades and Effect on Performance

As mentioned earlier, during an engine time on service, its components are exposed to a large number of deterioration effects that leads to a variety of changes in the blade airfoils, specifically in the HPC. These effects of wear include:

- Erosion on pressure and suction surfaces;
- Chord length reduction;
- Deformation of leading and trailing edges;
- Variation of stagger angles;
- Increase in tip clearances.

Marx *et al.* [20] conducted a statistical analysis on two full ex-service HPC blade sets. These engines had at the current moment of disassembling approximately 5,000 and 3,200 cycles since the last shop visit. The composition of each individual blade set were arbitrary (a mix of OVH and new blades), which is common for engines that have received at least one shop visit. Over 1,400 overhauled (OVH) blades and 300 new blades were scanned to account manufacture variations. After being digitalized with a 3D scanner, a CAD model for each blade was generated. In figure 3.11 is illustrated the variations of each specific parameter for all stages (averaged variations of all the blades of each stage) along the HPC channel height (h/H). A value greater or lower than 100% indicates that that property is above or under the geometry of the new condition and equal to 100% indicates that it is equal to a blade in the new condition. In figure 3.11a, a noteworthy change can be identified regarding chord length, beginning in stage 7 and further downstream, as well as maximum profile thickness and stagger angle in figures 3.11b and 3.11d. However, an increase in chord length is implausible regarding deterioration effects and could be explained by leading edge/trailing edge weld extension repair. Relatively to the leading edge radius and leading edge thickness (figures 3.11c and 3.11e), it can be seen that, although it is more distinguished in the downstream stages, significant variations in the first stages were verified. Nonetheless, the author concludes that it is possible that some span-wise and stage-wise trends of deterioration may have remained undetected due to the lack of documentation of the parts.

Reitz *et.al* [21], [22] studied the influence that the variation of the previous geometric properties will have on the HPC performance, by applying standard deviations to each property and taking into account that some properties are inter-connected, e.g., the leading edge radius and thickness. The results of this analysis can be seen in figure 3.12.

It is possible to verify that the leading edge thickness is the geometric property that most affected the rotor loss coefficient, followed by the blade chord and stagger angle (γ in figure 3.13b). In compressor rotor blades, the incidence angle is positive. Blades are designed to operate in the optimum incidence angle, i.e., the angle at which the losses are minimum, and so, small variations in the incidence angle will lead to an increase in blade profile losses. Reitz *et.al* [21], [22] concluded that decreasing the stagger

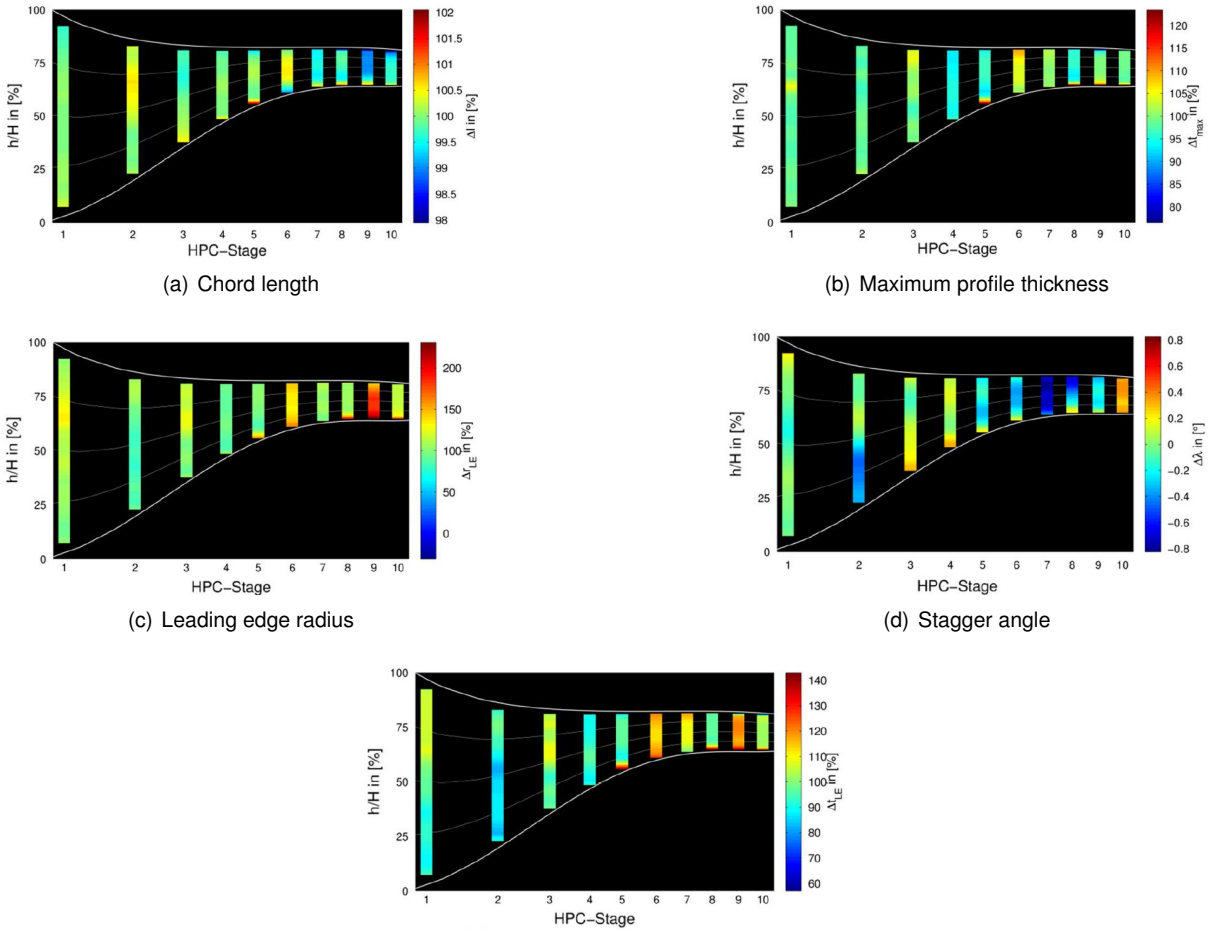

(a) Chord length

(b) Maximum profile thickness

(c) Leading edge radius

(d) Stagger angle

(e) Leading edge thickness

Figure 3.11: Overall HPC deterioration [20]

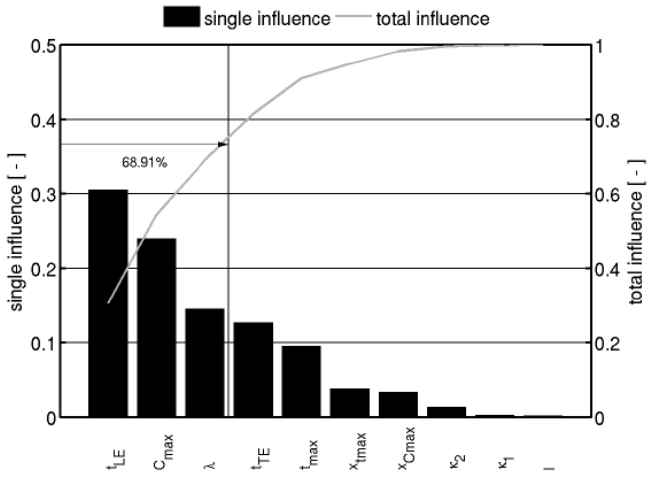

Figure 3.12: Pareto chart of the rotor loss coefficient at the 1st stage [22]

angle will strengthen the losses. Deviations in the incidence angle for blades that operate with positive incidence angles will lead to an increase in the loss coefficient, as seen in figure 3.13a.

These results indicate that regarding compressor performance and blade deterioration, it should be taken into account the various geometric properties, specifically those with respect to the leading edge.

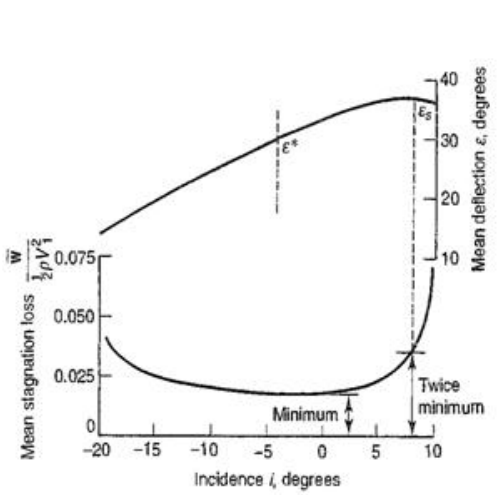

(a) Stagnation pressure loss as a function of incidence angle [23]

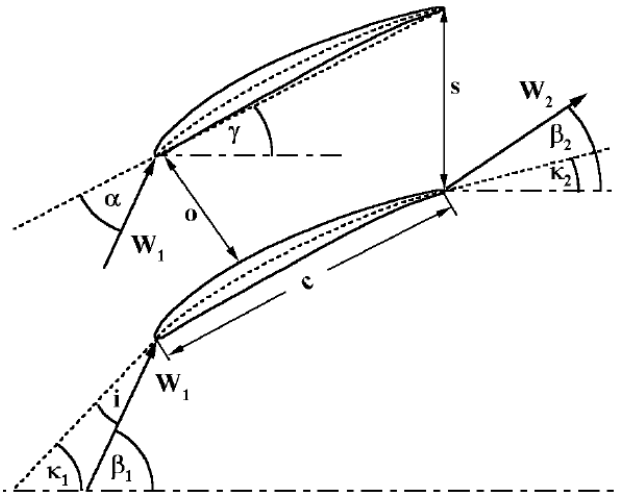

(b) Compressor blade cascade geometry [24]

Figure 3.13: Incidence angle and compressor blade cascade geometry

However, because this is not yet possible at TAP M&E, it will only be made reference to the blade chord, since this is the geometric variable that is possible to control as mentioned in section 3.3.

Tabakoff *et al.* [19], studied the influence that the HPC blade chord erosion of different stages will have on the overall HPC performance. It is visible in figure 3.14 that the erosion of the first stage resulted in a reduced mass flow and pressure ratio, while the erosion of stage eight had insignificant impact in the performance of the compressor. A similar result was obtained in the work of Martins [25], where it was compared the influence of the first three stages with the overall efficiency of the compressor.

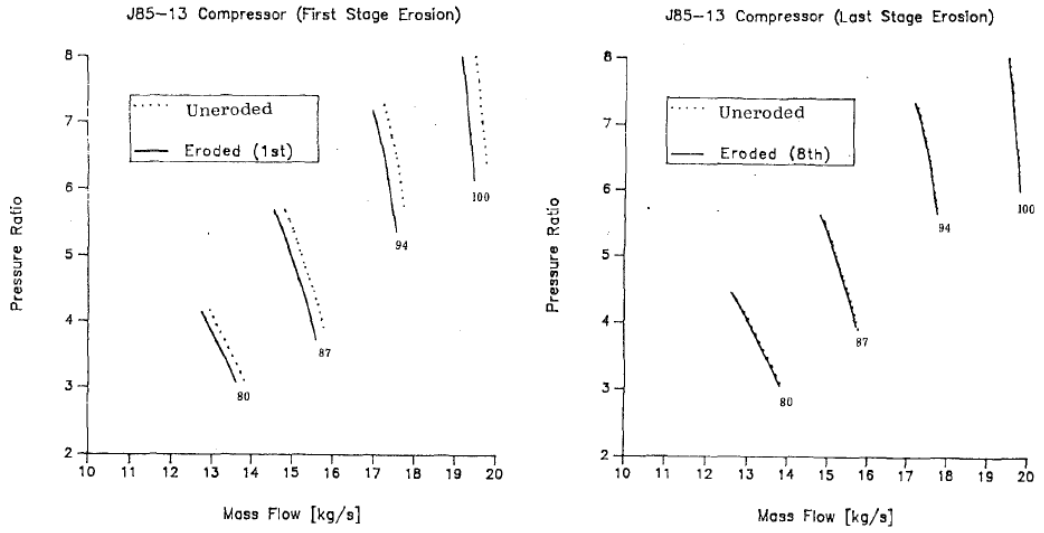

Figure 3.14: Effect of blade chord erosion of stage 1 and 8 in the HPC performance [19]

To summarize, the HPC performance has demonstrated to be more vulnerable to the first stages efficiency. In the following chapters, the developed 0-D thermodynamic of the CFM56-5B turbofan engine will be used to verify if the performance of its HPC, as well as the overall engine performance, is also more sensitive to the first stages efficiency, as previous studies have demonstrated.

Chapter 4

Thermodynamic Model of the CFM56-5B Turbofan Engine

In this section it will be described how the thermodynamic model of the engine was obtained. TAP M&E had available a thermodynamic model for the CFM56-5B that is described in reference [6], however after a thorough study, it was assessed that this model was unfit for performance studies due to some inaccurate assumptions. A more detailed explanation can be found in section 4.4. Because the objective is to develop a 0-D thermodynamic model, it is imperative that the measured data of the engine that is being modelled in the different stations is reliable, otherwise, it may not be possible to achieve a converged solution or to have an imprecise model. For the purpose of analysing other engines, it is also desirable that the engine is in good health condition, i.e., to have a low EGT. The engine that was modelled is the one described in subsection 4.2.

4.1 EGT Margin

The EGT is the temperature at the engine exhaust and it is a measure of an engine's efficiency in producing its design level thrust. The higher the EGT, the more wear and deterioration affects the engine. A high EGT is an indicator of an engine with degraded performance. When the EGT reaches a certain limit, it is performed maintenance actions in order to restore its EGT margin. The EGT margin is defined as the difference between the EGT red line (or limit) and the EGT that is measured. The EGT red line for a hot day (HD), that is for an outside air temperature (OAT) of 30^{o}C, is defined in the CFM56-5B engine shop manual in reference [26]. Beyond the EGT limit, the thermal loads are high enough that creep may occur. The EGT margin is a function of the OAT, as the OAT increases so does the EGT at a constant thrust, which consequently reduces the EGT margin. All commercial turbofan engines operate as a flat-rated engine. This means that the maximum take-off thrust is available up to a specific OAT, that is called Flat Rated Temperature (FRT). Beyond this temperature, the EGT margin is kept constant with the penalty of reducing the maximum available thrust [27]. Figure 4.1 illustrates the EGT margin and FRT concept.

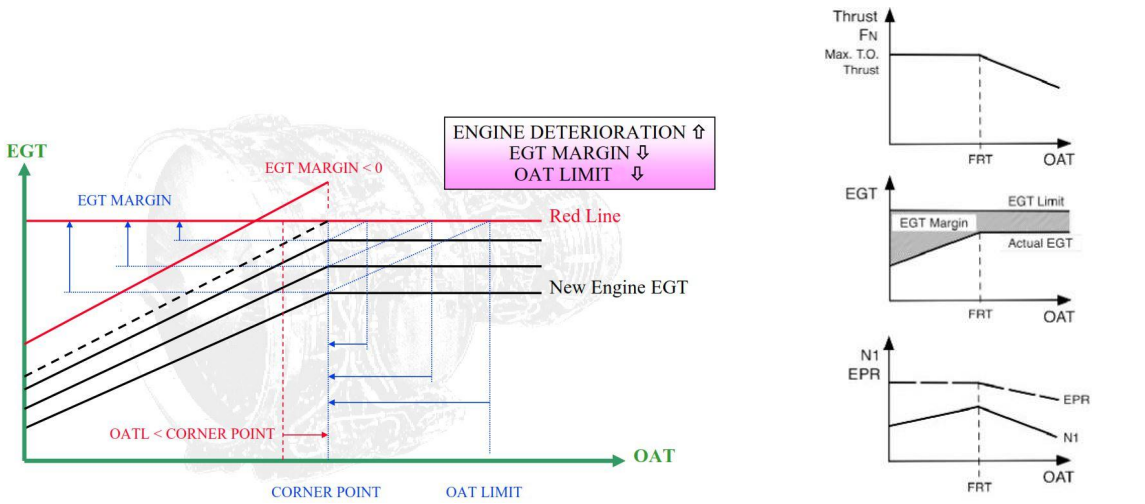

(a) EGT margin deterioration [28]

(b) EGT margin at FRT [27]

Figure 4.1: EGT margin and FRT concept

A new CFM56-5B3 engine in take off regime has an EGT hot day (HD) margin of approximately 64K. At TAP M&E the standards for a healthy CFM56-5B3, after performing heavy maintenance works, is to have an EGT HD margin greater than 40K.

In the thermodynamic cycle of the engine, the hottest section is the combustor discharge T4 but due to the harsh conditions present in that section, the risk of damaging the sensor and consequently, the components that follow is high, and so, it is undesirable to have sensors in that station. The LPT inlet T45 is affected by an air stream from the compressor discharge pressure (CDP), with the objective of cooling the LPT nozzle, thus the solution to measure the EGT was the inlet of the second stage of the LPT (station 49.5 at TAP test bed) with 11 sensors, and then averaged to avoid misreads due to temperature distortion (see section 2.2.1 for sensor locations).

4.2 Correlation Test Report and Correction Factors

The correlation engine is an engine whose performance was known by the manufacturer and it was considered a stable engine. The purpose of testing this engine is to correlate its performance in TAP test bed with the data from the CFMI facilities, where it had been previously tested and measurements were made at various stations. This allowed to correlate with deviations of measurements made at TAP test bed and calculate the Facility Modifiers (FM), that will permit to relate the performance of an engine in different test cells. The Correlation Test Report (CTR) in reference [29] is the document composed by CFMI where the performance report is documented and the FM are calculated. The FM are applied to the high pressure spool speed (N2), fuel flow (WF), air mass flow (W2), EGT and net thrust (FN) by multiplying the measured data with the FM. Each FM is a result of a polynomial equation of the type:

$$FM = A0 + A1 \times x + A2 \times x^2 + A3 \times x^3 + A4 \times x^4, \tag{4.1}$$

where x represents the measured thrust at TAP test bed and the "A's" are coefficients tabulated in reference [29]. P2 is also a function of the FM, the Low Pressure Spool Speed (N1) and Ambient Pressure and it can be calculated as:

$$PT2 = (A0 + A1 \times N1R) \times P_{amb} \tag{4.2}$$

Apart from the FM corrections, other measurements were made in the correlation engine such as Ambient Pressure and Temperature, T2, T3, T5, P13, Ps3 and P5. Because ambient conditions change from day to day, it is important to correct this data to Standard Day so that it is possible to establish a basis of comparison between the performance of different engines. To correct to Standard Day, the following equations were used for temperature and pressure measurements respectively:

$$\theta = \frac{T2_{read}}{T_{ambStd}} \tag{4.3a}$$

$$T_{corr} = \frac{T2_{read}}{\theta} \tag{4.3b}$$

$$\delta = \frac{P2_{read}}{P_{ambStd}} \tag{4.4a}$$

$$P_{corr} = \frac{P2_{read}}{\delta} \tag{4.4b}$$

The standard ambient temperature and pressure are 288.15K and 101.325KPa as defined by the International Standard Atmosphere (ISA) [23].

As described in section 4.1, for performance calculations regarding EGT HD margin, it is necessary to perform a series of corrections to the measured EGT. These corrections are described in reference [26], and applied as:

$$EGTK = [EGT_{read} \times \frac{1}{\theta \times EXP_{EGT}} \times KHEGT \times KCONDT] \tag{4.5a}$$

$$EGTK1 = [EGTK \times FMEGT] \tag{4.5b}$$

$$EGTK2 = [EGTK1 \times EGT_{ADJ}] \tag{4.5c}$$

$$EGTK3 = [EGTK2 + \Delta EGT] \tag{4.5d}$$

$$EGTHD = [EGTK3 \times \theta_{HD}^{EXP_{EGT}}], \tag{4.5e}$$

where KHEGT, KCONDT and EXP_{EGT} are an humidity, condensation and HPT clearance correction factor respectively. FMEGT is the FM correction, EGT_{ADJ} is a bellmouth adjustment and ΔEGT is the difference of the EGT between N1 rated and N1 measured which is approximately zero. θ_{HD} is the Standard Day correction for an (OAT) of 30°C.

In reference [26], the EGT HD limit for a CFM56-5B3 is 1210K. From the engine tested in the CTR, the EGT measured was 1088K. This raw data needs to be corrected for HD in order to verify the EGT margin and can only then be subtracted to the EGT HD limit to find the EGT HD margin. Following the procedure in equations (4.5), the EGT HD margin for the correlation engine is calculated as:

$$EGTHD_{margin} = EGTHD_{limit} - EGTHD_{CTR} = (937 + 273.15) - 1185.54 = 24.61K \tag{4.6}$$

where 937ºC is the EGTHD limit defined in the engine shop manual in reference [26].

4.3 GasTurb Program Scope

GasTurb® offers three different degrees of gas turbine simulation. These are: **Basic Thermodynamics** for only fundamental questions, **Performance** to study gas turbine cycles and off-design behaviour in more detail, and **More** to study preliminary engine design [4]. Since the objective is to develop an off-design performance prediction model of an existing engine, the **Performance** program is the one of interest. Within *GasTurb*®, various types of engines configurations are available. Being the CFM56-5B a turbofan engine, it is of interest in the *GasTurb*® menu the *Geared Unmixed Flow Turbofan* with a gear ratio equal to 1 considering that the fan and booster rotate at the same speed of the LPT and the HPC at the same speed as the HPT.

Firstly, a suitable cycle reference point is chosen and the model is tailored to the data of this point. Secondly, compressor and turbine maps are added and scaled such that they fit exactly to the cycle reference point. In this step, a second operating point is considered and the location of the cycle reference point in the component maps is adapted such that the simulation fits optimally to the given data of the second point. In a third step, the rest of the data are compared graphically with the model simulation [30].

4.4 Cycle Reference Point

The first step is to choose a cycle reference point from available data in the CTR. According to Kurzke [30], the ideal point would be the design point of the engine, however, any high power operating point is suited for that purpose for measurement accuracy reason because Reynolds number effects are negligible, i.e., where Reynolds number are high. Reynolds number is calculated as:

$$Re = \frac{\rho L V}{\mu}, \tag{4.7}$$

where ρ is the density, L is the characteristic length, V is the velocity and μ is the dynamic viscosity.

At high Reynolds numbers, if the boundary layer is turbulent and the surface is hydraulically rough, the Reynolds number has no effect on the losses. At low Reynolds numbers, viscous losses increase and this can have a significant effect on engine performance [4]. The Reynolds number effect on engine performance has been studied by Citavy *et al.* [31] and Wassel [32] where experimental setups of

compressor cascades were tested varying Reynolds number. The results are represented in figure 4.2a and 4.2b, where it is possible to see that a decrease in Reynolds number lead to a lower efficiency and pressure ratio of the compressor and to an increase of the loss coefficient (ξ). This is explained by the fact that for low Reynolds number, the separation of the laminar boundary layer takes places on the pressure surface of the blade near the trailing edge, and consequently increases the deviation angle (δ) [31].

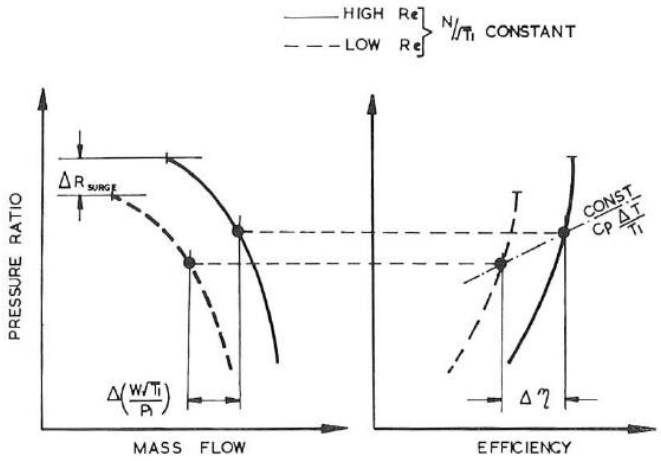

(a) Reynolds number effect on mass flow and efficiency [32]

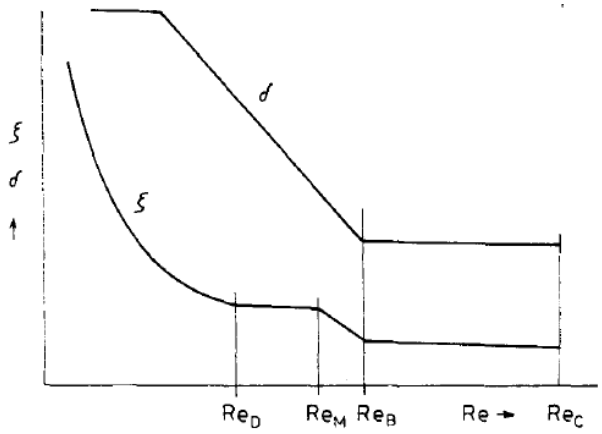

(b) Reynolds number effect on compressor losses [31]

Figure 4.2: Reynolds number effect on compressor performance

For that reason, the cycle reference point was defined as the highest available value of N1 in the CTR. Another important aspect to have defined the highest available N1 speed as the reference cycle point is due to the positioning of the VSV's and VBV's. These vanes and valves have a positioning schedule that will affect the mass flow and other parameters in the cycle. The CTR does not possess any information regarding their position, however it is known that for high speed regimes, the VBV's are closed and the VSV's are fully open. The internal air system also has to be defined. Cooling air from the HPC is deviated and bypasses the combustion chamber to cool the HPT nozzle guide vane (NGV), HPT rotor and the LPT NGV. Because this mass flow is unknown, it is recommended in the *GasTurb*® Manual [4] to use the default values which are common among turbofan engines.

By applying the FM and correcting the temperatures and pressures from the CTR to Standard Day,

as described in section 4.2, it is possible to begin the modelling of the cycle reference point. Mass flow and spool speeds (N1 and N2) are given as input and then it is necessary to select iteration variables and targets within *GasTurb*®. However, care must be taken when selecting them. For instance, it does not make sense to make as a variable the booster efficiency and as target the core nozzle area because they are not directly related. It is also important to define reasonable intervals in the variables, otherwise, it may not be possible to achieve a converged solution. In table 4.1, it is described the iterations that were defined.

Variable	Interval	Target	Value
Burner Exit Temperature (T4)	1000K - 2000K	Fuel Flow (Wf)	1.57666 Kg/s
Design Bypass Ratio (BPR)	5 - 6	LPT Exit Temperature (T5)	884.3K
Bypass Duct PR	0.5 - 1.0	Bypass Nozzle Area	$1.008944m^2$
Isentr. LPT Efficiency	0.7 - 1	LPT Exit Pressure (P5)	176.6818KPa
Isentr. HPC Efficiency	0.7 - 1	HPC Exit Temperature (T3)	860K
Isentr. IPC/Booster Efficiency	0.7 - 1	HPC Inlet Temperature (T25)	417K
Isentr. HPT Efficiency	0.8 - 1	HPC Exit Pressure (P3)	3459.6KPa
IP/Booster PR (P25/P21)	1 - 5	Overall Pressure Ratio (P3/P2)	34.14124
Bypass Nozzle Thrust Coeff.	0 - 2	Net Thrust	144.2KN
Outer Fan PR	1 - 2.5	Fan Outer Exit Pressure (P13)	171.24KPa
Design Core Nozzle Angle (º)	0 - 45	Core Nozzle Area	$0.309664m^2$
Inner Fan PR	1 - 2.5	Fan Inner Exit Pressure (P21)	131.418KPa

Table 4.1: Iteration variables and targets to model the cycle reference point

In figure 4.3 and figure 4.4 are represented all the parameters of the converged solution for the cycle reference point.

The BPR of the CMF56-5B is defined by CFM as 5.4, however, this is just a representative value and may not represent the real BPR of the engine. For that reason, it was decided that the BPR would be a variable instead of an iteration target. *GasTurb*® solution converged with a BPR of approximately 5.3 which represents a 1.85% deviation from the manufacturer value.

The iteration target P3 is not measured directly in the engine. Instead, it is measured the static pressure in station 3 (Ps3). In a study conducted by Kurzke [33], it was concluded that a good approximation for estimating P3 is, $P3 = \frac{Ps3}{0.97}$, since in station 3 the Mach number is low and fairly constant.

EGT was not used as an iteration target because this temperature is not among the normal *GasTurb*® output parameters, however, it can be calculated as a composed value. Kurzke [33] studied the temperature decrease within the four stage LPT. He assumed that the aerodynamic loading $\frac{\Delta H}{u^2}$ of all stages is equal and the temperature drop between stages varies along the LPT stages due to the mean rotor blade diameters being different, with the first stage being the smallest, and so, the temperature drop in the first stage will be the smallest as well. The value 0.217 is a guess for the relative temperature drop in the first stage of the LPT due to work extraction and 0.9664 is the recovery factor:

$$EGT = 0.9664 \times [T45 - 0.217 \times (T45 - T5)] \tag{4.8}$$

Station	W kg/s	T K	P kPa	WRstd kg/s
amb		288,15	101,325	
2	440,286	288,15	101,325	441,400
13	370,353	342,09	171,240	239,378
21	69,933	313,91	131,418	56,420
22	69,933	313,91	131,418	56,420
24	69,933	417,00	324,272	26,354
25	69,933	417,00	324,272	26,354
3	68,535	860,00	3459,361	3,477
31	60,842	860,00	3459,361	
4	62,419	1696,40	3286,393	4,681
41	65,915	1655,62	3286,393	4,883
43	65,915	1259,41	858,071	
44	70,111	1237,07	858,071	
45	71,510	1226,88	849,490	17,643
49	71,510	884,30	176,684	
5	71,510	884,30	176,684	72,016
8	71,510	884,30	174,917	72,743
18	370,353	342,09	170,902	239,851
Bleed	0,000	860,00	3459,361	

Efficiency	isentr	polytr	RNI	P/P
Outer LPC	0,8600	0,8699	1,000	1,690
Inner LPC	0,8600	0,8651	1,000	1,297
IP Compressor	0,8889	0,9020	1,172	2,467
HP Compressor	0,8483	0,8871	2,060	10,668
Burner	0,9995			0,950
HP Turbine	0,9100	0,8963	4,209	3,830
LP Turbine	0,8879	0,8669	1,536	4,808

HP Spool mech Eff 0,9900 Nom Spd 14736 rpm
LP Spool mech Eff 1,0000 Nom Spd 5051 rpm

P22/P21=1,0000 P25/P24=1,0000 P45/P44=0,9900

FN	=	144,20 kN
TSFC	=	10,9338 g/(kN*s)
WF	=	1,5767 kg/s
s NOX	=	1,4017
Core Eff	=	0,4776
Prop Eff	=	0,0000
BPR	=	5,2958
P2/P1	=	1,0000
P3/P2	=	34,14
P5/P2	=	1,7437
P16/P6	=	0,97704
P16/P2	=	1,68667
P6/P5	=	0,99000
A8	=	0,30966 m²
A18	=	1,00894 m²
XM8	=	0,93418
XM18	=	0,89782
WBld/W2	=	0,00000
CD8	=	0,99329
CD18	=	0,99502
PWX	=	0,0 kW
V18/V8,id	=	0,60694
WBLD/W22	=	0,00000
Wreci/W25	=	0,00000
Loading	=	100,00 %
e444 th	=	0,88164
WBLD/W25	=	0,00000
WHNGV/W25	=	0,05000
WHcl/W25	=	0,06000
P6/P5	=	0,9900
P16/P13	=	0,9980

Figure 4.3: Cycle reference point of the CFM56-5B3 in *GasTurb*®

Iteration converged after 1 loops.

Iteration Variables:

1:	Burner Exit Temperature K (1000...2000)	= 1696,4
2:	Design Bypass Ratio (5...6)	= 5,29581
3:	Bypass Duct Pressure Ratio (0,5...2)	= 0,998025
4:	Isentr.LPT Efficiency (0,7...1)	= 0,887917
5:	Isentr.HPC Efficiency (0,7...1)	= 0,848319
6:	IP Compressor Pressure Ratio (1...6)	= 2,46749
7:	Bypass Nozzle Thrust Coeff (0...2)	= 0,939064
8:	Outer Fan Pressure Ratio (1...5)	= 1,69001
9:	Design Core Nozzle Angle [°] (0...45)	= 2,82725
10:	Isentr.IPC Efficiency (0,5...1)	= 0,888949
11:	Isentr.HPT Efficiency (0,8...1)	= 0,91
12:	Inner Fan Pressure Ratio (1...3)	= 1,29699

Iteration Targets:

1:	Fuel Flow	= 1,57666
2:	LPT Exit Temperature T5	= 884,3
3:	Bypass Nozzle Area	= 1,00894
4:	LPT Exit Pressure P5	= 176,682
5:	HPC Exit Temperature T3	= 860
6:	Overall Pressure Ratio P3/P2	= 34,1412
7:	Net Thrust	= 144,2
8:	Fan Outer Exit Press P13	= 171,24
9:	Core Nozzle Area	= 0,309664
10:	HPC Inlet Temperature T25	= 417
11:	HPC Exit Pressure P3	= 3459,36
12:	Fan Inner Exit Press P21	= 131,418

Figure 4.4: Converged iterations targets

To measure the EGT, the air has to enter four holes and flow through the thermocouple tip, which reduces the dynamic head of the gas. This leads to a recovery factor lower than 1. Figure 4.5 illustrates

the EGT measurement in station 49.5.

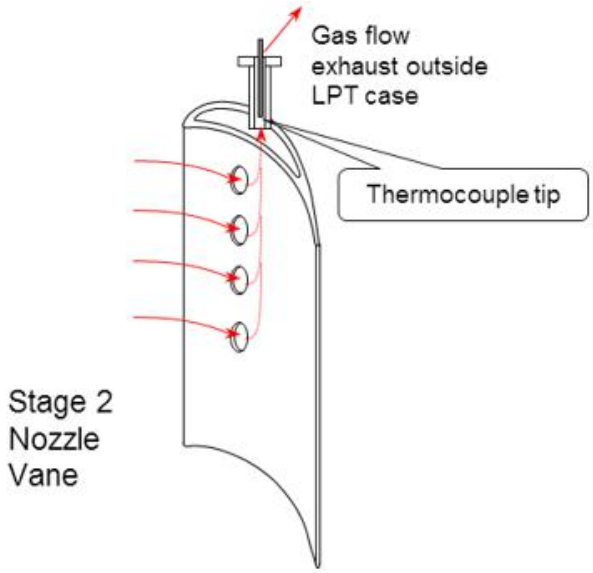

Figure 4.5: EGT thermocouple [33]

The recovery factor can be calculated using equation (4.9). This leads to a recovery factor of 0.9664.

$$r = \frac{T_{ind}}{T_{true}} \tag{4.9}$$

Remarks about unavailable stations and modelling assumptions: In the CTR, no information regarding station 25 is available. This is a crucial station to determine the HPC efficiency. Also in the CTR, the temperature T3 for a speed N1 of 5051rpm is 1086.54K. *GasTurb*® did not achieve any converged solution for this value of T3, and when that iteration target was removed, it would converge to a T3 of approximately 880K. This implied that it was possible that the readings from the CTR for that station were not reliable. To confirm that, various tests runs of the CFM56-5B temperature T3 in take off regime were checked, and then averaged, which resulted in a T3 of 860K. An identical approach was made to the temperature T25. Another possible approach that was considered to resolve this situation was to simply remove T25 and T3 iteration targets, and let the iteration process find a solution. However, that solution revealed unsuitable due to the efficiencies that resulted. In figure 4.6, it is possible to see that that approach resulted in an underestimation of the booster efficiency and an overestimation of the LPT efficiency. Although it may not seem a problem, this cycle reference point would be improper to perform comparisons of other engines due to that unbalance.

Efficiency	isentr	polytr
Outer LPC	0,8600	0,8699
Inner LPC	0,8600	0,8538
IP Compressor	0,8113	0,8390
HP Compressor	0,8218	0,8671
Burner	0,9995	
HP Turbine	0,9100	0,8957
LP Turbine	0,9337	0,9210

Figure 4.6: Cycle reference point efficiencies without iteration targets for T25 and T3

Station 21 also revealed very important due to the limitations of TAP test bed, as there are no available sensors in that station. An incorrect modelling of this station would translate to an incorrect analysis of the fan and booster. Because no measurements were made in station 21 of the correlation engine, it is unknown what the pressure ratio of the fan actually is. To bypass this situation, Martins [25] and Ridaura [34], used in their work of modelling the CFM56-3, an inner fan pressure ratio equal to 1. This solution revealed of poor accuracy. The fan acts like a compressor rotor, except that it is larger, where the pressure rise results from the energy imparted to the air in the rotor which increases the air velocity [1]. That effect can be seen if figure 4.7.

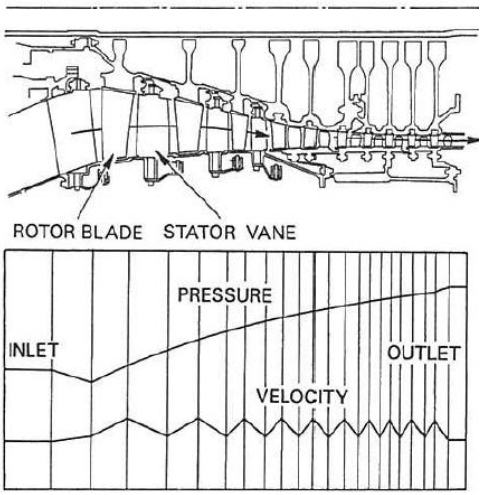

Figure 4.7: Pressure and velocity distribution of an axial compressor [1]

The solution was to investigate if any data was available for this station in a CFM56-5B engine or in any other engine of the CFM56 family. Figure A.1 in Appendix A illustrates the temperature, pressure and velocity distribution throughout the different stations of the CFM56-3 engine. By using a digitizer software, it was possible to retrieve the data from station 21. Because this image is of the CFM56-3, the fan pressure ratio differs from the CFM56-5B. In the interest of having the most accurate possible model, the inner fan pressure ratio was extrapolated because it was known the outer fan pressure ratio of both engines. This resulted in a P21 of 131.418KPa and an inner fan pressure ratio of 1.297. According to reference [1], typical values of the outer and inner fan pressure ratio are of 1.6 and between 1.3 and 1.4 respectively, which complies with assumptions made in the cycle reference point modelling. In figure 4.8 it is possible to clearly see why the previous model was inadequate to evaluate the performance of other engines. In all cases, the efficiency is very high, and in some cases it is greater than 1. This is a violation of the Second Law of Thermodynamics, which states that it is impossible for any system to operate in a way that entropy is destroyed. Entropy production may be positive or zero but never negative. Thus, entropy production is an indicator of whether a process is possible or impossible [35].

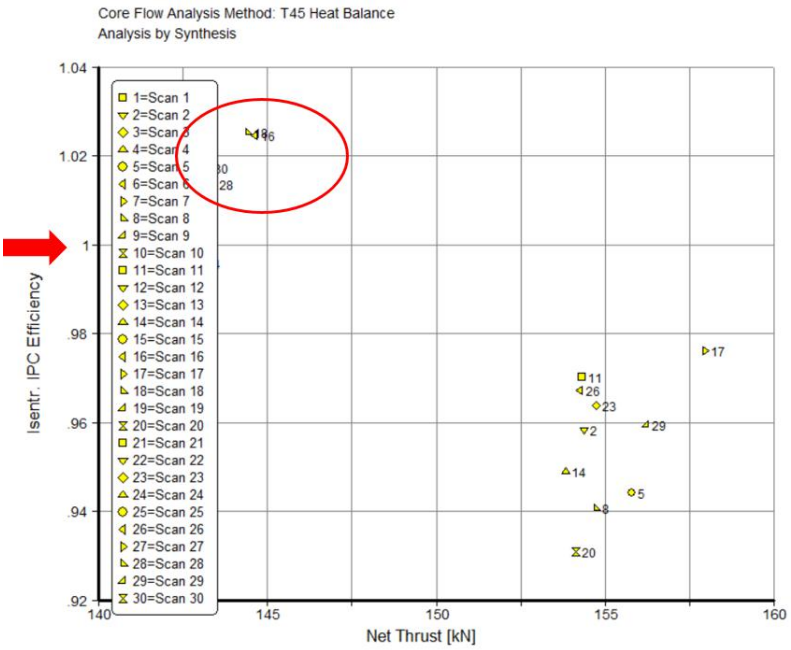

Figure 4.8: Booster efficiency of some analysed engines

4.5 Off-Design Modelling

After achieving a converged cycle reference point, the next phase is to begin the off-design modelling, where the objective is to model the behaviour of the engine at different rotational speeds. It is evident that all components of the engine will be required to operate at conditions far from the design point, e.g., engine starting, idling, acceleration, deceleration and others. Thus, it is clear that the components must be capable of a satisfying performance over a wide range of rotational speeds [23].

In *GasTurb*®, the off-design modelling begins by selecting the components maps. Suitable maps are required to predict the component efficiencies at conditions deviating from the cycle design point [30]. Since the original maps are not accessible because original equipment manufacturers (OEM) do not share that information, the best alternative is to use the maps from the *GasTurb*® library. A generic compressor map is presented in figure 4.9.

The component map has on the y-axis the Pressure Ratio and on the x-axis the Corrected Mass Flow. To tune the map to fit an operational line from the correlation engine, i.e., the parameters at different rotational speeds, it is necessary to scale the cycle reference point in the compressor for pressure ratio, mass flow and efficiency in order to match to the engine operational line. Each compressor map yields two correlations along an operational line:

1. Corrected Mass Flow - Efficiency

2. Corrected Mass Flow - Corrected Speed

Efficiencies are not available in the report of the correlation engine, however, as long as the model agrees with the temperatures and pressures in the different stations, the efficiencies are naturally correct. It is also necessary to adjust the relative Corrected Speed. These changes in the map will define the

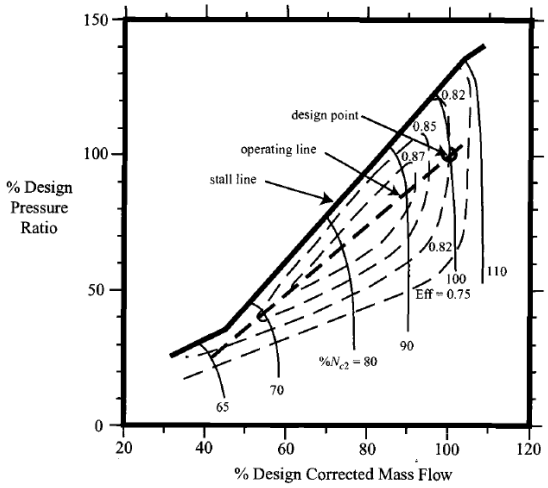

Figure 4.9: Generic compressor map [36]

coordinate in the cycle reference point. In figure 4.10a) is presented the standard *GasTurb*® map, that is in this case an unscaled HPC map, and in figure 4.10b) a scaled HPC map.

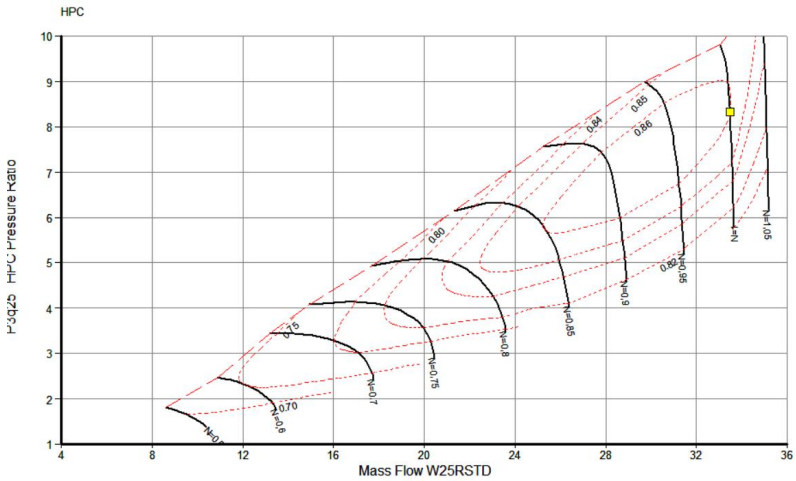

(a) Unscaled map

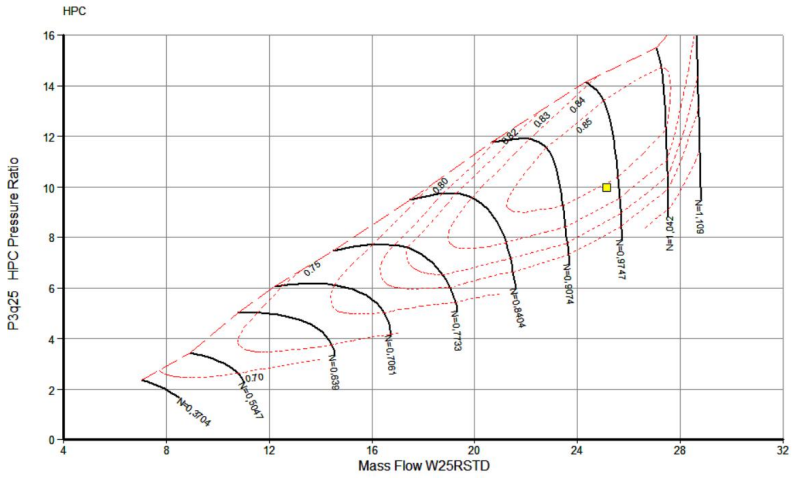

(b) Scaled map

Figure 4.10: HPC unscaled and scaled map

To select an appropriate coordinate in the component map, it will be followed the procedure recommended in reference [30]. It is recommended to deal with both correlations separately, beginning with efficiency correlation in order to verify the impact of the changes. In the end, both correlations should be in agreement with the operational line from the correlation engine. By locating the cycle reference point in a map region with poor efficiency, the efficiency will increase towards part load, while locating the reference point in the peak efficiency region will decrease it for any off-reference operation. This is an iterative approach, where it is necessary to constantly verify the effects of changes, until a reference point is found for all components maps that is in agreement with the off-design operation.

Another important aspect to take in consideration in the off-design modelling is the schedule of the VBV's and VSV's. TAP M&E does not possess their operation schedules for the CFM56-5B. Nonetheless, because it is of interest the high power regimes, and at this setting the VBV's and VSV's do not affect the engine operation, it is decided to discard their implementation in the model. In figure 4.11 it is presented the schedule of the VSV's and VBV's of the CFM56-3 engine, illustrating why it is possible to neglect their effect in high power regimes.

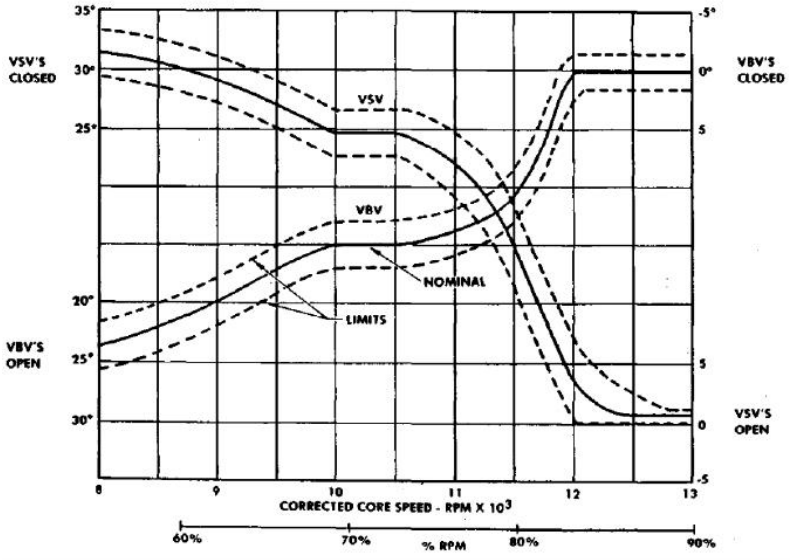

Figure 4.11: VSV's and VBV's schedule for the CFM56-3 engine [37]

Verification and Validation: After achieving suitable reference points in the components maps, it should be verified if the model is in agreement with the operational lines of the correlation engine. Figure 4.12 presents the specific fuel consumption, net thrust, EGT and T5, which are usually the parameters most difficult to attain compliance. The purple points represent the operational points of the correlation engine and the yellow points the model operational points. The remaining parameters and the components maps can be consulted in figures B.1 and B.2.

By analysing figure 4.12, it is possible to verify that the model is in compliance with CTR data at high speed regimes. The performance of the developed model matches with cycle reference point since these points were used as iteration targets. It is now possible to use this model as a benchmark for other engines, and so, TAP M&E has now in its possession, a tool that will allow to analyse the performance of

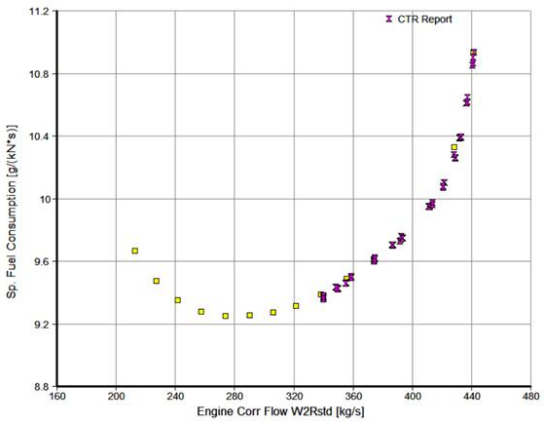

(a) SFC validation

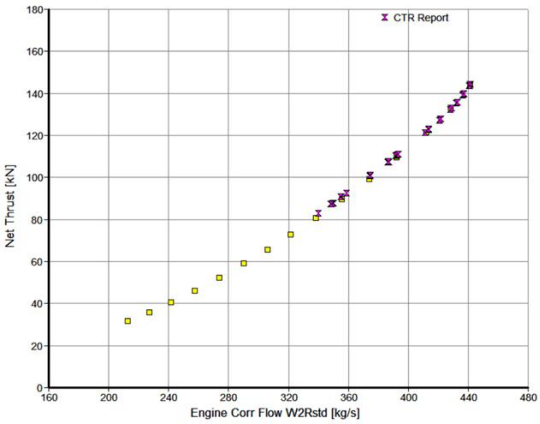

(b) Net thrust validation

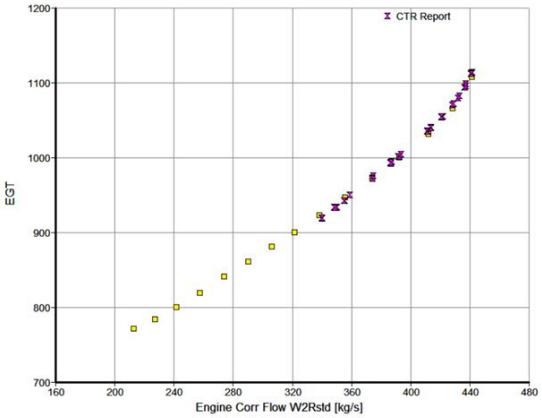

(c) EGT validation

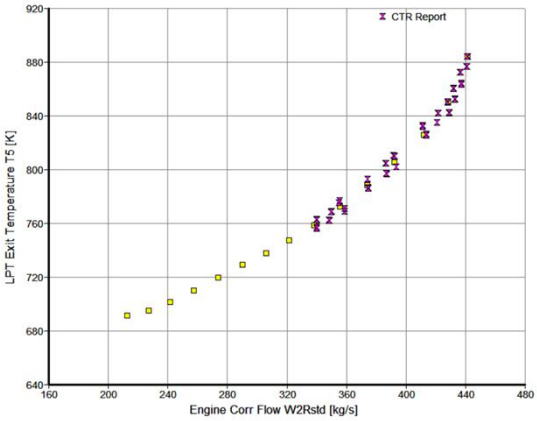

(d) T5 validation

Figure 4.12: Model validation

other CFM56-5B engines. By performing such analysis, it is possible to allocate the financial and human resources in engine modules that have poor performance. This analysis will be done in the following chapter.

Chapter 5

Model Applications

In this chapter it will be demonstrated the potential that the CFM56-5B model developed in the previous chapter can have to TAP M&E. It is possible that an engine that was subjected to heavy maintenance works still fails the performance acceptance test. This situation may occur because, for some reason, one or more of the engine's component are under performing despite being in an overhauled (OVH) condition. It is not an uncommon situation, it happened in the past and will happen again in the future at MRO companies. With a reliable model it is possible to identify which components are performing below expectations and, by doing so, save valuable time and financial resources in troubleshooting.

5.1 Modifiers Tool

One of the first exercises that can be done is to verify the impact that the deterioration of a specific component has in the performance of the engine. This can be done in *GasTurb*® with the Modifiers Tool. It is possible to increase and/or decrease the components efficiency and analyse its effect in the performance of the engine. To corroborate this analysis, it will be compared with a similar study conducted by General Electric (GE) in reference [38].

An analysis was made by individually applying a deterioration of 1% efficiency in each component. The results are illustrated in table 5.1 where it is possible to see the impact they have on EGT, fuel flow, core spool speed (N2), fuel flow/Ps3, booster efficiency and thrust.

In the performance diagnostics table (table 5.1), of the 30 analysed parameters, 28 are in compliance. The ones that are not in compliance are denoted by arrows in red. In all cases the EGT increased, which is an expected result since the engine tries to compensate the poor efficiency with additional fuel burn in order to achieve the desired thrust. The core spool speed (N2) increases for low efficiency of the components that belong to low pressure spool (N1), which indicates that the HPT and HPC will rotate faster to compensate the low efficiency of these components. The core spool speed (N2) decreases in a situation of low efficiency of the core components and this is a direct consequence of the low efficiency. The only parameter that was not sustained by the GE study was the booster efficiency for the cases of HPC and HPT low efficiency, where a slight increase was noted.

Issue	Analysis	Symptom					
		EGT	Fuel Flow (Wf)	N2	Wf/Ps3	Booster Eff.	Thrust
Low Fan Efficiency	GE	↑	↑	↑	↑	→	↑
	GasTurb®	↑	↑	↑	↑	→	↑
Low Booster Efficiency	GE	↑	↑	↑	→	↓	→
	GasTurb®	↑	↑	↑	→	↓	→
Low HPC Efficiency	GE	↑	↑	↓	↑	→	→
	GasTurb®	↑	↑	↓	↑	↑	→
Low HPT Efficiency	GE	↑	↑	↓	↑	→	→
	GasTurb®	↑	↑	↓	↑	↑	→
Low LPT Efficiency	GE	↑	↑	↑	↑	→	↑
	GasTurb®	↑	↑	↑	↑	→	↑

Table 5.1: GE and *GasTurb*® performance diagnostics comparison

In table 5.1 it is possible to verify the effect that an efficiency deterioration of a component has on the performance of the engine. Yet, it will be more useful to quantify what that effect is. In figure 5.1 it is presented a bar chart that quantifies the consequence of having low efficiency in the individual components.

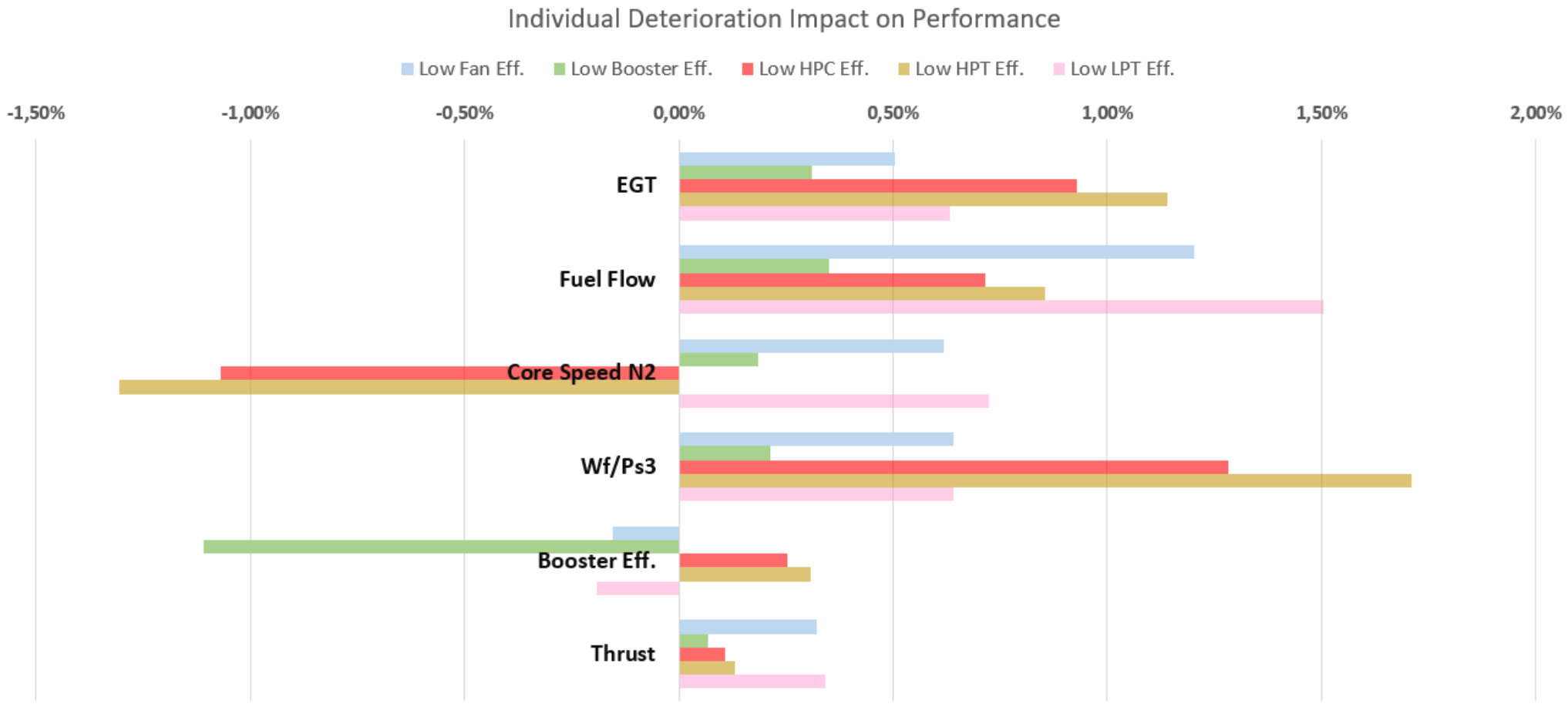

Figure 5.1: Individual deterioration impact on performance

It is possible to draw some conclusions by analysing figure 5.1:

- EGT is most affected by core components, being the HPT performance the most important, followed by the HPC and LPT;
- Fuel Flow is most affected by the LPT, followed by the Fan, HPT and HPC;
- Core Speed N2 is directly linked to HPC and HPT and so it is natural that these components influence its speed the most;
- Wf/Ps3 is also affected the most by core components, HPT and HPC respectively;
- Thrust is most influenced by the LPT and the Fan, which is also natural since these components are linked by the low pressure spool N1 and the Fan generates approximately 80% of the engine thrust.

5.2 Model Based Test Analysis

Another exercise that can be performed is based on the Model Based Test Analysis (MBTA). MBTA is one of *GasTurb*® tools that allow to evaluate how each engine components is performing by comparing its performance with a reference, which in this case is the thermodynamic model of the engine that was developed in chapter 4. If an engine does not meet the performance requirements, it is possible to identify which component is performing below expectations. For an MRO company this is the most useful tool that *GasTurb*® can offer.

MBTA is also known as *Analysis by Synthesis (AnSyn)*. When performing an analysis by synthesis, the model of the engine is automatically matched to the test data. This is done with scaling factors (AnSyn factors) applied to the mass flow and efficiency of the components that close the gap between the measured data and the model. For example, an Ansyn factor greater than 1 implies that the component is performing better than the model and vice-versa [4]. The AnSyn factors are calculated as:

$$AnSynEfficiencyFactor = \frac{MeasuredEfficiency}{ModelEfficiency} \tag{5.1a}$$

$$AnSynFlowFactor = \frac{MeasuredCapacity}{ModelCapacity} \tag{5.1b}$$

To perform a MBTA, the first step is to input in *GasTurb*® the measured data. Ideally, all the input data should be real measured data from the engine tested, so that all the components are isolated to evaluate their true state. However, because this is not yet possible in TAP test bed, some of the input data has to be complemented with data from the model. This has some implications: if one of the components has no sensors upstream and downstream, an AnSyn factor of 1 will always be calculated because it is in perfect agreement with the model. In table 5.2 it is possible to verify which data is measured and which has to be complemented with data from the model. For instance, no measurements are made at

the fan exit in stations 13 and 21. In these circumstances, an analysis to the fan is compromised and in turn it contaminates the booster analysis as well. The booster AnSyn factors will always be an average of both the fan and booster performance due to those conditions, since station 25 is instrumented with a temperature sensor. Another problem that was encountered that introduces a limitation in the analysis is the engine mass flow (W2). After inspecting different performance reports of engines, it was found that the mass flow calculated by TAP test bed was not congruent, since these values were much lower (approximately 150lb/s) than expected. The mass flow is not directly measured, instead it is calculated as a function of the LP spool speed N1 and the static pressure at the inlet (Ps2). Later it was found that the Ps2 sensors had leaks, and so, it was decided that this flow measure will not be used in the MBTA. To bypass this situation, *GasTurb*® allows to iterate an unknown value by sacrificing one of the AnSyn factors. In this case, the engine mass flow was iterated to match the fan flow factor equal 1.

Measured Data	Availability
Relative Humidity	✓
Mass Flow W2	✓
LP Spool Speed	✓
HP Spool Speed	✓
Inlet Temperature T2	✓
Inlet Pressure P2	✓
Fan Outer Exit Temperature T13	N/A
Fan Outer Exit Pressure P13	N/A
Fan Inner Exit Temperature T21	N/A
Fan Inner Exit Pressure P21	N/A
Booster Exit Temperature T24	✓
Booster Exit Pressure P24	N/A
HPC Exit Temperature T3	✓
HPC Exit Pressure P3	✓
Fuel Flow Wf	✓
HPT Exit Pressure P44	N/A
LPT Inlet Temperature T45	Extrapolated from eq. (4.8)
LPT Outlet Pressure P5	N/A
LPT Outlet Temperature T5	✓
Ambient Pressure	✓
Measured Thrust	✓

Table 5.2: *GasTurb*® MBTA input data availability

It is possible to introduce the measured data in *GasTurb*® manually or create a .mea file that allows to analyse several engines at the same time. In figure 5.2 it is illustrated part of a .mea file with data from analysed engines tests. A .mea file is similar to a Notepad file, where in each column is a specific parameter with the nomenclature that *GasTurb*® uses, and the lines are filled with different engine tests. Measured temperatures and pressures have to be corrected to standard day using equations (4.3) and (4.4). Since the data from the model has already been corrected to standard day, there is no need to apply any further corrections. However, it is necessary to limit the LP spool speed N1 in *GasTurb*® to match the speed of the engine tested to extract correctly the model data and complement the input data

that is not measured in TAP test bed, which can be done in the limiters tab.

ScanId	humid!	W2!	XN_LP_A!	XN_HP_A!	T2!	P2!	T13!	P13!	T21!	P21!	T24!
Tolerances											
1	1	1	1	1	1	1	1	1	1	1	1
Measured Data											
1	70,18	409,50319	5039	14709,6	288,15	101,325	341,89	171,096	313,81	131,356	
2	60,12	404,06008	5043	14721,4	288,15	101,325	341,95	171,144	313,84	131,377	
3	73,61	409,18568	5038	14738,4	288,15	101,325	341,87	171,085	313,80	131,351	
4	59,44	402,20035	5035	14691,8	288,15	101,325	341,82	171,049	313,77	131,336	
5	63,60	404,01472	5038	14688,1	288,15	101,325	341,87	171,085	313,80	131,351	
6	77,49	401,42925	5034	14720,6	288,15	101,325	341,80	171,037	313,76	131,331	
7	49,23	343,73230	5053	14744,0	288,15	101,325	342,12	171,263	313,92	131,428	
8	54,97	353,80205	5044	14723,4	288,15	101,325	341,97	171,156	313,85	131,382	
9	79,48	407,32595	5028	14706,9	288,15	101,325	341,70	170,966	313,72	131,300	
10	35,98	408,00634	5044	14718,0	288,15	101,325	341,97	171,156	313,85	131,382	
11	75,27	403,15290	5033	14677,6	288,15	101,325	341,79	171,025	313,76	131,325	
12	45,05	410,27430	5053	14753,3	288,15	101,325	342,12	171,263	313,92	131,428	
13	65,06	410,68253	5026	14695,9	288,15	101,325	341,67	170,942	313,70	131,290	
14	67,00	409,82071	5042	14772,0	288,15	101,325	341,94	171,133	313,83	131,372	
15	62,42	405,05799	5032	14640,6	288,15	101,325	341,77	171,013	313,75	131,320	

Figure 5.2: Part of a .mea file with MBTA input data

In Analysis by Synthesis, a Core Flow Analysis Method, also known as Matching Scheme, must be selected. This is the element that defines the way the engine synthesis will be modified to match the measured cycle and, therefore, is a fundamental piece of the AnSyn analysis. It will represent the choice of parameters in the engine model that will not be modified, the ones that will be scaled and the ones that will be used as reference. In *GasTurb*® 11, four different methods can be selected:

- **HP Turbine Capacity** - matches the HPT capacity of the model with the engine tested;
- **LP Turbine Capacity** - matches the LPT capacity of the model with the engine tested;
- **T45 Heat Balance** - matches the T45 measured with T45 of the model;
- **T5 Heat Balance** - matches the T5 measured with T5 of the model.

According to reference [39], the AnSyn factors should be applied to the candidates with the greatest modelling uncertainty, i.e, the selected Matching Scheme should be based in measurements that are reliable, so that the AnSyn factors can directly reflect physical phenomenons that were not taken into account in the model and allow a better comprehension of the components behaviour. These factors are only a way of calibrating the model to a particular engine in the tested conditions, they are not part of the physical model, only a correction to it. If these factors are not applied to the components that are really causing the deviations, their anomalous behaviour will indirectly appear in other AnSyn factors, which makes the physical interpretation more difficult [39]. This is the situation that occurs with the fan and booster described earlier and it is the reason why these components will not be taken into consideration in the MBTA. Also, if a measurement is thought to be inaccurate, it may be better not to use it because it will have an influence in the whole matching process. Measurement problems will appear as unexpected AnSyn factors. For example, if the HPC compressor temperature T3 is higher than the real one, the AnSyn analysis will output low HPC efficiency and high HPT efficiency simultaneously. By inspecting the definition of isentropic efficiency for the compressor and turbine, given respectively by equations (5.2a) and (5.2b) it is possible to see why that situation occurs. With increasing temperature

downstream of the compressor (or T02 in eq. (5.2a)), the isentropic efficiency of the compressor is lower. At the same time, the temperature downstream of the turbine (T04 in eq. (5.2b)) is an accurate measurement, and so, the difference between the inlet and outlet temperature of the turbine is higher than the real one, resulting in a high isentropic efficiency of the turbine. This was the case with one of the engines that was analysed which will be discussed in section 5.2.1.

$$\eta_{is,c} = \frac{T_{01}}{T_{02} - T_{01}} \left[\left(\frac{P_{02}}{P_{01}} \right)^{\frac{\gamma-1}{\gamma}} - 1 \right] \tag{5.2a}$$

$$\eta_{is,t} = \frac{T_{03} - T_{04}}{T_{03} \left[1 - \left(\frac{P_{04}}{P_{03}} \right)^{\frac{\gamma-1}{\gamma}} \right]} \tag{5.2b}$$

To analyse the engine performance, different thrust ratings can be evaluated. The engine ratings are [40]:

- Take-off, that corresponds to the maximum thrust that the engine is certified to produce and it is generally specified for short periods of time;
- Maximum climb, that is the maximum thrust that the engine is certified to produce for normal climb operation, which corresponds to 90% to 93% of the take-off rating;
- Maximum Cruise, that is the maximum thrust that the engine is certified to produce for normal cruise, which corresponds to 80% of the take-off rating.

In the performance acceptance test the engines run at these different ratings and remain in it for a few minutes to stabilize the temperatures and pressures measurements. Since the take-off rating is the most important to evaluate the EGT HD margin and that operation range is near the cycle reference point described in section 4.4, the take-off rating will be the main focus in the MBTA. In figure 5.3 it is presented an example of the MBTA, where it is illustrated the AnSyn factors defined in equation (5.1). *GasTurb*® also outputs the cycle parameters as in figure 4.3 and the position in the component maps.

Because the selected Matching Scheme is the **T45 Heat Balance**, in all MBTA's, the T45 measured and the T45 calculated will always be equal.

5.2.1 MBTA Results and Analysis

In this section it will be presented the MBTA results obtained and their analyses. In this study, it was possible to gather a sample of 18 performance tests of different engines. Because the correlation engine was tested in the CFM56-5B3 rate, only engines that were tested in this rate should be analysed since the model is not suited to analyse other rates.

GasTurb® only has as performance parameters the efficiency and flow factors, however, it is pertinent as well to evaluate the TSFC and the EGT. For that reason, besides the AnSyn factors, efficiencies, TSFC and EGT are also exported from the MBTA analyses. A database was created using Excel VBA macros to ease the data processing and treatment. In figure 5.4 it is presented one of the engines

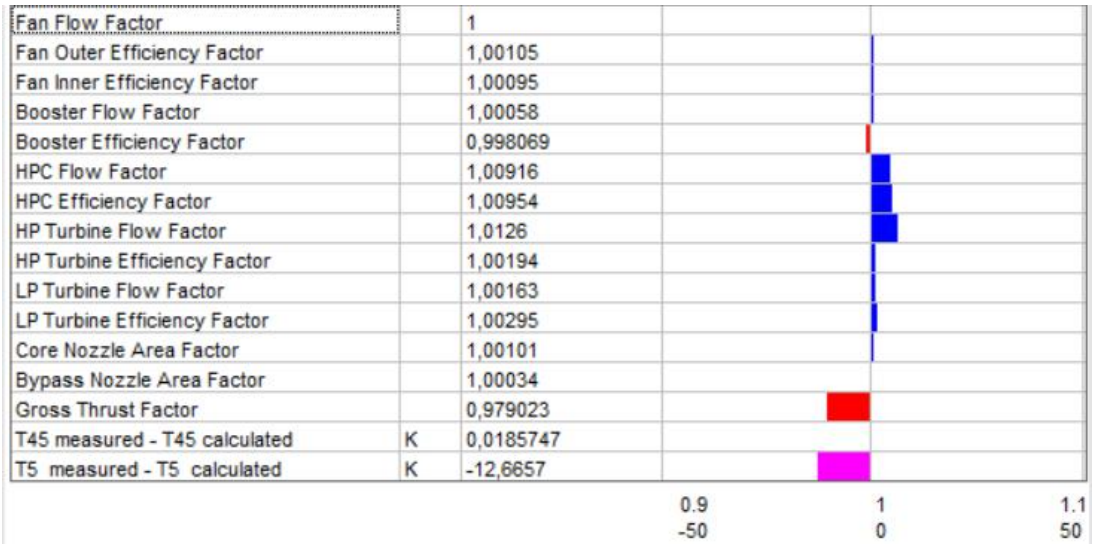

Figure 5.3: MBTA example of one of the analysed engines

that was analysed. In cell ”C2” it is possible to search from a drop down list a particular engine, that for confidentiality reasons is omitted. Efficiencies and AnSyn factors will be automatically updated for the searched engine. Along column ”C” and ”D” it is possible to check the respective AnSyn factor and the variation in percentage from the model. In column ”E”, it is possible to verify the average difference (delta) percentage deviation from the model, and in column ”F” the percentage deviation from the average. Along lines ”12”, ”13” and ”14” is presented the EGT HD, the EGT HD margin and the EGT HD margin difference from the model (presented in eq. (4.6)). In column ”F” is represented the difference to the average values of the quantities mentioned before (if it is above or below the average), and in cell ”G13” the difference of the EGT HD margin between the average and the respective engine. Along cell ”16” is presented the TSFC, the average TSFC and the percentage difference. Along columns ”G”, ”H”, ”I” and ”J” is applied the same logic for the component capacity.

This Excel tool will allow to evaluate all the component’s performance for a specified engine and help identify which component is performing below expectations. However, because it is known that the model developed is not an exact model due to the lack of parameters that were not measured in the correlation engine and use of component maps that are not from the real engine, the model is important to establish a basis, however, the real focus of comparison between engines should be the percentage deviation from the average.

In figures 5.5 and 5.6 it is presented a plot where the efficiency and flow percentage deviations from the model are represented for the HPC, HPT and LPT as a function of the EGT HD margin. The searched engine is automatically circulated in the graph to help identify its position. The green dashed line represents the average of the EGT HD margin, and so, all engines that are to the right of the line are performing better than average and to the left are performing worse. Linear trend lines were added just to verify the tendency of the points due to the many points represented. They do not represent a performance prediction since the EGT depends on the performance of all the components, although it is known that some components influence the EGT more than others as supported by figure 5.1, which

states the HPT is the component that affects the most the EGT. It is possible to see in figures 5.5 and 5.6 that as the components perform better regarding efficiency and capacity, the EGT HD margin is greater. Regarding figure 5.5, the slope of the linear functions of the HPC and HPT is similar, demonstrating that these components have an identical effect on the EGT HD margin and the LPT linear function slope being the smallest, demonstrating that this component is the one that least affects the EGT HD margin. As mentioned earlier, the fan and booster were not considered in this analysis, and so, it is not possible to draw any conclusions regarding those components. Regarding figure 5.6, the slope of the linear functions is greater in the HPT, followed by the HPC and the LPT, demonstrating as well that the capacity of the HPT has more impact on the EGT HD margin than the other components.

	A	B	C	D	E	F	G
1			Spot Engine				
2			purposely blank				
3							
4		Efficiency	Eff. AnSyn Factor	Eff. Delta Percentage (%)	Average Eff. Delta Percentage (%)	Eff. [Above / Below Average]	
5	Fan Outer	0,86162	1,00151	0,151%	0,106%	0,044%	
6	Fan Inner	0,86151	1,00138	0,138%	0,101%	0,037%	
7	Booster	0,90231	1,01242	1,242%	1,013%	0,229%	
8	HPC	0,84599	0,99487	-0,513%	-1,514%	1,000%	
9	HPT	0,90853	0,99832	-0,168%	0,750%	-0,918%	
10	LPT	0,89483	1,00775	0,775%	-0,080%	0,855%	
11						Average EGT HD	
12	EGT HD (K)	1173,85				1179,36	
13	EGT HD Margin (K)	36,30				30,79	5,51
14	EGT HD Margin Difference (K)	11,69				6,17	
15						Average TSFC (g/(N*s))	
16	TSFC (g/(N*s))	11,0091				11,139	-1,166%

	G	H	I	J
	Flow Factor	Flow Delta Percentage	Average Flow Delta Percentage	Flow [Above/Below Average]
Fan Outer	1,00000	0,000%	0,000%	0,000%
Fan Inner				
Booster	0,99328	-0,672%	-0,461%	-0,211%
HPC	0,98226	-1,774%	-1,270%	-0,504%
HPT	0,98480	-1,520%	0,214%	-1,734%
LPT	0,98568	-1,432%	-0,727%	-0,705%

Percentage Delta (%)	
PD> 1%	
0,1%<PD<1%	
-0,1%<PD<0,1%	
-1%<PD<-0,1%	
PD<-1%	

Figure 5.4: MBTA analysis of an engine

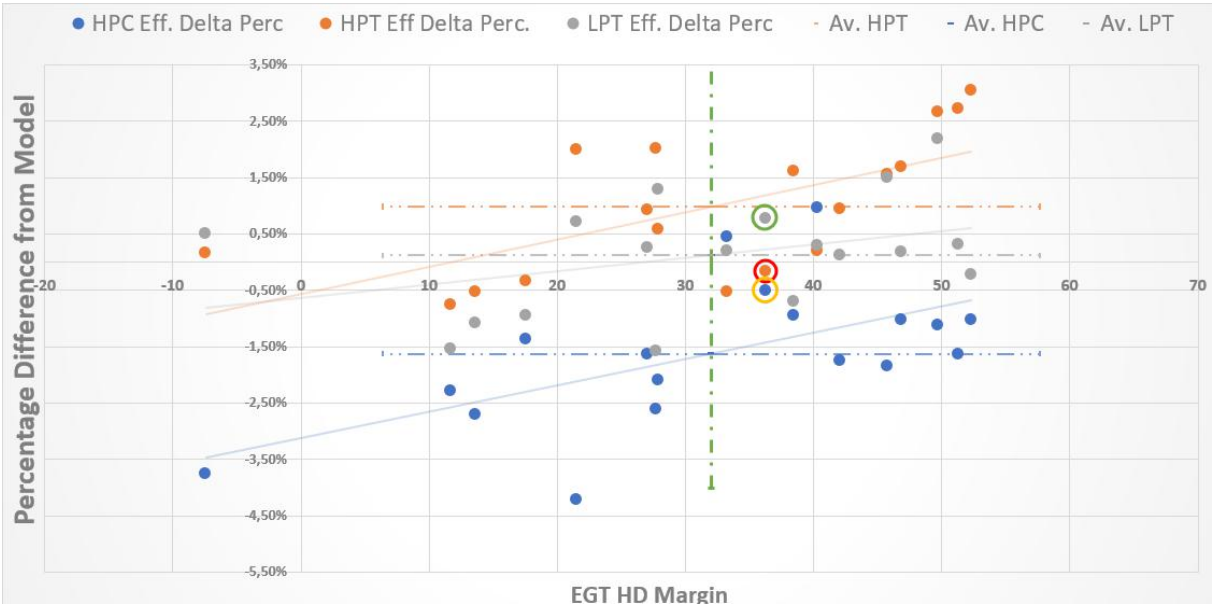

Figure 5.5: Efficiency percentage difference from model as a function of EGT HD margin

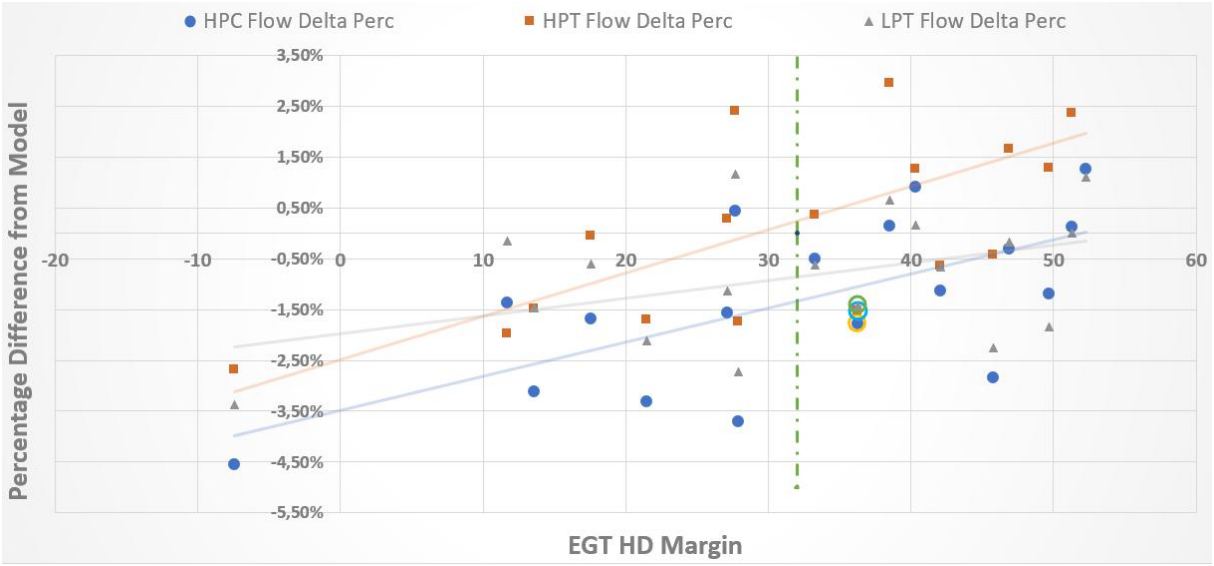

Figure 5.6: Flow percentage difference from model as a function of EGT HD margin

In figure 5.7 it is represented TSFC as a function of the EGT HD margin. The result is coherent, in the sense that a lower TSFC is a good performance indicator. It is also plotted a red dot that represents the average TSFC and EGT HD margin with extended black lines to help identify if the engine performance is above or below average. A linear trend line was also added to help identify the tendency.

In figures 5.8 and 5.9, a similar exercise is represented as in the previous figures but as a function of TSFC. It is possible to identify that for lower efficiencies, TSFC tends to increase, which is consistent. In this case, the LPT linear function is the one with greater slope, demonstrating that the LPT is the component that most affects the TSFC. The HPC and the HPT linear functions have similar slopes, which means that these components have similar impacts on the engine TSFC. These results are consistent with the results presented in figure 5.1. However, that relation is not visible regarding the components

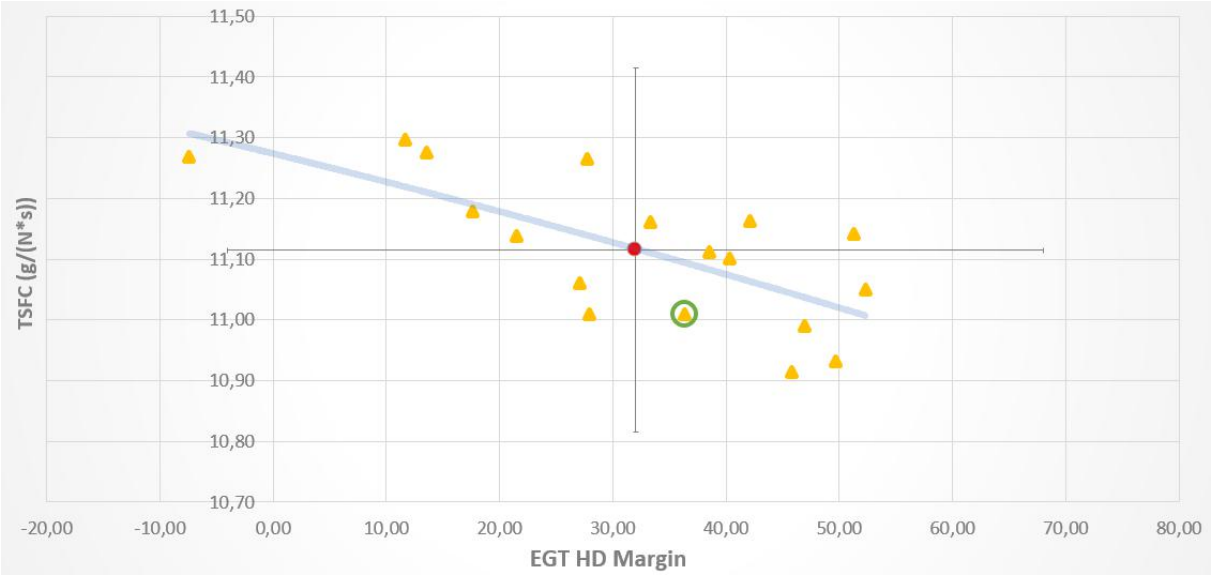

Figure 5.7: TSFC as a function of EGT HD margin

capacity as the slope of the LPT linear function is positive, meaning that as the capacity of the LPT is lower, the TSFC is decreasing, thus increasing the engine performance which is implausible. By inspecting equation (5.3), it is possible to verify that, as the engine tries to compensate the lower efficiencies of the components with an increasing fuel flow and thrust is kept constant, TSFC will naturally increase.

$$TSFC = \frac{FuelFlow}{Thrust} \tag{5.3}$$

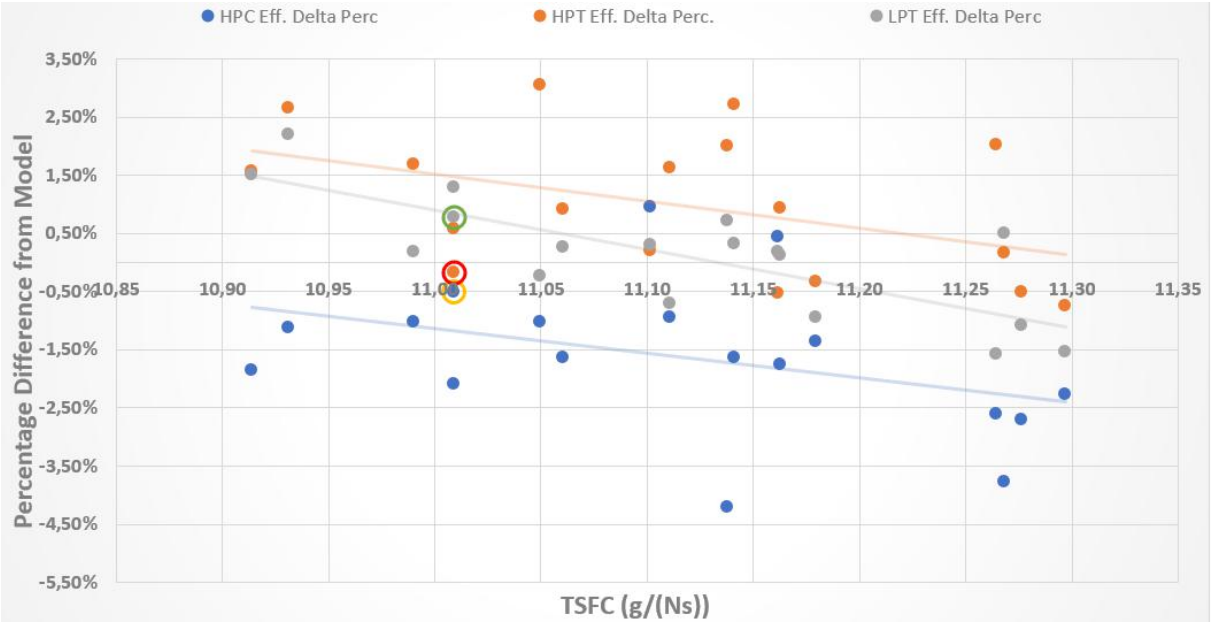

Figure 5.8: Efficiency percentage difference from model as function of TSFC

As mentioned earlier, if one sensor is giving wrong measurements, that engine should not be added to the database, because it will not be possible to correctly analyse the performance of the components and this way as well avoiding influencing the average values of performance, as these will be the bench-

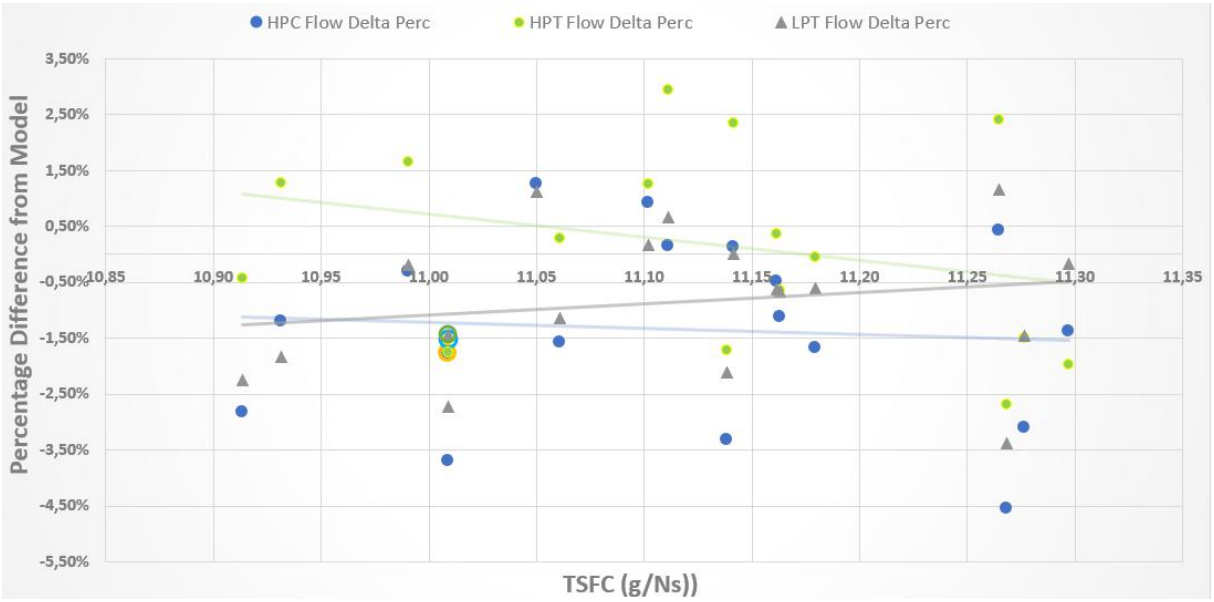

Figure 5.9: Flow percentage difference from model as function of TSFC

mark to evaluate a component performance. *GasTurb*® also has the capability of analysing the reliability of the sensor measurements by performing a *Sensor Check* that is a function of the postulated value of the model, the measurement and the tolerance defined which in this case is always 1%. By running the *Sensor Check* tool, *GasTurb*® outputs a ”decision” regarding the sensors. A sensor indicator close to 0 means that the measurement is in agreement with the postulated value of the model and a value close to 1 means that the measurement is not sustained by the model. The engine with the inaccurate measurement it will be labelled engine ”X” and is represented in figure 5.10. By inspecting figures 5.10a and 5.10b, it is possible to verify that for this specific engine, the sensor indicator is higher than usual when comparing with the other sensor indicators. Sensor T25 gave a reading lower than what it postulated by the model. By analysing equation (5.2a) it is possible to see that this would result in a higher efficiency of the booster and also in a lower efficiency of the HPC. In figure C.2, it is represented the Engine ”X” MBTA, where that exact phenomenon occurs. A very high efficiency of the booster, 5% above the model and 3.57% above average, which is higher than usual, and a low efficiency of the HPC (3% lower than the model and 1.2% lower than average). For these reasons, engine ”X” was excluded from the database.

Sensor	Reading R	Postulated P	abs(R-P)/Tol	Indicator	Decision
Meas. Rel.Humidity @ T2&P2 [%]	65,06	65,06	0,00	0,0006	
Meas. Mass Flow W2	410,683				
Meas. LP Spool Speed [RPM]	5026	4966,86	1,19	0,0000	
Meas. HP Spool Speed [RPM]	14695,9	14532,6	1,12	0,0000	
Meas. Inlet Temperature T2	288,15	288,148	0,00	0,0000	
Meas. Inlet Pressure P2	101,325	101,34	0,01	0,0000	
Meas. Fan Exit Temp. T13	341,67	341,67	0,00	0,0000	
Meas. Fan Exit Press. P13	170,942	170,87	0,04	0,0001	
Meas. Fan Exit Temp. T21	313,7	313,7	0,00	0,0000	
Meas. Fan Exit Press. P21	131,29	131,578	0,22	0,0092	
M. Booster Exit Temp. T24	410,9	416,377	1,32	0,6275	suspect
M. Booster Exit Press. P24	322,023	309,57	4,02	0,0883	
Meas. Compr.Exit Temp. T3	858,4	851,639	0,79	0,0364	
Meas. Comp. Exit Press. P3	3410,69	3429,01	0,53	0,0035	
Meas. Fuel Flow WF	1,5297	1,55378	1,55	0,0542	
Meas. HPT Exit Press. P44	850,247	839,03	1,34	0,0188	
Meas. LPT Inlet Temp. T45	1218,59	1207,25	0,94	0,0490	
Meas. Turb. Exit Press. P5	175,232	174,41	0,47	0,0004	
Meas. Turb. Exit Temp. T5	830,17	830,17	0,00	0,0000	
Meas. Amb. Pressure Pamb	101,756	101,756	0,00	0,0000	
Meas. Gross Thrust	140,479	140,479	0,00	0,0000	

(a) Sensor check

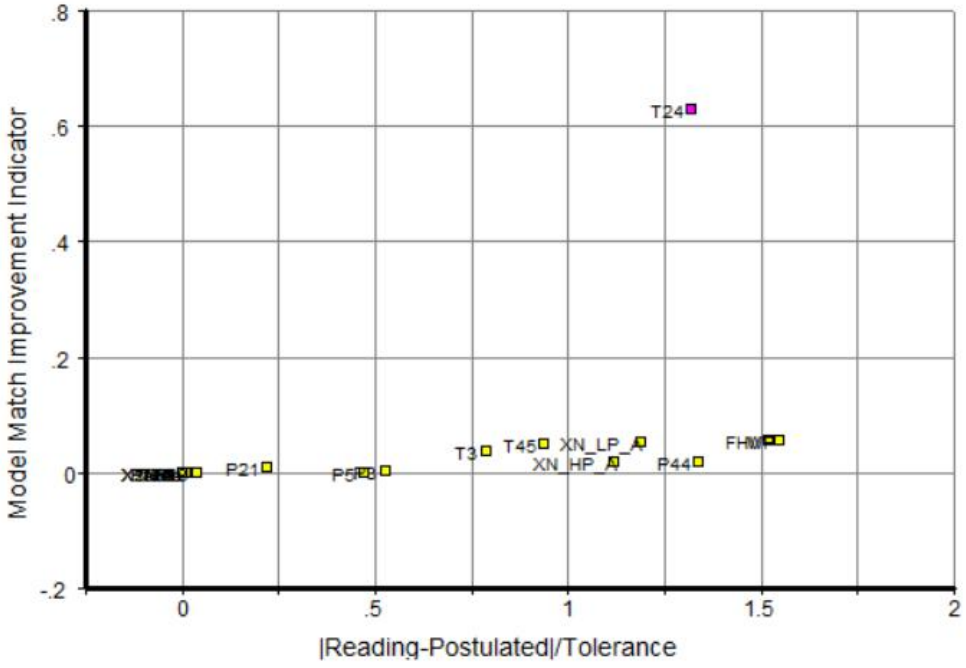

(b) Sensor check graph

Figure 5.10: Sensor check procedure

5.3 GasTurb Tool Summary

With the *GasTurb*® tool, it was possible to study the engine performance regarding its components and the impact that their performance have on the overall engine performance. With the developed MBTA Database, it is possible to identify which components are under performing of a specific engine and, if necessary, to focus performance restoration tasks to that component. This will allow TAP M&E to focus their human and financial resources.

With the Modifiers Tool it was possible to verify the impact that and increase or decrease of the component efficiency has on the overall engine performance.

With the *Sensor Check Tool*, TAP M&E has in its possession, a tool that can help identify inaccurate sensors, which, otherwise would make difficult the troubleshooting of an engine when it is necessary.

In the following chapter it will be studied the impact that HPC blades of the different stages have on the performance of the HPC itself. This will allow to estimate the performance of the HPC, thus helping the TAP M&E team taking into consideration which performance restoration tasks will be accomplished in a specified engine.

Chapter 6

HPC Rotor Blades Impact on Performance

In this chapter it will be studied the impact that HPC blades of the different stages have on its performance. This study will also complement the analysis made in chapter 7 where increases of the HPC efficiency was studied.

With respect to the HPC, the choice of installing new or OVH blades can represent a penalty in the HPC performance. As mentioned in section 2.2, the CFM56-5B has 9 rotors. From stage 4 to 9 the repair process of the blades can be done without restrains, meaning that the blade can be repaired in regard to all geometric properties and attain the shape as if it were a blade in the new condition. From stage 1 to 3 the blades are made of a titanium alloy that is very difficult to weld. For that reason, the blades of these stages cannot be fully repaired regarding all geometric properties, specifically its chord. Its shape will be different from a blade in the new condition, even if in its repair process the airfoil, maximum thickness, blade angles and other geometric properties are optimized to the new chord.

In the following sections it will be analysed the *GasTurb*® MBTA results and the percentage of blades in the new condition that were installed in that specific compressor. An analytical study was also conducted to help understand which stages affect the HPC performance the most.

6.1 HPC Rotor Blades Analysis with MBTA

In table 6.1 it is presented the number of total blades per stage, the chord in a blade in the new condition, the minimum chord standards of the manual, the difference between the new and minimum chord and the possible chord loss (chord loss is the blade chord that was eroded due to particles in the air).

As mentioned earlier, it will be taken into account the possible chord loss in the first three stages, since it is not recoverable in these stages, however, as it was mentioned in section 3.3 and 3.4, the chord is not the only parameter that is changed with engine operation nor it was found to be the most important geometric parameter in the compressor stage performance.

The different stages of the compressor will also have different effects on the overall compressor

Stage	Total Blades	Min. Chord (mm)	Δ (mm)	Chord Loss (mm)
1	38	57.84	2.50	98
2	53	41.22	0.91	48.23
3	60	32.23	1.11	66.6
4	64	25.86	1.58	101.12
5	71	22.00	0.99	70.29
6	78	19.43	0.85	66.3
7	78	19.13	0.54	42.12
8	76	20.14	0.61	46.36
9	72	20.83	1.10	79.2

Table 6.1: Go/NoGo tool minimum chord standards [10]

performance, as demonstrated by Tabakoff *et al.* [19]. In a multi-stage compressor, the reduction in blade chord of the first stages will have a greater influence on the overall performance of the compressor when comparing with the last stages as seen in figure 3.14.

The HPC blades are represented in figure 6.1, where it is possible to compare the dimensions between stages.

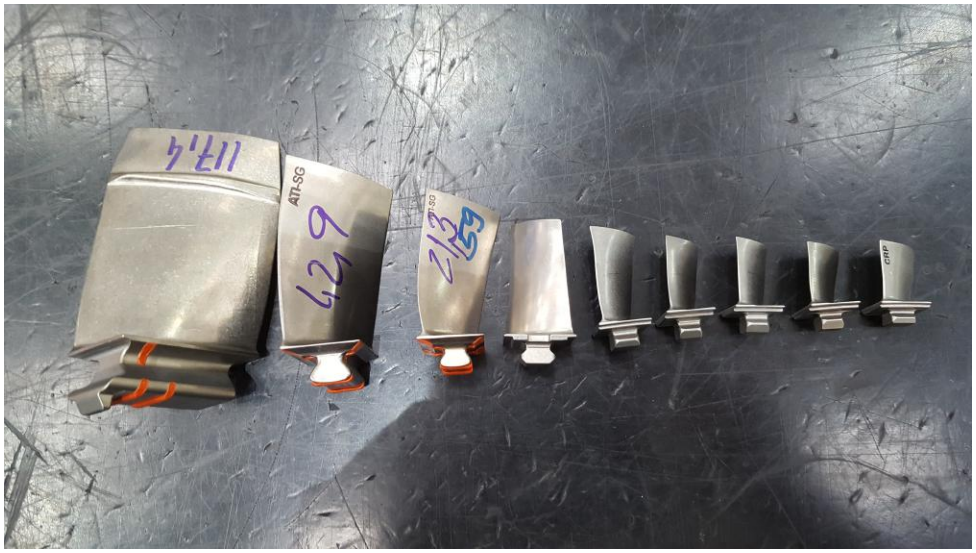

Figure 6.1: Blades from the CFM56-5B HPC: stage 1 to 9

The composition lists of the engines that were analysed in the MBTA were inspected to study if the HPC efficiency is related with the use of new and OVH blades. These lists possess all the information of parts that were installed in the engine. Some of the engines analysed had been tested over 10 years ago and it proved difficult to access this type of information, which resulted in a sample of only 10 engines.

It was considered the percentage of new blades of the first three stages only and also considering all the stages. The results are plotted in figure 6.2. The ”first three stages” points are represented with a polynomial cubic function and the ”all stages” points are represented with a polynomial quadratic function. The R^2 of the functions is low and, although the trend line shows that increasing the percentage of new blades installed in the HPC increase its efficiency, these functions should not be used to predict

the HPC performance due to the data not being fit to the regression lines. Other polynomial functions did not increase the R^2 significantly. It is possible to verify that the use of new blades will influence the HPC efficiency, especially when considering the first three stages. However, the points of the first three stages have to analysed separately (see table 6.2). For instance, the engine that is circulated in pink had 50% of new blades in stage 1. The red and blue circulated engines had 100% of new blades in stage 1, which can explain why the HPC performed better. Between the blue and red circulated engines, it is notable that the blue had a significant amount of new blades in the first three stages as well as in the remaining stages, which can explain why the trend line (orange) grows exponentially.

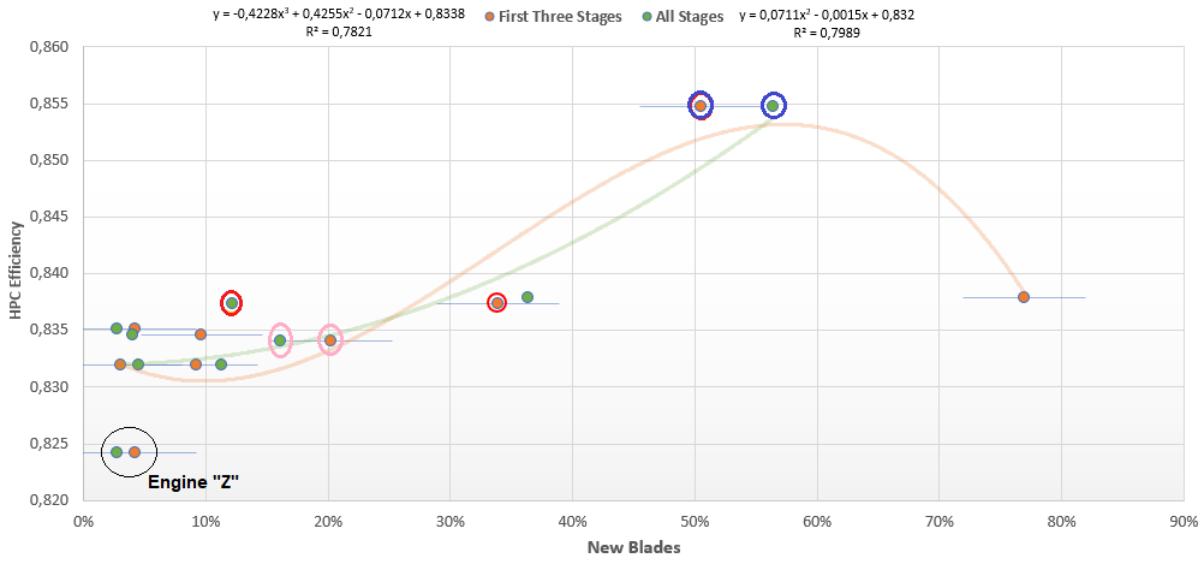

Figure 6.2: HPC efficiency as a function of the percentage of new blades

Engine	Stage	Percentage of New Blades
Pink Circulated	1	50
	2	5.7
	3	5
Red Circulated	1	100
	2	0
	3	1.7
Blue Circulated	1	100
	2	41.5
	3	10

Table 6.2: HPC new blades percentage per stage of 3 engines

In figure 6.3 it is presented a bar chart with the new blades percentage per stage as a function of the HPC efficiency. All stages play an important role in the HPC performance, however the first stage appears to influence the HPC efficiency the most. Polynomial trend line functions were added for the first four stages. It is possible to verify that, in the case of the three most efficient compressors, the percentage of new blades installed in the first stage is high, and it is accompanied by a high efficiency. However, these statistical results are of poor accuracy to predict the performance for a HPC due to the

low R^2 and small sample of engines.

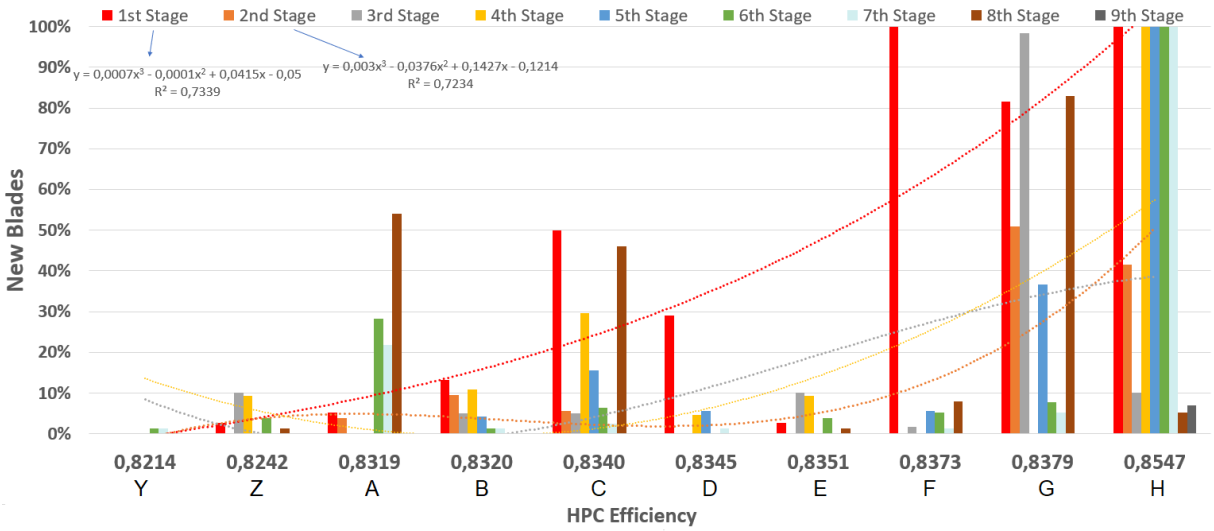

Figure 6.3: HPC efficiency and new blades per stage

These results are not unexpected. According to Marx *et al.* [20], it is hardly surprising that the performance of an OVH compressor may differ considerably from one that was newly manufactured. The quality of the airfoil repairs and the aerodynamic impact of disregarded geometry parameters will affect considerably the overall performance of the HPC.

6.2 HPC Stage Performance Calculation and Impact on Overall Compressor Efficiency

Stage efficiency is dependent on total drag coefficients for each of the blade rows comprising the stage, and, in order to evaluate these quantities, it is necessary to revert them to loss measurement. From the values of mean loss ϖ, the drag C_D and lift C_L coefficients can be obtained. To determine these coefficients, the methodology described in Gas Turbine Theory [23] will be used.

The total or stagnation pressure of a fluid is given by:

$$P_0 = P_s + P_{dyn}, \tag{6.1}$$

where the dynamic pressure is equal to $P_{dyn} = \frac{1}{2}\rho V^2$. Referring to the diagram of forces acting on the cascade, represented in figure 6.4, the static pressure rise across the blades is given by:

$$\Delta P = P_2 - P_1 = (P_{02} - \frac{1}{2}\rho V_2^2) - (P_{01} - \frac{1}{2}\rho V_1^2) \tag{6.2}$$

where P_0 is the stagnation pressure, ρ is the air density and V_1 and V_2 are the inlet and outlet flow velocity.

Since the variations in the fluid density are relatively small, the flow can be considered to be incompressible. Using cascade notation for velocities and angles:

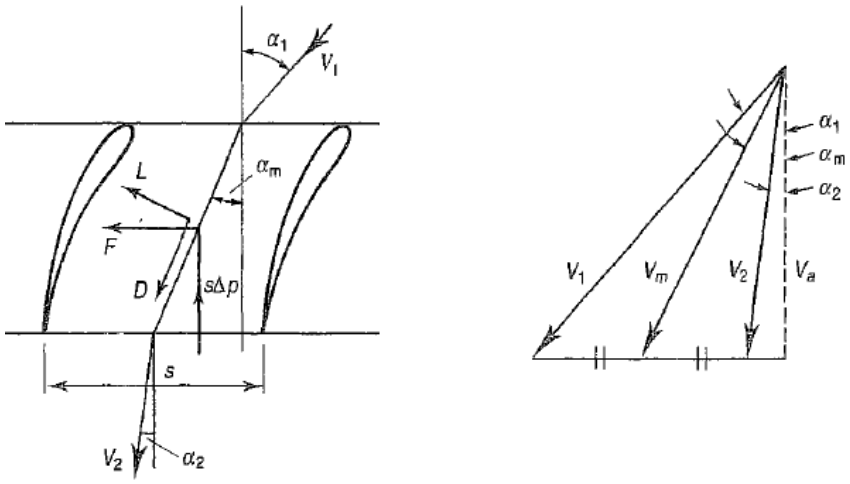

Figure 6.4: Forces acting on the compressor cascade [23]

$$\Delta P = \frac{1}{2}\rho(V_2^2 - V_1^2) - \varpi = \frac{1}{2}\rho V_a^2(\tan^2\alpha_1 - \tan^2\alpha_2) - \varpi, \tag{6.3}$$

where α_1 and α_2 are inlet and outlet blade angles, and the axial velocity V_a is assumed to be constant at the inlet and outlet. The force acting along the cascade is given by:

$$F = s\rho V_a^2(\tan\alpha_1 - \tan\alpha_2), \tag{6.4}$$

where s is the cascade pitch. The coefficients C_D and C_L are based on a vector mean velocity V_m defined by the velocity triangles in figure 6.4.

$$V_m = V_a \, sec\,\alpha_m, \tag{6.5}$$

where α_m is given by:

$$\tan\alpha_m = [\tfrac{1}{2}(V_a\tan\alpha_1 - V_a\tan\alpha_2) + V_a\tan\alpha_2]/V_a = \tfrac{1}{2}(\tan\alpha_1 + \tan\alpha_2) \tag{6.6}$$

Drag and lift forces act along and perpendicular respectively to the direction of the mean vector velocity. Resolving along the mean vector:

$$D = \tfrac{1}{2}\rho V_m^2 c\, C_{DP} = F\sin\alpha_m - s\Delta P\cos\alpha_m \tag{6.7}$$

where c is the blade chord and C_{DP} is the profile drag coefficient. From equations (6.3) and (6.4) and resolving for C_{DP} the equation reduces to:

$$C_{DP} = \left(\frac{s}{c}\right)\left(\frac{\varpi}{\frac{1}{2}\rho V_1^2}\right)\left(\frac{\cos^3\alpha_m}{\cos^2\alpha_m}\right) \tag{6.8}$$

Resolving for the perpendicular direction:

$$L = \tfrac{1}{2}\rho V_m^2 c C_L = F\cos\alpha_m + s\Delta P \sin\alpha_m \tag{6.9}$$

Therefore:

$$C_L = 2\left(\frac{s}{c}\right)(\tan\alpha_1 - \tan\alpha_2)\cos\alpha_m - C_{DP}\tan\alpha_m \tag{6.10}$$

Because the term C_{DP} is relatively small, it can be neglected in equation (6.10). By determining C_L, it is possible to read C_{DP} from figure 6.5. A digitizer software was used to extract the points of figure 6.5, thus using the polynomials equations from the points extracted to determine C_{DP}. Using equation (6.8) it is now possible to calculate the pressure loss factor $\frac{\varpi}{\frac{1}{2}\rho V_1^2}$.

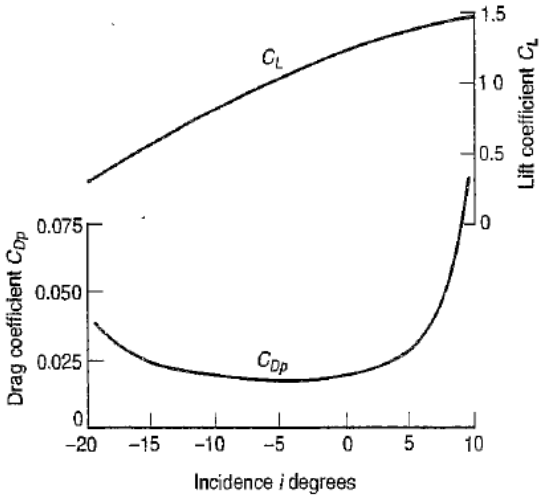

Figure 6.5: Lift and drag coefficients for cascade of fixed geometry [23]

Before these coefficients can be applied to the blade rows of the compressor stage, two additional factors must be taken into account: drag effects due to the walls of the compressor annulus (C_{DA}) and the secondary loss due to trailing edge vortices and tip clearance (C_{DS}). The following empirical formulas developed by Howell [14] were used:

$$C_{DS} = 0.018\, C_L^2 \tag{6.11a}$$

$$C_{DA} = 0.02\left(\frac{s}{h}\right) \tag{6.11b}$$

An overall drag coefficient can now be calculated, by summing the previous drag coefficients:

$$C_D = C_{DP} + C_{DS} + C_{DA} \tag{6.12}$$

The argument used in deriving equation (6.8) for the profile drag coefficient in the case of a straight cascade also applies to the annular case by substituting C_{DP} for C_D thus enabling the loss coefficient $\frac{\varpi}{\frac{1}{2}\rho V_1^2}$ to be determined. Equation (6.8) becomes:

$$C_D = \left(\frac{s}{c}\right)\left(\frac{\varpi}{\frac{1}{2}\rho V_1^2}\right)\left(\frac{\cos^3 \alpha_m}{\cos^2 \alpha_m}\right) \tag{6.13}$$

The theoretical static pressure rise in the blade row can be determined by equalling the loss to zero in equation (6.3), which gives:

$$\frac{\Delta P_{th}}{\frac{1}{2}\rho V_1^2} = 1 - \frac{\cos^2 \alpha 1}{\cos^2 \alpha 2} \tag{6.14}$$

The efficiency of the blade row η_b, which is defined as the ratio of actual pressure rise to the theoretical pressure rise can be found from:

$$\eta_b = 1 - \frac{\frac{\varpi}{\frac{1}{2}\rho V_1^2}}{\frac{\Delta P_{th}}{\frac{1}{2}\rho V_1^2}} \tag{6.15}$$

A compressor stage comprises both a rotor and a stator. The increase in enthalpy in the stage is shared by both the rotor and stator where the degree of reaction can determined through:

$$R = \frac{\Delta H_{rotor}}{\Delta H_{stator}} \tag{6.16}$$

Considering symmetrical blading in the stage and a stage reaction of 50% in the mean diameter of the blade will lead to symmetrical velocity triangles as represented in figure 6.6. In these conditions the blade row efficiency η_b will be the same for the rotor and stator.

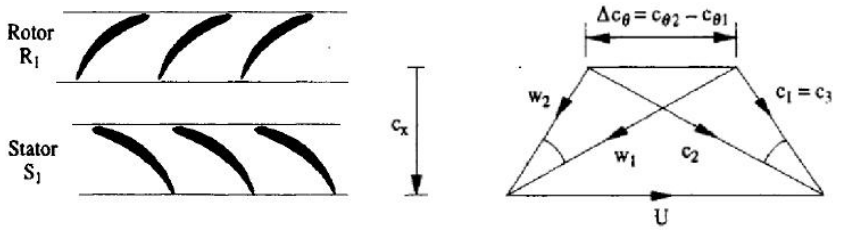

Figure 6.6: Velocity triangles for a 50% reaction compressor stage [41]

However, the blade row efficiency still has to be related to the isentropic efficiency of the whole stage, which was demonstrated by Cohen *et al.* in reference [23] that $\eta_s = \eta_b$. In the case of 50% reaction compressor stage, the stage efficiency will be:

$$\eta_{stg} = \frac{1}{2}(\eta_{b:rotor} + \eta_{b:stator}) \tag{6.17}$$

Since the study focus only on the rotor, the efficiency of the stage will be considered to be equal to the efficiency of the rotor. The static pressure ratio across a compressor stage can be found by:

$$\frac{P_2}{P_1} = \left[1 + \frac{\eta_s \Delta T_s}{2T_1}\right]^{\frac{\gamma}{\gamma-1}} \tag{6.18}$$

It is of interest the efficiency of the stage considering the stagnation temperatures, however for the common case when the inlet and outlet velocities are equal ($C_3 = C_1$) there is no need to elaborate any

further since the difference between the stagnation and static temperatures are equal ($\Delta T_{0s} = \Delta T_s$).

To obtain an estimate of the overall efficiency of the compressor it is necessary to repeat the previous methodology for all the compressor stages. The product of the pressure ratios will then yield the overall pressure ratio, and hence the compressor efficiency can be calculated using equation (5.2a).

Many correlations are available to estimate compressor losses. The reduction of blade chord in such correlations do not reflect the performance loss of a compressor, as by evaluating equation (6.10), the small chord reduction will result in a higher lift coefficient C_L which will lead to a lower or higher profile drag coefficient C_{DP} depending of the original C_L value (figure 6.5). Such correlations are intended to help the compressor designer and not to evaluate deterioration effects. A more precise correlation such as the Koch & Smith [42] yielded the same results, where a chord reduction would result in an increase of the overall HPC efficiency.

6.2.1 Blade Measurements

HPC blades in the new condition represented in figure 6.1 were measured in chord and in height with a digital pachymeter represented in figure 6.7. Blade angles and pitch were not possible to measure at the engine shop since a mounted HPC rotor was necessary to perform those measurement and none was available. To bypass this situation it was decided to use the blade angles that were measured in the CFM56-3 in the work developed by Martins [25] and the angles of the third stage were used in the remaining stages. Since the objective was to evaluate which stages affected the most the overall HPC performance and why, these measurements were only necessary to calculate a reference efficiency.

Figure 6.7: Digital pachymeter

In table 6.3 it is presented the measurements used in the methodology described earlier.

6.2.2 Results

In table 6.4 it is presented the results of the HPC performance using the Howell correlation [14]. As mentioned earlier, the objective is to understand why the HPC performance is more sensitive to the first stages, rather than obtaining an estimate of the HPC efficiency.

By applying decrements of the stage efficiency η_s in equation (6.18) and calculating the HPC efficiency using equation (5.2a), it is possible to perform a sensitivity analysis in the HPC. In figure 6.8 it

Stage	Total Blades	New Cond. Chord (mm)	Height (mm)	α_1 (deg)	α_2 (deg)	s (mm)
1	38	60.34	87.6	66.18	51.63	3.66
2	53	42.13	65.94	72.41	44.9	2.62
3	60	33.34	53.66	71.29	45.01	2.31
4	64	27.44	43.06	-	-	-
5	71	22.99	35.345	-	-	-
6	78	20.28	28.32	-	-	-
7	78	19.67	24.98	-	-	-
8	76	20.75	23.625	-	-	-
9	72	21.93	23.18	-	-	-

Table 6.3: HPC rotor blade measurements

Stage	C_L	C_D	$\frac{\varpi}{\frac{1}{2}\rho V_1^2}$	$\frac{\Delta P_{th}}{\frac{1}{2}\rho V_1^2}$	PR	η_{Stg}	$\eta_{is,HPC}$
1	0.599	0.0385	0.0864	0.5769	1.398	0.8502	
2	1.165	0.0509	0.0914	0.8179	1.369	0.8882	
3	1.219	0.0550	0.0889	0.7941	1.330	0.8880	
4	1.285	0.0603	0.0926	0.7941	1.296	0.8834	
5	1.303	0.0621	0.0940	0.7941	1.270	0.8817	0.8446
6	1.217	0.0561	0.0909	0.7941	1.250	0.8855	
7	1.165	0.0534	0.0903	0.7941	1.231	0.8863	
8	1.062	0.0480	0.0891	0.7941	1.216	0.8877	
9	0.964	0.0445	0.0909	0.7941	1.201	0.8856	

Table 6.4: HPC performance calculation

is demonstrated the overall HPC efficiency as a function of each stage efficiency. The results demonstrate that the previous stage is more relevant than the next one. These results are identical to the ones presented in reference [25], except that it is extended to all the stages of the HPC. The conclusions are however somewhat different. The reason why the first stages have a greater influence in the HPC performance is related to the pressure ratio of each stage. Since the pressure ratio of each stage continuously decreases along the compressor, the first stages will naturally influence the compressor performance the most. The pressure ratio of each stage is summarized in table 6.4 and illustrated in figure 6.9, and the overall compressor pressure ratio can be calculated using equation (6.19).

$$PR_{HPC} = PR_{Stg1} \times PR_{Stg2} \times PR_{Stg3} \times PR_{Stg4}... \tag{6.19}$$

By evaluating equation (6.18) it is possible to verify why this is an expected result. Since the increase in temperature ΔT_s is equal for all stages, the inlet temperature of the stage T_1 will increase by an amount of ΔT_s for the subsequent stages, thus decreasing the pressure ratio of the following stages.

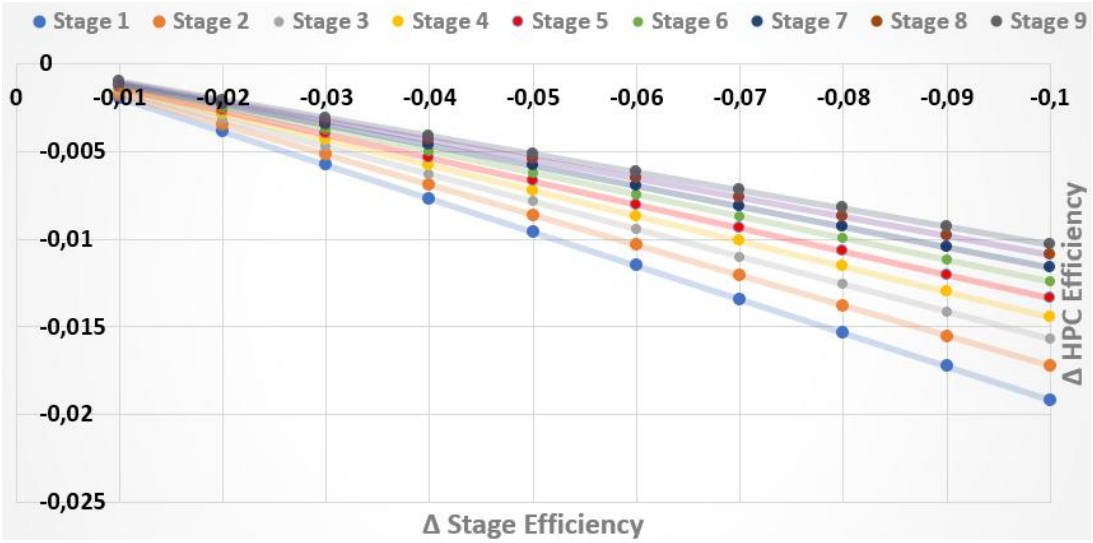

Figure 6.8: HPC sensitivity analysis

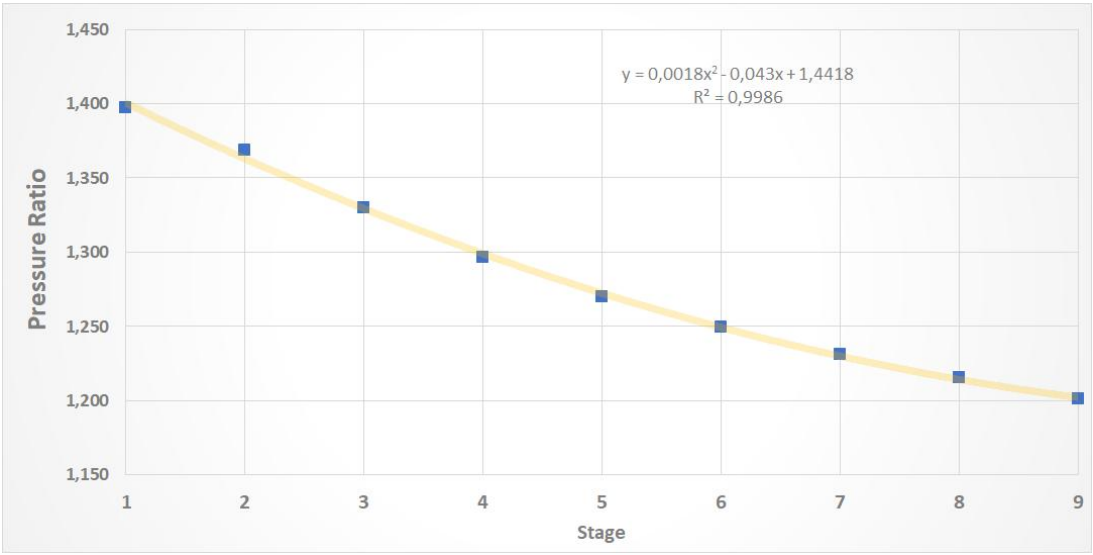

Figure 6.9: Pressure ratio per stage of the HPC

Chapter 7

Maintenance, Performance and Cost Analysis

In this section it will be given two examples to illustrate the benefit that this model and the database can have when troubleshooting in an engine is necessary. It will be used as an example an engine that failed the performance acceptance test, which will be labelled Engine ”Y”, and an engine that had an average performance, which will be labelled Engine ”Z”. A cost analysis for every engine that was analysed with MBTA which demonstrated that a maintenance/performance plan can lead to potential savings in the HPC maintenance.

7.1 Performance Analysis

Test Case Engine ”Y”

In the performance acceptance test, Engine ”Y” had an EGT HD margin of -7K. By analysing figures 7.1 and 7.2 it is possible to verify that all components, with exception of the LPT, are below average in efficiency as in capacity. Since both the booster and the fan are outside of this thesis scope (for the reasons mentioned in section 5.2), the HPC component stands out, as its performance is approximately 2.25% below average. By possessing this knowledge of the components performance, maintenance tasks can be redirected to that specific component that is in fault. The next step would be to estimate what would the gain be in the overall performance of the engine if an increase in the HPC efficiency was achieved. This can be done using again the *Modifiers Tool*. At this point, the current engine performance is known, therefore, the AnSyn factors can be replicated in the *Modifiers Tool* to match the model with the performance of Engine ”Y”.

Spot Engine

Engine "Y"

	Efficiency	Eff. AnSyn Factor	Eff. Delta Percentage (%)	Average Eff. Delta Percentage (%)	Eff. [Above / Below Average]
Fan Outer	0,86168	1,00126	0,126%	0,106%	0,020%
Fan Inner	0,86159	1,00115	0,115%	0,101%	0,014%
Booster	0,88029	0,98259	-1,741%	1,013%	-2,754%
HPC	0,82138	0,96232	-3,768%	-1,514%	-2,254%
HPT	0,90909	1,00162	0,162%	0,750%	-0,587%
LPT	0,89407	1,00493	0,493%	-0,080%	0,573%

		Average EGT HD	
EGT HD (K)	1217,55	1179,36	
EGT HD Margin (K)	-7,40	30,79	-38,19
EGT HD Margin Difference (K)	-32,01	6,17	
		Average TSFC (g/(N*s))	
TSFC (g/(N*s))	11,2682	11,139	1,160%

Flow Factor	Flow Delta Percentage	Average Flow Delta Percentage	Flow [Above/Below Average]
1,00000	0,000%	0,000%	0,000%
0,98118	-1,882%	-0,461%	-1,421%
0,95445	-4,555%	-1,270%	-3,285%
0,97319	-2,681%	0,214%	-2,895%
0,96630	-3,370%	-0,727%	-2,644%

Figure 7.1: Engine ”Y” MBTA

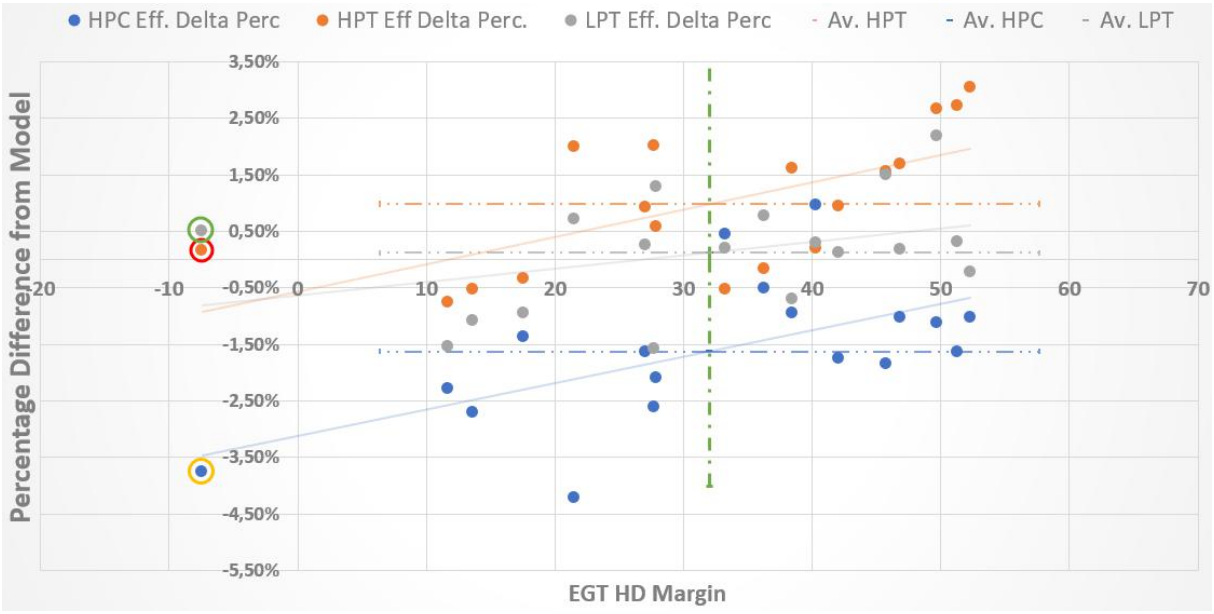

Figure 7.2: Engine ”Y” MBTA graph efficiency location

A compressor with poor efficiency will usually also show low flow capacity. In *GasTurb*® this dependence is automatically taken into account [4]. In figure 7.3 that dependence is visible. The difference between the operation points in figures 7.3a and 7.3b is a decrease of 3% in the HPC efficiency, which resulted in a shifting of the operation point in the map to a lower efficiency and capacity point.

In figure 7.4a, Engine ”Y” AnSyn factors are replicated in *GasTurb*® *Modifiers* (Original Modifiers) and the cycle is ran. The LP spool speed N1 should be limited to match the engine performance test and this way avoiding the cycle to converge out of range of the LP spool speed. The performance parameters such as efficiencies, thrust, TSFC and EGT are exported. By applying a delta modifier of 1% in the HPC efficiency, the Resulting Modifiers are calculated and are again used in *GasTurb*®. Note that the HPC efficiency Modifier changed from -3.768% to -2.768%, which is the equivalent to a 1% gain in efficiency. The performance parameters are again exported and compared with the Original Cycle. In figure 7.4b, it is possible to evaluate the improvement in the overall performance of the engine. Regarding the fan, booster, LPT and thrust, the variation is insignificant as in some cases it is lower than 0.1%. A gain in the HPC and the HPT was noted, although much smaller in the case of the HPT. The most notable improvements were regarding the TSFC with a gain of -0.7% and EGT with a gain of -1.075%, which translates into an increase of the EGT HD margin of approximately 13K.

Although it may give some guidance to identify which component is in fault, this methodology does not pinpoints the exact problem of the specific component, and so, a more scrutinized investigation of the maintenance works has to be done.

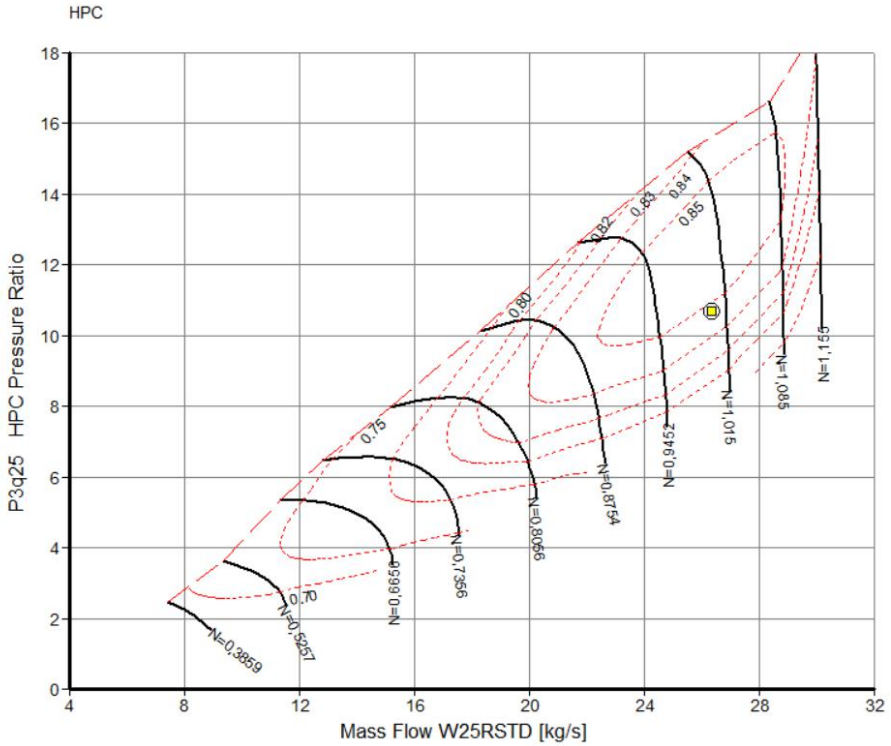

(a) Design point in the HPC map

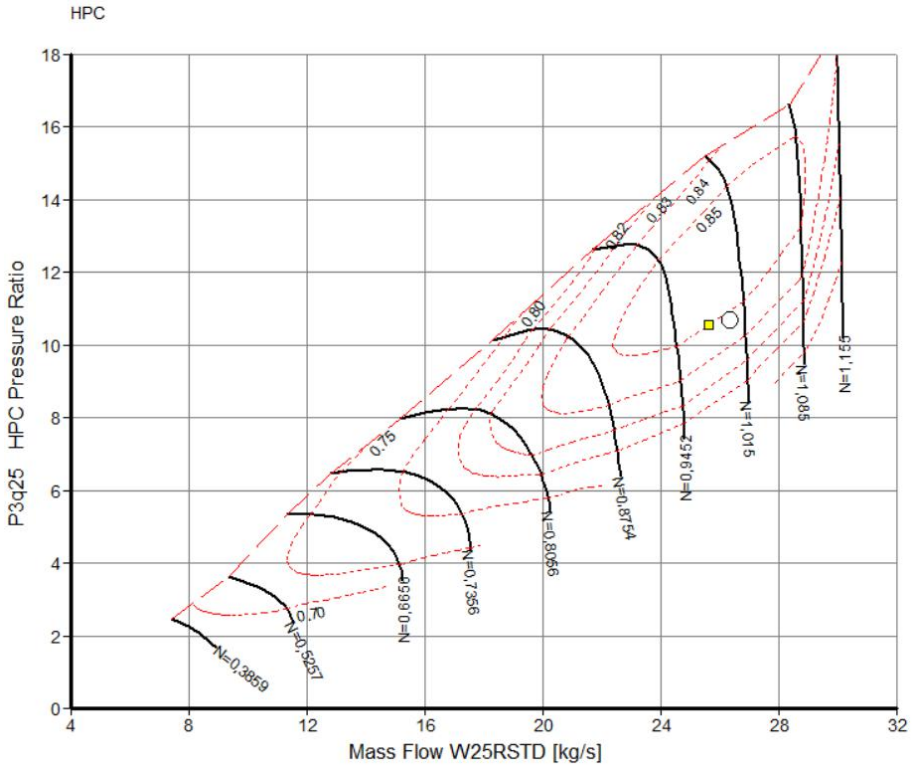

(b) Operation point with a decrease in the HPC efficiency

Figure 7.3: Efficiency and capacity dependence

Engine S/N		Original Modifiers	Delta Modifier (%)	Resulting Modifiers
Engine "Y"	Delta LPC (Fan) Capacity	0,000%	0%	0,000%
	Delta Outer LPC Efficiency	0,126%	0%	0,126%
	Delta Inner LPC Efficiency	0,115%	0%	0,115%
	Delta Booster/IPC Capacity	-1,882%	0%	-1,882%
	Delta Booster/IPC Efficiency	-1,741%	0%	-1,741%
	Delta HPC Capacity	-4,555%	0%	-4,555%
	Delta HPC Efficiency	-3,768%	1%	-2,768%
	Delta HPT Capacity	-2,681%	0%	-2,681%
	Delta HPT Efficiency	0,162%	0%	0,162%
	Delta LPT Capacity	-3,370%	0%	-3,370%
	Delta LPT Efficiency	0,493%	0%	0,493%

(a) Original, delta and resulting modifiers of engine "Y"

Original Cycle Output		Resulting Cycle Output		Gain / Loss	
Isentr. Outer LPC Efficiency	0,86367	Isentr. Outer LPC Efficiency	0,86328		-0,039%
Isentr. Inner LPC Efficiency	0,86356	Isentr. Inner LPC Efficiency	0,86317		-0,039%
Isentr. IPC Efficiency	0,87961	Isentr. IPC Efficiency	0,87828		-0,132%
Isentr. HPC Efficiency	0,81626	Isentr. HPC Efficiency	0,82559		0,933%
Isentropic HPT Efficiency	0,90780	Isentropic HPT Efficiency	0,91029		0,249%
Isentropic LPT Efficiency	0,89586	Isentropic LPT Efficiency	0,89558		-0,028%
Net Thrust (kN)	143,900	Net Thrust (kN)	143,71845	-0,182	-0,126%
TSFC (g/(N*s))	10,996	TSFC (g/(N*s))	10,91809	-0,077	-0,704%
EGT (K)	1147,15	EGT (K)	1134,80908	-12,336	-1,075%
EGT HD (K)	1208,58	EGT HD (K)	1195,59	-12,997	-1,075%
EGT HD Margin (K)	1,57	EGT HD Margin (K)	14,56	12,997	830,267%

(b) Original and resulting cycle with the respective gains of engine "Y"

Figure 7.4: Modifiers analysis

Test Case Engine ”Z”

Engine ”Z” had an EGT HD margin of 27.7K, which is a relatively close value to the average of the analysed engines, as seen in figure 7.5. It is, however, noticeable that two components are performing below average, -1.1% and -1.4% for the HPC and LPT respectively. In chapter 6, the percentage of new blades used in the HPC and their effect on its performance was studied. In figure 6.2 engine ”Z” is identified, and it is possible to verify that this engine had very few blades in the HPC that were in the new condition (4.2% regarding the first three stages and 2.7% if considering all stages). Although the engine performance is acceptable, it could be improved if it were decided to replace overhauled for new blades. As in the example of engine ”Y”, an increase of 1% in the HPC efficiency was applied with the *Modifiers Tool*. In figure 7.6 it is possible to verify that this increase of the HPC performance resulted in a gain of -0.541% of TSFC and a gain of approximately 9.8K in the EGT HD margin.

According to the engine manufacturer [43], a new CFM56-5B3 engine possesses an EGT HD margin of approximately 63K. Until it reaches an EGT HD margin of 0K, it has the capability to fly 42,300 hours, taking into account only performance restoration, i.e, disregarding any possible shop visits due to life limited parts. By performing a linear extrapolation, it is possible to verify what the gain would be in terms of engine flight hours. The new EGT HD margin would add to the engine approximately 7,000 flight hours.

	A	B	C	D	E	F
1			Spot Engine			
2			Engine "Z"			
3						
4		Efficiency	Eff. AnSyn Factor	Eff. Delta Percentage (%)	Average Eff. Delta Percentage (%)	Eff. [Above / Below Average]
5	Fan Outer	0,86337	1,00011	0,011%	0,106%	-0,096%
6	Fan Inner	0,86316	0,99986	-0,014%	0,101%	-0,115%
7	Booster	0,90023	1,01461	1,461%	1,013%	0,449%
8	HPC	0,82421	0,97383	-2,617%	-1,514%	-1,103%
9	HPT	0,92740	1,02015	2,015%	0,750%	1,266%
10	LPT	0,87445	0,98424	-1,576%	-0,080%	-1,495%
11						Average EGT HD
12	EGT HD (K)	1182,45				1179,36
13	EGT HD Margin (K)	27,70				30,79
14	EGT HD Margin Difference (K)	3,09				6,17
15						Average TSFC (g/(N*s))
16	TSFC (g/(N*s))	11,2646				11,139

G	H	I	J
Flow Factor	Flow Delta Percentage	Average Flow Delta Percentage	Flow [Above/Below Average]
1,00000	0,000%	0,000%	0,000%
1,00309	0,309%	-0,461%	0,770%
1,00429	0,429%	-1,270%	1,699%
1,02408	2,408%	0,214%	2,195%
1,01158	1,158%	-0,727%	1,885%

Percentage Delta (%)	
PD> 1%	
0,1%<PD<1%	
-0,1%<PD<0,1%	
-1%<PD<-0,1%	
PD<-1%	

Figure 7.5: Engine ”Z” MBTA

Engine S/N		Original Modifiers	Delta Modifier (%)	Resulting Modifiers
Engine "Z"	Delta LPC (Fan) Capacity	0,000%	0%	0,000%
	Delta Outer LPC Efficiency	0,011%	0%	0,011%
	Delta Inner LPC Efficiency	-0,014%	0%	-0,014%
	Delta Booster/IPC Capacity	0,309%	0%	0,309%
	Delta Booster/IPC Efficiency	1,461%	0%	1,461%
	Delta HPC Capacity	0,429%	0%	0,429%
	Delta HPC Efficiency	-2,617%	1%	-1,617%
	Delta HPT Capacity	2,408%	0%	2,408%
	Delta HPT Efficiency	2,015%	0%	2,015%
	Delta LPT Capacity	1,158%	0%	1,158%
	Delta LPT Efficiency	-1,576%	0%	-1,576%

(a) Original, delta and resulting modifiers of engine "Z"

Original Cycle Output		Resulting Cycle Output		Gain / Loss	
Isentr. Outer LPC Efficiency	0,85968	Isentr. Outer LPC Efficiency	0,85935		-0,033%
Isentr. Inner LPC Efficiency	0,85943	Isentr. Inner LPC Efficiency	0,85910		-0,033%
Isentr. IPC Efficiency	0,90124	Isentr. IPC Efficiency	0,89831		-0,293%
Isentr. HPC Efficiency	0,82036	Isentr. HPC Efficiency	0,82904		0,868%
Isentropic HPT Efficiency	0,92920	Isentropic HPT Efficiency	0,93074		0,154%
Isentropic LPT Efficiency	0,87187	Isentropic LPT Efficiency	0,87142		-0,044%
Net Thrust (kN)	145,198	Net Thrust (kN)	145,06381	-0,134	-0,093%
TSFC (g/(N*s))	11,193	TSFC (g/(N*s))	11,13270	-0,061	-0,541%
EGT (K)	1121,40	EGT (K)	1112,09840	-9,301	-0,829%
EGT HD (K)	1181,46	EGT HD (K)	1171,66	-9,799	-0,829%
EGT HD Margin (K)	28,69	EGT HD Margin (K)	38,49	9,799	34,156%

(b) Original and resulting cycle with the respective gains of engine "Z"

Figure 7.6: Modifiers analysis

7.2 Maintenance and Cost Analysis

In terms of performance, it is desirable that the HPC is fitted with new blades only since the results demonstrate that this approach maximizes the performance of the HPC. However, in general, this maintenance practice is not sustainable due to the high cost of the rotor blades. A rotor blade in the OVH condition costs approximately 10% the price of a new blade. For that reason, the installation of new blades is done only when the contractualized performance of the engine justifies it so.

The following table presents the price of one HPC rotor blade for each stage:

Stage	Price
1	$ 1,012.00
2	$ 483.75
3	$ 405.50
4	$ 296.75
5	$ 284.50
6	$ 254.75
7	$ 252.50
8	$ 228.00
9	$ 224.00

Table 7.1: CFM56-5B HPC rotor blades price

Due to confidentiality reasons, the prices presented in table 7.1 are fictitious, however, the price difference between stages are proportional to the real prices. It is noticeable that the blades of the first three stages are the most expensive ones and that the blades of the first stage cost more than double than the blades of the second stage.

In the next table it is presented the investment of each HPC of every engine that was analysed with *GasTurb*® MBTA. It is presented the HPC efficiency, the cost of blades in new condition installed in first three stages, the cost of blades in new condition installed in stages 4 to 9, the total investment in the HPC regarding rotor blades and the investment (in percentage) in terms of the total cost regarding the first three stages and stages 4 to 9.

It is noticeable that engines with a good performance (engines ”F” ”G” and ”H”) are the ones where a greater investment was made, with the exception of engine ”C”, where a total investment of $40,422.25 in new HPC rotor blades was made, and the HPC performance was still below other engines. By comparing engines ”C” and ”F”, where the total investment difference was approximately $2,200, it is possible to verify that in the the case of engine ”F”, 91.14% of the total investment was made in the first three stages, while in the case of engine ”C”, 54.17% of the total investment was made in the first three stages. As demonstrated in chapter 6, the first three stages influence the HPC performance more when compared to the latter stages, which can justify the difference in performance of these two engines, although the total investment is similar. Some engines HPC perform better than others even though the total investment is lower, as is the case of engines ”D” and ”E” when compared to engines ”A” and ”B”. Because no documentation is generated regarding used HPC rotor blades, it is difficult to assess the

Engine	HPC Eff.	Cost of New Blades				
		Stages 1-3	Stages 4-9	Total	Invest. Stg. 1-3	Invest. Stg. 4-9
Y	0,8214	$ 0	$ 507.25	$ 507.25	0%	100%
Z	0,8242	$ 3,445	$ 2,772.75	$ 6,217.75	55.41%	44.59%
A	0,8319	$ 2,991.5	$ 19,245	$ 22,236.5	13.45%	86.55%
B	0,8320	$ 8,695.25	$ 3,438	$ 12,133.25	71.66%	28.34%
C	0,8340	$ 21,895.75	$ 18,526.5	$ 40,422.25	54.17%	45.83%
D	0,8345	$ 11,132	$ 2,280.75	$ 13,412.75	83%	17%
E	0,8351	$ 3,445	$ 2,772.75	$ 6,217.75	55.41%	44.59%
F	0,8373	$ 38,861.5	$ 3,777.5	$ 42,639	91.14%	8.86%
G	0,8379	$ 68,357.75	$ 24,299.5	$ 92,657.25	73.77%	26.23%
H	0,8547	$ 51,531.5	$ 80,789	$ 132,320.5	38.94%	61.06%

Table 7.2: Investment in the HPC rotor blades of the engines analysed with MBTA

degradation level of each blade, since, as long as the blades are within the minimum standards of the Go/NoGo tool, they can be installed in the HPC. In the case of engines ”D” and ”E”, it is possible that the installed blades in the HPC have low degradation levels, however it is only a mere possibility and not a conclusion due to the lack of information. Nonetheless, with an accurate statistical model that relates the HPC performance and the chord of its blades, it would be possible to estimate and have a better control of the investment made in the HPC rotor blades, since it is not of the interest of TAP M&E to not reach or largely exceed the contractualized performance of the engine considering that it will result in fines or a lower profit margin.

Although it was not possible to develop a statistical performance model for the HPC within this thesis, by using the chord of the blade as data instead of classifying the blades simply as new or OVH, this statistical model may allow TAP M&E to estimate the HPC performance. Assuming that this statistical model was already available, figure 7.8 demonstrates how it could be used. Every blade of the HPC would have to be measured and register its chord. This process would have to automatized since it would be very time consuming performing it manually. The development of a support device that holds all the blades and allows the coordinate measuring machine (CMM) to perform all the measurements, would greatly simplify this process (illustrated in figure 7.7).

By possessing the knowledge of the average chord of each stage, the next step would be to rely on the statistical model. Depending on the contractualized performance, it would be installed new or with low degradation level blades, which would increase the average chord at least for the first three stages, or in the case of a low contractualized performance, OVH blades could be installed. The resulting performance would then be added to the statistical model.

Figure 7.7: Coordinate measuring machine [44]

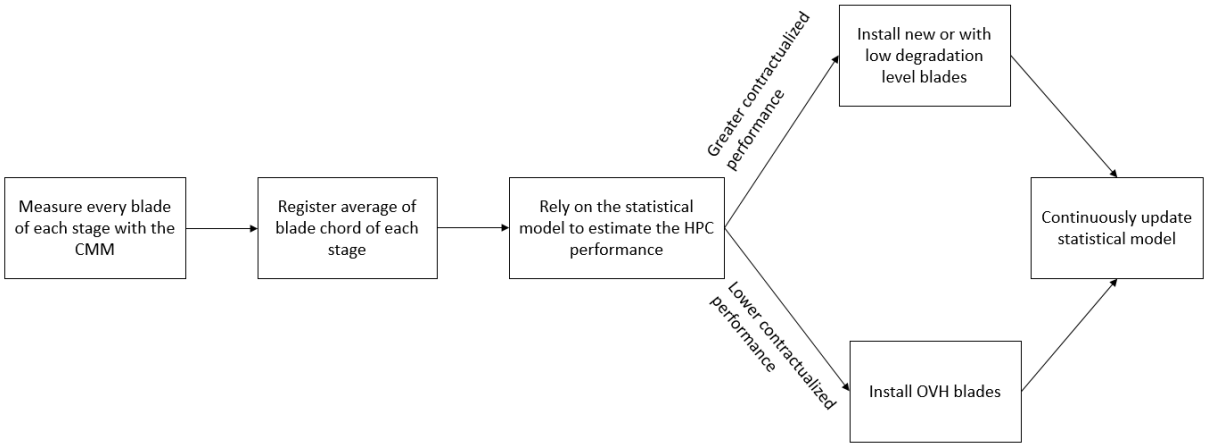

Figure 7.8: HPC maintenance/performance plan

Chapter 8

Conclusions

In the present chapter it will be presented the achievements of the work conducted in this thesis, the difficulties encountered throughout its development and lastly a list with proposed recommendations and suggestions for future work in this area.

The objective of this thesis was to evaluate the impact that the HPC performance has on the overall performance of the CFM56-5B engine. To aid that purpose, a 0-D thermodynamic model of the engine was available at TAP M&E, developed using the *GasTurb*® software. In order to develop the model, the performance parameters of the TAP test bed correlation engine were used. However, after conducting some MBTA's, the available model proved to be unsuited for performance studies, since the results were unrealistic regarding the booster performance. The problem that led to such results was diagnosed and corrected, which implied to rebuild the model. The first step was to define the engine cycle reference point. Once the cycle reference point was defined, the next step was to model the engine off-design operation. The newly developed model was able to replicate the correlation engine with precision in Maximum Continuous and Take Off regimes, that is above 80% of its maximum thrust.

Chapter 5 dealt with model validation and exercising using the tools provided by *GasTurb*®. The model behaviour was compared with a study conducted by GE, where decrements of efficiency were applied individually to each of the engine components. Of the 30 analysed parameters studied, the developed model complied with 28. A sensitivity analysis was conducted to the same parameters. The EGT revealed to be more sensitive to the engine core (HPT and HPC respectively) while thrust is more sensitive to the fan and LPT performance. Several CFM56-5B engines that were tested in the past were selected and a MBTA was conducted. A database was created using Excel VBA macros to ease the data processing and analysis. Since the original component maps are proprietary information of the manufacturer, standard *GasTurb*® maps were used. For that reason and although the model is precise, it is not exact, and so the database will allow to compare a specific engine performance with others engines. *GasTurb*® also has the capability to identify sensor measurements that may be imprecise. The sensor check procedure revealed useful in one of the analysed engines.

In chapter 6 it was studied the influence that HPC Rotor Blades have on the overall HPC performance. Because there are some limitations in the repair process of the blades regarding the chord of the first

three stages, the aerodynamic performance of such blades can vary when compared to a blade in the new condition. However, this analysis only took into account the condition of the blades used in the HPC, as no geometric properties were documented. The HPC performance analysis revealed a significant increase in the HPC efficiency with the use of blades in the new condition, specially for the first three stages. Nonetheless, it was not possible to relate the rotor blade chord with the HPC performance as other geometric properties are also reshaped with blade erosion, such as the leading edge geometry. Computational methods as CFD analysis would be required to relate the blade geometry and the HPC performance. With the use of empirical formulas, it was possible to conclude why in the HPC, the performance of the previous stage is more important than the next one. By applying decrements of the stage efficiency, it was possible to verify which stage affected the overall HPC performance the most. Because the stage pressure ratio decreases along the HPC, the overall pressure ratio of the compressor decreases in a greater magnitude when the first stages are less efficient.

By using the Modifiers Tool and the results of the MBTA analysis it is possible to replicate the analysed engine performance in the model and help TAP M&E to decide where to take action regarding overhauling or replacement of engine components. Two test cases were used as example (Test Case ”Y” and ”Z”), where an increment of 1% in the HPC efficiency was made. In both cases an improvement was achieved regarding the TSFC and EGT HD margin. By applying this methodology, TAP M&E has the possibility of estimating what the performance gains are, and by doing so, analyse in which component the financial and human resources should be applied, thus avoiding unnecessary costs in components that are performing well, which translates to better operational results of TAP M&E.

In conclusion, this thesis provided to TAP M&E very useful tools that will allow to assess the overall engine performance and provide guidance about the most adequate repairs that yield the targeted overall engine performance recovery. The created database will allow to store the engine components performance and compare a specific engine performance, thus permitting to evaluate which components are in fault. The HPC rotor blades study revealed that the use of blades in the new condition improved the overall HPC performance, thus allowing TAP M&E to take that fact into account when an engine comes to the shop for maintenance works.

8.1 Achievements

The major achievements of this thesis can now be described:

1. Improvement of the CFM56-5B thermodynamic model for high thrust settings;
2. Study of which components efficiencies influenced certain engine parameters the most;
3. Creation of a database using Excel VBA macros to store engine components performance and allow to compare the performance of a specific engine;
4. Implementation of various performance tests in *GasTurb*® Model Based Test Analysis;
5. Study of the overall performance gains when an increase of the HPC efficiency is achieved;

6. Analysis of the HPC rotor blades and its impact on the overall HPC performance;

7. Study of HPC stage efficiency and its effect on the overall compressor performance.

8.2 Future Work

Similar studies regarding the blades that constitute other components can be conducted, such as the fan, booster, HPT and LPT to assess its effect on the overall performance. However, to do so, it is required more test cell instrumentation, specifically in the stations before and after the component in study. Sensors can be designed at TAP M&E to allow to conduct such studies.

If the acquisition of a 3D scanner is possible, the geometry of blades can be digitalized and analyse with computational methods the performance of blades with different levels of deterioration, and ultimately analysing with MBTA to see if that performance deterioration is noted.

With these recommendations, a more precise estimation of the overall engine performance could be achieved by allowing the analyses of the performance of other components that currently are not instrumented.

Bibliography

[1] Rolls-Royce, editor. *The Jet Engine*. Rolls-Royce plc, Derby, England, 1986.

[2] M. P. Boyce. *Gas Turbine Engineering Handbook*. Gulf Professional Publishing, 2nd edition, 2002.

[3] S. Ackert. Engine maintenance concepts for financiers, September 2011. 2nd Edition.

[4] *GasTurb 12, Design and Off-Design Performance of Gas Turbines*. GasTurb Gmbh, 2015.

[5] P. M. A. Ribeiro. *Análise de Performance da Familía de Motores de Avião CFM56-3*. Master's thesis, Instituto Superior de Engenharia de Lisboa, Lisboa, Portugal, November 2012.

[6] J. Pabiot. Performance analysis on cfm56-5b. Internship Report, September 2015.

[7] P. C. . F. Trimouille. *Correlation Report of TAP Test Cell for CFM56-3 Engines*. CFMI, October 1991.

[8] G. Yanley and Z. Yanpei. Airworthiness management of cfm56 products in faa and easa. *The 2nd International Symposium on Aircraft Airworthiness*, 17:588–594, 2011. doi:10.1016/j.proeng.2011.10.074.

[9] Jet engine specifications. http://www.jet-engine.net/civtfspec.html, 2017.

[10] CFMI. *Training Manual CFM56-5B, Basic Engine*, December 2000.

[11] J. T. Borges. *Propulsão, Folhas de Apoio*. Instituto Superior Técnico, 2014/2015.

[12] J. Denton. Loss mechanisms in turbomachines. *Journal of Turbomachinery*, 115:621–656, 1993. doi:10.1115/1.2929299.

[13] W. J. Swift. *Modelling of Losses in Multi-Stage Axial Compressors with Subsonic Conditions*. Master's thesis, Potchefstroom University for Christian Higher Education, October 2003.

[14] A. R. Howell. Design of axial compressors. *Proc. Instn. Mech. Engrs.*, 1945.

[15] S. Dixon. *Fluid Mechanics and Thermodynamics of Turbomachinery*. Butterworth-Heinemann, 4th edition, 1998.

[16] N. Chen. *Aerothermodynamics of Turbomachinery, Analysis and Design*. John Wiley & Sons, 1st edition, 2010.

[17] C. B. M. Homji, M. A. Chaker, and H. M. Motiwala. Proceeding of the 30th turbomachinery symposium. In *Gas Turbine Performance Deterioration*, 2001.

[18] M. S. Grewal. *Gas Turbine Engine Performance Deterioration Modeling and Analysis*. PhD thesis, Cranfield Institute of Technology, Bedford, England, 1988.

[19] W. Tabakoff, A. Lakshimnarasimha, and M. Pasin. Simulation of compressor performance deterioration due to erosion. *Journal of Turbomachinery*, 112:78–83, 1990. doi: 10.1115/1.2927424.

[20] J. M. . J. S. . G. R. . J. Friedrichs. Investigation and analysis of deterioration in high pressure compressors due to operation. *German Aerospace Congress*, 2014. doi:10.1007/s13272-014-0118-z.

[21] G. R. . S. S. . J. Friedrichs. Design of experiments and numerical simulation of deteriorated high pressure compressor airfoils. In ASME, editor, *Proceedings of ASME Turbo Expo 2016*, June 2016.

[22] G. R. . A. K. . S. S. . J. Friedrichs. Comparison of sensitivities to geometrical properties of front and aft high pressure compressor stages. *Institute of Jet Propulsion and Turbomachinery*, 2016. Deutscher Luft- und Raumfahrtkongress.

[23] H. C. . C. R. . H. Saravanamutto. *Gas Turbine Theory*. Longman Group Limited, 4th edition, 1996.

[24] R. H. Aungier. *Axial-Flow Compressors, a Strategy for Aerodynamic Design and Analysis*. ASME Press, 1st edition, 2003.

[25] D. Martins. *Off-Design Performance Prediction for the CFM56-3 Aircraft Engine*. Master's thesis, Instituto Superior Técnico, Lisboa, Portugal, November 2015.

[26] *CFM56-5B Engine Shop Manual, Engine Assembly Testing 003 - Engine Acceptance Test, Task 72-00-00-760-003*. CFMI, 2016.

[27] A. Linke-Diesigner. *Systems of Commercial Turbofan Engines*. Springer, 1st edition, 2008.

[28] Egt margin by cfm. https://www.slideshare.net/RicardoCcoyureTito1/05-egt-margin-by-cfm, 2017.

[29] R. G. . D. Mosny. *Correlation Report of TAP Test Cell for CFM56-5B Engines*. CFMI, May 1999.

[30] J. Kurzke. How to create a performance model of a gas turbine from a limited amount of information. In S. ASME Turbo Expo 2005: Power for Land and Air, editors, *Proceedings of GT2005*, June 2005.

[31] J. C. . J. Jilek. The effect of low reynolds number on straight compressor cascades. In ASME, editor, *Proceedings of Gas Turbine and Aeroengine Congress and Exposition*, June 1990.

[32] A. B. Wassel. Reynolds number effect in axial compressors. *Journal of Engineering for Power*, 1968.

[33] J. Kurzke. *CFM56-3*, 2010. TAP - Private Communication.

[34] J. Ridaura. *Correlation Analysis Between HPC Blade Chord and Compressor Efficiency for the CFM56-3*. Master's thesis, Instituto Superior Técnico, Lisboa, Portugal, October 2014.

[35] M. J. M. . H. N. S. . D. D. B. . M. B. Bailey. *Fundamentals of Engineering Thermodynamics*. John Wiley & Sons Inc., 7th edition, 2011.

[36] J. D. M. . W. H. H. . D. T. Pratt. *Aircraft Engine Design*. American Institute of Aeronautics and Astronautics Inc., 2nd edition, 2002.

[37] *CFM56-3 Basic Engine, B737-300. Formação Profissional TAP. Revision 3*. TAP Portugal, 1992.

[38] *Power Plant Engineering for Commercial Engines 2016*. GE Proprietary Information, 2016.

[39] X. C. . F. K. . P. Sahm. Generation of physically based analysis factors to improve synthesis models of jet engines. In *Proceedings of GT2005*. Rolls-Royce Deutschland Ltd & Co KG, 2005.

[40] T. C. Corke. *Design of Aircraft*. Pearson Education, Inc., 1st edition, 2002.

[41] R. I. Lewis. *Turbomachinery Performance Analysis*. Elsevier Science & Techonolgy Books, 1st edition, 1996.

[42] C. C. K. . L. H. S. Jr. Loss sources and magnitudes in axial-flow compressors. *Journal of Engineering for Power*, 1976.

[43] CFM. *CFM56-5B Workscope Planning Guide*. CFMI, June 2016.

[44] Mitutoyo coordinate measuring machines catalogue. http://ecatalog.mitutoyo.com/Coordinate-Measuring-Machines-C101.aspx, 2017.

Appendix A

CFM56-3 Data

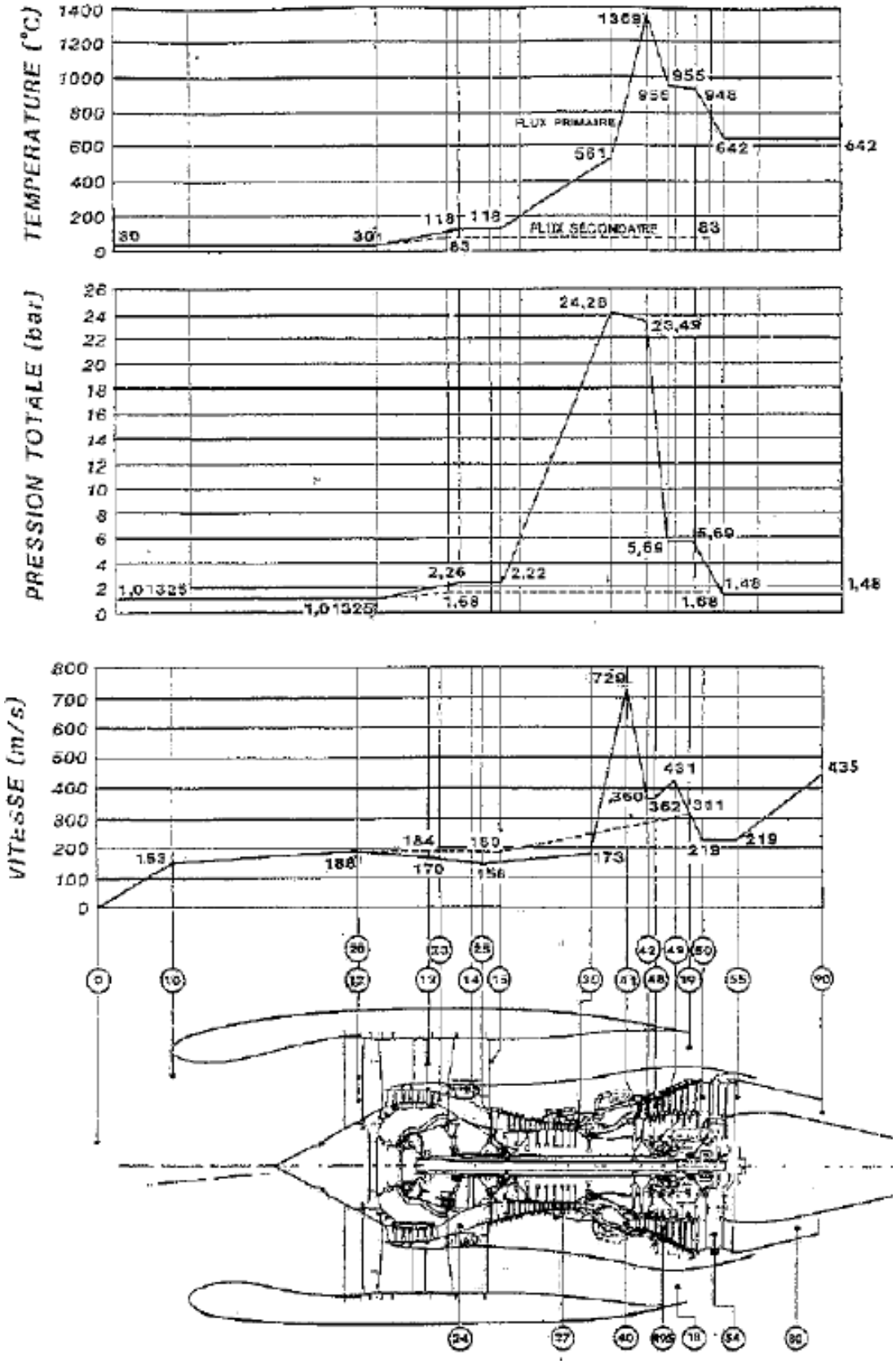

Figure A.1: Pressure, temperature and velocity distribution the CFM56-3 [Source:CFM]

Appendix B

Model Validation

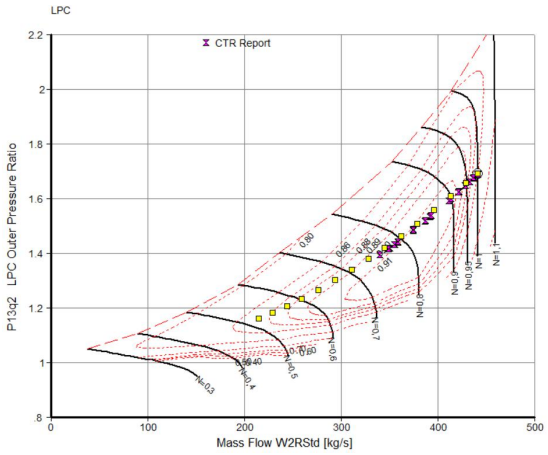

(a) LPC Map

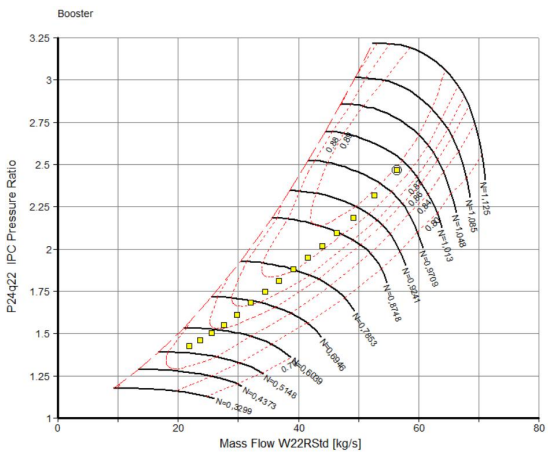

(b) Booster Map

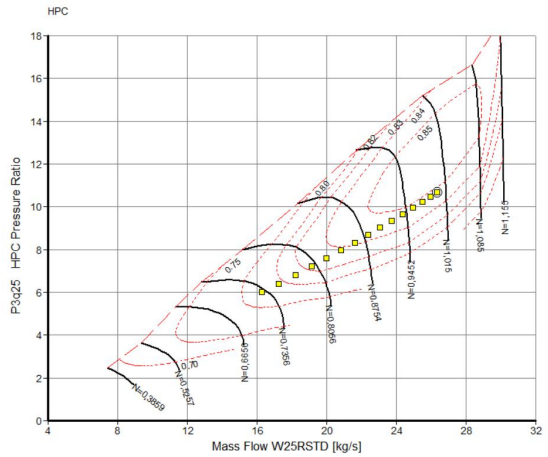

(c) HPC Map

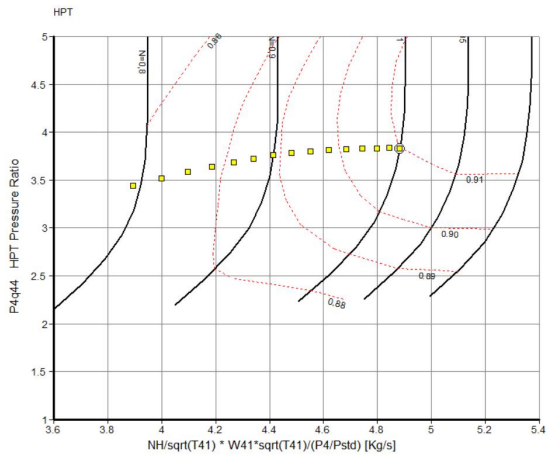

(d) HPT Map

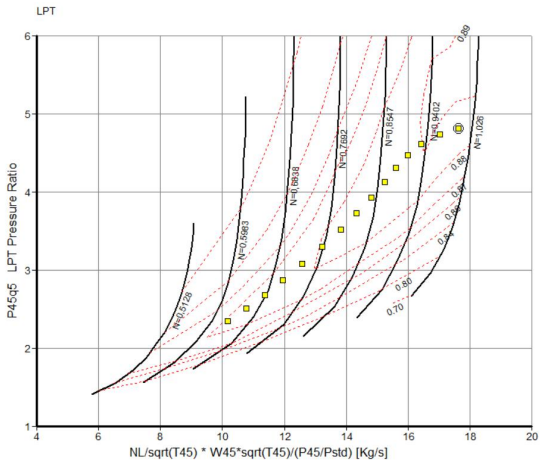

(e) LPT Map

Figure B.1: Components maps

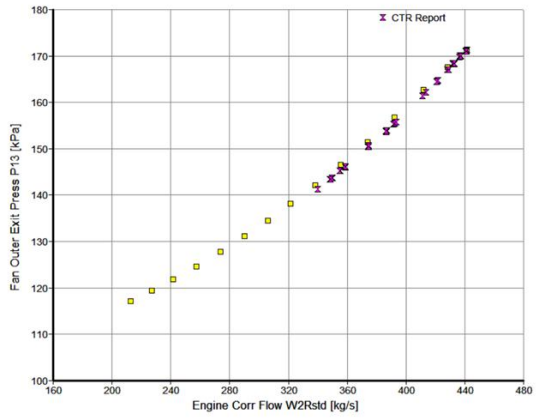

(a) P13

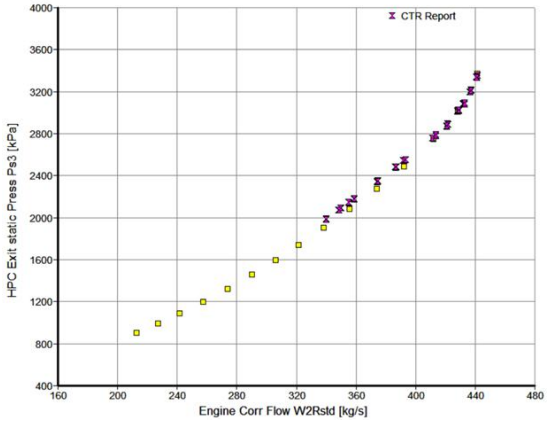

(b) Ps3

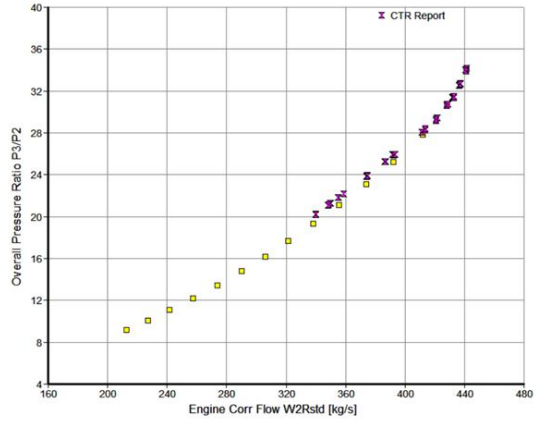

(c) P3/P2

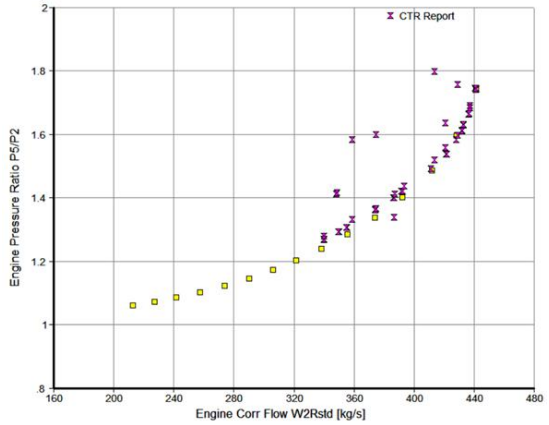

(d) P5/P2

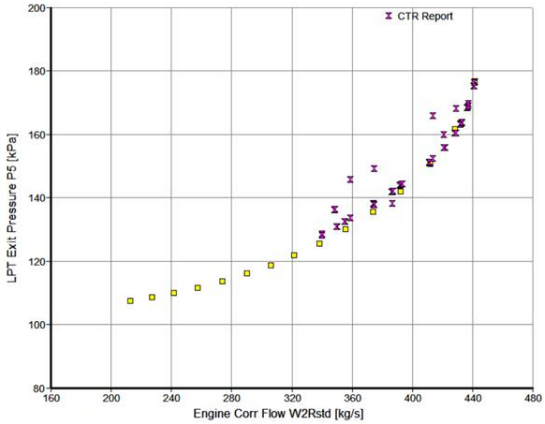

(e) P5

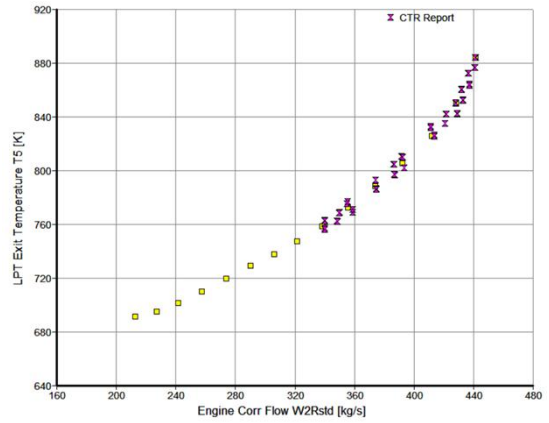

(f) T5

Figure B.2: Parameters validation

Appendix C

Engine ”X” Data

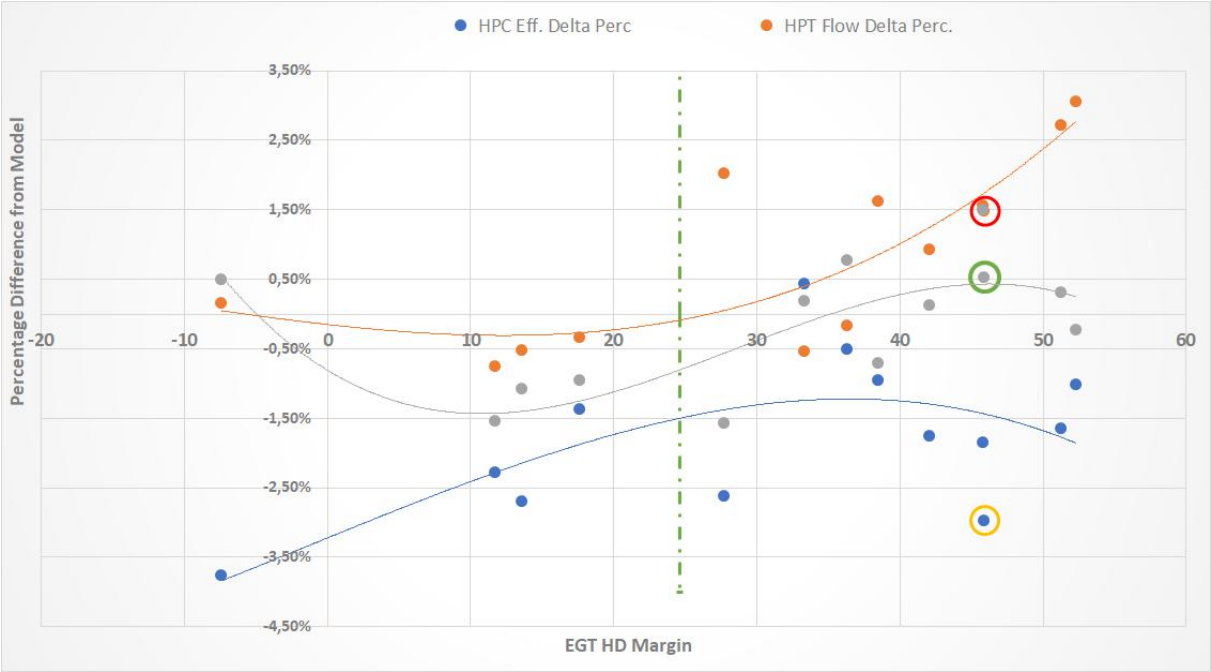

Figure C.1: Engine ”X” MBTA efficiency graph

Spot Engine

Engine "X"

	Efficiency	Eff. AnSyn Factor	Eff. Delta Percentage (%)	Average Eff. Delta Percentage (%)	Eff. [Above / Below Average]
Fan Outer	0,86397	1,00090	0,090%	0,108%	-0,017%
Fan Inner	0,86391	1,00084	0,084%	0,102%	-0,018%
Booster	0,93618	1,05000	5,000%	1,425%	3,574%
HPC	0,82555	0,97030	-2,970%	-1,771%	-1,199%
HPT	0,92324	1,01482	1,482%	0,862%	0,620%
LPT	0,89272	1,00531	0,531%	-0,167%	0,698%

		Average EGT HD	
EGT HD (K)	**1164,25**	**1178,71**	
EGT HD Margin (K)	**45,90**	**31,44**	14,46
EGT HD Margin Difference (K)	**21,29**	**6,83**	
		Average TSFC (g/(N*s))	
TSFC (g/(N*s))	**10,8892**	**11,133**	-2,187%

Flow Factor	Flow Delta Percentage	Average Flow Delta Percentage	Flow [Above/Below Average]
1,00000	0,000%	0,000%	0,000%
0,99271	-0,729%	-0,463%	-0,266%
0,97070	-2,930%	-1,379%	-1,551%
0,98715	-1,285%	0,169%	-1,454%
0,98090	-1,910%	-0,733%	-1,177%

Figure C.2: Engine ”X” MBTA